Examination of cellular and molecular changes associated with Neuronal Thioredoxin-1 Deficiency

by

Tetiana Shcholok

A thesis submitted to the Faculty of Graduate Studies of

The University of Manitoba

In partial fulfilment of the requirements of the degree of

MASTER OF SCIENCE

Department of Physiology and Pathophysiology

University of Manitoba

Winnipeg, Canada

August 2023

Abstract

Introduction: Oxidative distress is a potent inducer and modulator of pro-neurodegenerative processes, although the exact mechanisms that underlie these changes remain controversial. Based on the pathomorphological features, all neurodegenerative disorders commonly express a set of so-called hallmarks of neurodegeneration, i.e., accumulation of protein aggregates, cytoskeleton impairments, decreased mitochondrial metabolism, etc. Numerous attempts to tackle these traditional targets did not yield any clinically efficient treatment of neurodegenerative disorders. Therefore, there is an urgent need for a profound investigation into the pathophysiology of neurodegeneration that might lead to the development of novel strategies in diagnostics, prevention, and treatment. The involvement of oxidative distress in neurodegenerative disorders is well-documented by increased levels of oxidized proteins, lipids, and nucleic acids in neural tissues. Thioredoxin-1 (Trx-1) is a thiol antioxidant protein responsible for the reduction of disulfide bonds in oxidized proteins. Altered Trx-1 activity is reported in various neurodegenerative disorders. However, the knowledge about the role of Trx-1 system in the prevention of neurodegenerative processes remains limited. *In vitro* reports from our lab and others have demonstrated that downregulation of Trx-1 disrupts several vital cellular processes in neurons, including alteration of nuclear integrity. Trx-1 is involved in the prevention of nuclear lamina invagination, a newly identified mechanism typical for several neurodegenerative diseases known as laminopathy. The events consequent to nuclear lamina damage are currently the area of active investigation in neurodegeneration research. Functional, morphological, aand molecular changes associated with Trx-1 downregulations in neurons remain to be studied in animal models.

Hypothesis: Trx-1 neuronal depletion is sufficient for induction of neurodegenerative-associated pathophysiology.

Methods: Trx-1 neuron-specific knockout mice (Trx-nKO) were generated using Cre-Lox recombination. Synapsin-1 Cre-driver was used to achieve Trx-1 depletion in all mature neurons. I then performed phenotypical (mean survival, body weight, hindlimb circumference measurements), behavioural (hindlimb clasping test, rotarod challenge, sensory-motor, novel object recognition, and Y-maze tests), morphological (MRI), histological (immunofluorescence and H&E staining), and molecular (western blotting and enzymatic activity assay) assessments on 4- and 8-week-old animals.

Results: Neuron-specific knockout of Trx-1 in mice results in severe phenotypical abnormalities as evidenced by significantly shortened lifespan, decreased body weight and muscular volume. These mice have dramatic motor deficits with no significant change in cognitive functions. Morphologically, the knockouts have significantly reduced brain and spinal cord size as well as prominent deterioration in white matter organization. Thus, these animals have significantly reduced corpus callosum thickness and lower number and diameter of axons in spinal cord and sciatic nerve. These findings coincided with a significant reduction in myelin content and perinuclear accumulation of axon-specific proteins. Molecular and histological characterization revealed significantly increased incidence of nuclear lamina damage in cortices and lumbar spinal cords of the knockouts. These mice also demonstrated a significant increase in c-Jun kinase (JNK)-medicated Tau phosphorylation and TAR DNA-binding protein (TDP-43) mislocatization and phosphorylation, pathological hallmarks typical for several neurodegenerative disorders. Altered neuronal homeostasis triggered glial responses in cortex and spinal cord of the mutants. There was a significant increase in the density of astroglia however, no significant signs of pro-inflammatory activation in the microglia population.

Conclusion: This study pioneered the characterization of novel neuron-specific Trx-1 knockout in rodents. It demonstrates the significance of Trx-1 antioxidant system for neuronal homeostasis as evidenced by severe phenotypical, behavioural, morphological, and molecular abnormalities identified in Trx-nKO mice. Detailed examination of molecular players involved in activation of pro-neurodegenerative changes is beneficial for designing novel tools for diagnostics, prevention, and treatment of neurodegeneration.

Acknowledgements

First and foremost, I would like to express my deepest gratitude to my supervisor, Dr. Eftekhar Eftekharpour, for his excellent guidance, caring and patience during the course of my research work. It would not have been possible to accomplish this work without his continuous support, mentoring, and contribution to my development as a scientist. I also appreciate my Advisory Committee members, Dr. Paul Fernyhough and Dr. Michael Jackson, for their contribution to the project through the feedback they have given during our annual meetings. The critique they provided helped to strengthen the weaknesses in my knowledge and in the project.

I owe my profound gratitude to our team members, who were always open to sharing their experiences and providing methodological guidance in various laboratory techniques. Special thanks to Dr. Md Imamul Islam for helping me to acquire the right skill set for basic medical research, the critique and advice he has been continuously providing on my project. I also appreciate Shakila Sultana and Parisa Tabeshmehr, my fellow graduate students, who were always a shoulder to lean on. I highly value the feedback and methodological guidance I've received from Dr. Shiva Nemati and Mojtaba Hosseini, my colleagues from Spinal Cord Research Centre.

I am thankful to Dr. Soheila Karimi for the expert advice she provided on the project, and an excellent opportunity for scientific discussion. I profoundly appreciate the contribution of Dr. Peter Vitiello, who came up with the idea of creating Trx-1 neuronal knockout mice, the main focus of my project.

I would also like to thank Mitacs for providing me with such an opportunity to do my MSc in Canada. I deeply admire their dedication to opening new horizons to talented youth with an interest in research, and the financial and informational support they provide.

Finally, special and great appreciation is due to my family, my most powerful stimulus to grow and achieve new heights. I am grateful to my husband Danyyl and my parents for their emotional support, patience, and belief in me throughout the study.

Table of Contents

Abstract **2**

Acknowledgements **5**

Table of Contents **7**

List of Tables **9**

List of Figures **10**

List of Abbreviations **11**

1. Introduction **15**

1.1 The burden of neurodegenerative diseases *15*
1.2 Pathophysiology of neurodegenerative diseases *16*
1.3 The role of reactive oxygen species (ROS) in neurodegeneration *18*
1.4 The evidence of oxidative distress in common neurodegenerative diseases *19*
1.5 Thioredoxin system *23*
1.5.1 Isoforms of mammalian Thioredoxin *25*
1.5.2 The structure of Trx-1 *26*
1.5.3 General functions of Trx-1 ***28***
1.5.3.1 Regulation of Cell Proliferation *29*
1.5.3.2 Antioxidant activity *29*
1.5.3.3. Regulation of apoptosis *31*
1.5.3.4 Regulation of autophagy *33*
1.5.3.5 Cytoskeleton organization *35*
1.5.3.6 Interaction with transcription factors *39*
1.5.3.7 The role of Trx-1 in maintenance of nuclear lamina integrity *42*
1.5.4 Neuron-specific functions of Trx-1 ***47***
1.5.4.1 The role of Trx-1 in neuronal differentiation *47*
1.5.4.2 Trx-1 in axonogenesis and regeneration *48*
1.5.4.3 Trx-1 functions in synaptic terminals *50*
1.5.4.4 Dysregulation of Trx-1 system in neurological diseases *51*
1.6 Hypothesis and Research objectives **53**

2. Materials and Methods **54**

2.1 Generation and maintenance of Trx-nKO mice colony *54*
2.2 Genotyping procedures *56*
2.3 Trx-nKO phenotype characterization *57*
2.3.1 Body weight *57*
2.3.2 Hindlimb circumference *57*
2.3.3 Racine scale for seizure activity assessment *58*

2.4 Tissue collection and processing *58*
2.5 Immunohistochemistry *60*
2.6 Image acquisition and quantitative analysis *61*
2.7 Western Blot *64*
2.8 Trx-1 activity assay *66*
2.9 Behavioral assessments *67*
2.9.1 Hindlimb clasping test *68*
2.9.2 RotaRod *68*
2.9.3 Sensory-motor test ("adhesive removal" test) *69*
2.9.4 Novel object recognition test *69*
2.9.5 Y-Maze *70*
2.10 Mouse magnetic resonance imaging (MRI) *70*
2.12 Statistical analysis *71*
3. Results **71**
3.1 Confirmation of Trx-1 neuron-specific knockout *71*
3.2 Phenotypical characterization of Trx-nKO mice *74*
3.3 Sensory and motor behavioural assessments reveal severe motor deficits in Trx-nKO mice *76*
3.4 Trx-1 neuronal knockout results in changes in CNS morphology and cellular organization *78*
3.5 Trx-1 knockout in neurons is associated with white matter deficits *80*
3.6 Trx-1 deficiency in neurons is associated with nuclear lamina damage *84*
3.7 Trx-1 depletion in neurons is associated with increased neurodegeneration *86*
3.8 Trx-nKOs exhibit increased Tau phosphorylation *88*
3.9 Trx-1 depletion results in disruption of intracellular transport *91*
3.10 Trx-1 depletion results in accumulation of neurofilaments and axonal deformation *94*
3.11 Trx-1 depletion in neurons is associated with increased protein oxidation *96*
3.12 Trx-1 depletion in neurons evokes glial responses *97*
4. Discussion **99**
4.1 Variable efficacy of Syn-Cre recombination underlies the mosaic pattern of Trx-nKO across the brain regions. *100*
4.2 Trx-1 is essential for normal nucleo- and cytoskeleton morphology *102*
4.3 Trx-nKO recapitulates the features of TDP-43 pathology *104*
5. Conclusion **106**
6. Limitations and Future Directions **107**
7. References **110**

List of Tables

Table 1.1 Molecular hallmarks of neurodegenerative diseases 17

Table 1.2 Characterization of Trx isoforms 28

Table 1.3 Trx-1 mediated redox regulation 44

Table 1.4 The status of Trx-1 in neurological diseases 51

Table 2.1 Modified Racine scale for seizure scoring 58

Table 2.2 Nuclear lamina structure scale 64

Table 2.3 List of antibodies used in experiments 66

List of Figures

Figure 1.1 CNS regions and subtypes of neurons affected in common neurodegenerative disorders 16

Figure 1.2 The principle of function of the Trx system 24

Figure 1.3 A simplified schematic of the axonal cytoskeleton 37

Figure 1.4. Schematic overview of nuclear envelope proteins involved in cytoskeleton/nucleoskeleton coupling 43

Figure 2.1 Quantification of corpus callosum thickness 62

Figure 3.1 Generation and confirmation of Trx-1 neuron-specific knockout in mice 73

Figure 3.2 Phenotypical characterization of Trx-nKO mice 75

Figure 3.3 Behavioral assessments reveal severe motor deficits in Trx-nKO mice 77

Figure 3.4 Trx-1 neuronal knockout results in changes in CNS morphology and cytoarchitectonics 79

Figure 3.5 Trx-1 knockout in neurons is associated with white matter deficits 82

Figure 3.6 Trx-1 deficiency in neurons is associated with nuclear lamina damage 85

Figure 3.7 Trx-nKO pathology includes elements of neurodegeneration 87

Figure 3.8 Trx-1 knockout in neurons is associated with activation of stress-related kinase JNK 90

Figure 3.9 Trx-1 deficiency in neurons is associated with TDP-43 proteinopathy 93

Figure 3.10 Trx-nKOs exhibit changes in axonal morphology along with decrease in myelin content 95

Figure 3.11 Trx-1 depletion enhances protein oxidation in neurons 96

Figure 3.12 Trx-1 depletion in neurons evokes glial responses 98

List of Abbreviations

ACC	anterior cingulate cortex
ACSF	artificial spinal cord fluid
AD	Alzheimer's disease
ALS	amyotrophic lateral sclerosis
AMPK	5' adenosine monophosphate-activated protein kinase
AP-1	activator protein 1
ARE	antioxidant response element
ASK-1	apoptosis signalling kinase
ATG	autophagy-related genes
ATG-4	autophagy-related gene 4
ATG-7	autophagy-related gene 7
BS	brain stem
BSA	bovine serum albumin
CA	cornu ammonis
cAMP	cyclic adenosine monophosphate
ChAT	choline acetyl transferase
CNS	central nervous system
Cntl	control
COS-7 cells	monkey kidney fibroblast cell line
Cre	Cre-recombinase
CREB	cAMP response element-binding protein
CRMP2	Collapsin response mediator 2
CSF	cerebrospinal fluid
Cys	Cysteine
DALY	disability-adjusted life year
DAPI	4′,6-diamidino-2-phenylindole
DMV	dorsal motor nucleus of the vagus
DNA	desoxyribonucleic acid
DNP	Dinitrophenylhydrazine
EC	entorhinal cortex
ECL	enhanced chemiluminescence
EDTA	ethylenediaminetetraacetic acid
EGTA	ethylene glycol tetraacetic acid
ERK 1/2	extracellular signal-regulated kinases 1 and 2
FAD	flavine adenine dinucleotide
FC	frontal cortex
FI	frontal insula
fl	floxed
FTD	frontotemporal dementia

FUS	fused in sarcoma RNA-binding protein
GABA	γ-Aminobutyric acid
GAPDH	glyceraldehyde 3-phosphate dehydrogenase
Gly	Glycine
gRNA	guide RNA
Grx	glutaredoxin
GSH	glutathione
H2AX	H2A histone family member X
HD	Huntington's disease
HeLa cells	immortalized cervical cancer cell line
HIF-1α	hypoxia-induced factor-1α
HP	hippocampus
HRP	horse radish peroxidase
Iba1	ionized calcium-binding adaptor molecule 1
IHC	immunohistochemistry
IL-1b	interleukin 1b
JNK	c-Jun N-terminal kinase
KEAP1	Kelch-like-ECH-associated protein 1
LC III	Microtubule-associated proteins 1A/1B light chain 3B
LC	locus coeruleus
LINC	Linker of Nucleoskeleton and Cytoskeleton
MAG	myelin-associated glycoprotein
MAPK	mitogen-activated protein kinase
MBP	myelin basic protein
MES	2-(N-morpholino)ethanesulfonic acid
MNC	motor neocortex
MRI	magnet resonance imaging
mRNA	messenger RNA
MSN	medium spiny neurons
MsrA	methionine sulforeductase A
MsrB	methionine sulforeductase B
MST-1	mammalian STE-20-like kinase-1
mTOR	mammalian target of rapamycin
NADPH	reduced nicotinamide adenine dinucleotide phosphate
NeuN	neuronal nuclear protein
NF-κB	nuclear factor kappa-light-chain-enhancer of activated B cells
NFH	neurofilament heavy (neurofilament 200)
NGF	nerve growth factor
NHEJ	non-homologous end joining
NOX	nitric oxide

NPC	neural progenitor cell
Nrf-2	nuclear erythroid 2-related factor
OB	olfactory bulb
OCT	optimal chamber temperature
Oct-1	Octamer-binding transcription factor 1
Oct-4	Octamer-binding transcription factor 4
p53	tumor protein p53
p62	Sequestosome 1
PAM	protospacer adjacent motif
PBS	phosphate-buffered saline
PC12 cells	Rat pheochromocytoma cell line
PCR	polymerase chain reaction
PD	Parkinson's disease
PolyQ	polyglutamine
Pro	Proline
Prx	peroxiredoxin
pTau	phosphorylated Tau
PVDF	polyvinylidene fluoride
Ref-1	redox factor-1
rhTrx-1	recombinant human thioredoxin-1
RIPA	radioimmunoprecipitation assay
RNA	ribonucleic acid
RNR	ribonucleotide reductase
ROS	reactive oxygen species
SC	spinal cord
SDS	sodium dodecyl sulfate
SDS-PAGE	Sodium dodecyl-sulfate polyacrylamide gel electrophoresis
SEM	standard error of the mean
Sema 3A	Semaforin 3A
SNpc	substantia nigra pars compacta
SOD1	superoxide dismutase 1
SUN	SAD1/UNC-84 homology
Syn-1	synapsin 1
TAE	Tris-acetate-EDTA
TBP	TATA-binding protein
TBS	Tris-buffered saline
TBST	Tris-buffered saline with Polysorbate-20 (Tween-20)
TC	temporal cortex
TDP-43	TAR DNA-binding protein 43
Thr	Threonine

TNF-α	tumor necrosis factor-alpha
Trp	Tryptophan
Trx	thioredoxin
Trx-1	thioredoxin-1 protein
Trx-2	thioredoxin-2 protein
Trx-3	thioredoxin-3 protein
Trx-80	truncated thioredoxin
Trx-nKO	thioredoxin neuronal knockout
TrxR	thioredoxin reductase
TrxR1	thioredoxin reductase 1
TrxR2	thioredoxin reductase 2
Tuj	beta-tubulin
Txn1	thioredoxin-1 gene
Txn2	thioredoxin-2 gene
UTR	untranslated region
UV	ultraviolet
WHO	World Health Organization
WT	wild type
β2-AR	β2-adrenergic receptors

1. Introduction

1.1 The burden of neurodegenerative diseases

Neurodegenerative diseases are the spectrum of neurological and psychiatric disorders caused by progressive loss of structure and functions of neuronal cells through a process known as neurodegeneration[1]. Based on the clinical presentation, neurodegenerative diseases of Central Nervous System (CNS) are classified as extrapyramidal and pyramidal movement disorders (Huntington's disease (HD), Parkinson's disease (PD) and Parkinsonism, Amyotrophic lateral sclerosis (ALS), Multiple sclerosis, etc.) and cognitive or behavioural disorders (Alzheimer's disease (AD), Dementia with Lewy bodies deposition, frontotemporal dementia (FTD), stroke-related cognitive dysfunction, epilepsy-associated cognitive decline, etc.)[2].

Neurodegenerative diseases are among the top causes of disability in developed countries. To illustrate, AD and other dementias are ranked third in the list of disorders associated with significant limitations in professional and social activity with 1100 DALYs per 100 000 of the population (WHO, 2023). Major advances in the treatment of several prevalent infectious and non-infectious diseases led to a significant increase in life expectancy across populations in the world[3]. Global aging, being one of the leading risk factors of neurodegeneration, resulted in a dramatic increase in the prevalence of these disorders in developed countries[3]. For instance, in Canada, the DALY index for neurodegenerative diseases experienced a dramatic increase of more than 150% within the 20-year period between 1990 and 2010[4]. Neurodegeneration is also among the leading causes of premature death in developed countries having raised from 22nd rank in 1990 (0.9% of total deaths) to 7th rank in 2010 (3.2% of death; 247% increase)[4].

The problem of neurodegeneration is not limited to healthcare systems or personal impact on the patients with neurodegeneration, their families, and caregivers, but it also has a significant negative influence on the global economy. A US Government report indicated the expenditure of over 655 billion USD on both direct medical and non-medical (from lost productivity and uncompensated caregiving hours) expenses associated with neurodegenerative disorders[5].

1.2 Pathophysiology of neurodegenerative diseases

Neurodegenerative diseases are identified by the loss of neurons in specific regions or neuronal subtypes CNS[6]. Considering the limited ability of endogenous neural stem cells to replace the damaged and lost neurons, loss of functions in these diseases is permanent and results in life-lasting disabilities[7]. The CNS regions and subtypes of neurons affected in the most common neurodegenerative disorders are summarized in **Figure 1.1**.

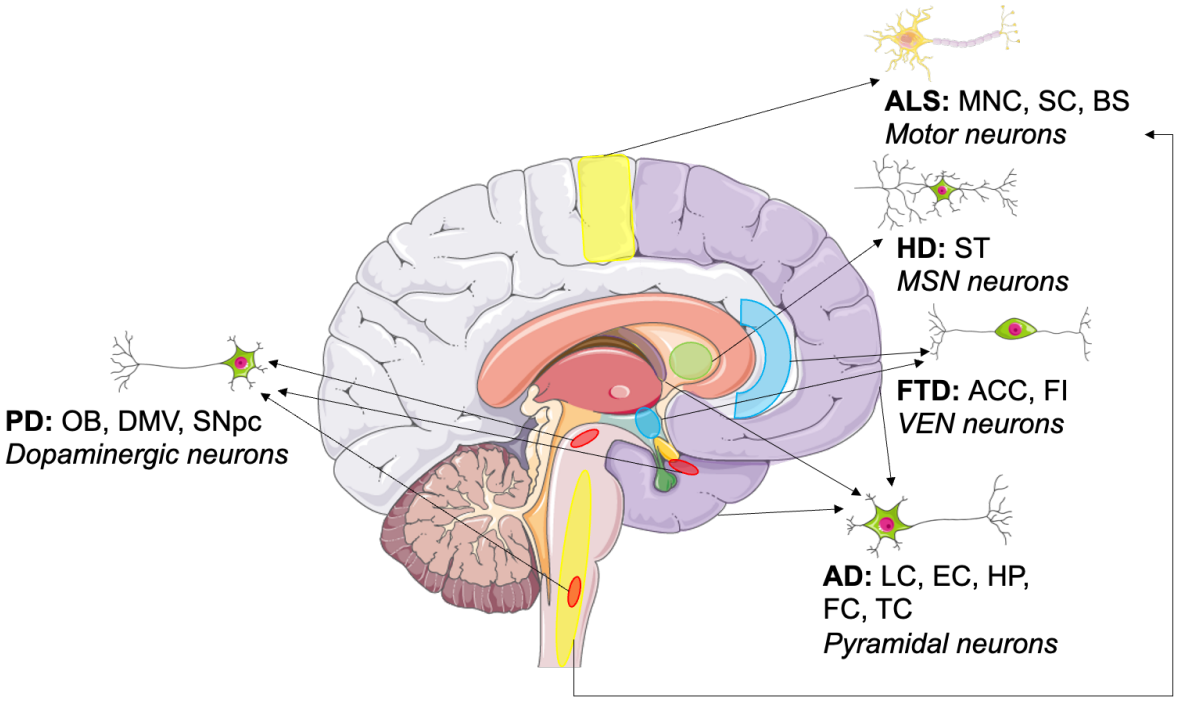

Figure 1.1 CNS regions and subtypes of neurons affected in common neurodegenerative disorders

Early affected regions in various neurodegenerative diseases are indicated with different colors. **Amyotrophic Lateral Sclerosis (ALS)**: motor neurons in motor neocortex (MNC), spinal cord (SC), brain stem (BS); **Huntington's disease (HD)**: medium spiny GABAergic neurons (MSN) in striatum (ST); **Frontotemporal dementia (FTD):** large bipolar spindle-shaped von Economo neurons in anterior cingulate cortex (ACC) and frontal insula (FI); **Alzheimer's disease (AD):** pyramidal neurons in locus coeruleus (LC), hippocampus (HP), entorhinal cortex (EC), frontal cortex (FC), and temporal cortex (TC); **Parkinson's disease (PD):** dopaminergic neurons in olfactory bulb (OB), dorsal motor nucleus of the vagus (DMV), substantia nigra pars compacta (SNpc).

Decades of research have revealed genetic biochemical and morphological alterations involved in neurodegeneration. Despite the variety of clinical presentations, neurodegenerative disorders are united with common molecular and histological impairments called "hallmarks of neurodegeneration"[8]. **Table 1.1** provides a summary of typical markers of neuronal degeneration in most common neurodegenerative diseases.

Table 1.1 Molecular hallmarks of neurodegenerative diseases

Marker	**AD**	**ALS**	**PD**	**HD**
Protein deposits	Extracellular and intercellular Amyloid plaques[9], Neurofibrillary tangles[10]	Bunina bodies[11]	Lewy bodies[12]	Aggregated huntingtin[13]
Aggregating proteins	pTau[10], Amyloid-Beta-42[9], TDP-43[14]	TDP-43[15], pTau[16], SOD1[17], FUS[18], p62[19], neurofilaments[20,21]	Alpha-synuclein[22], pTau[23]	huntingtin[24], PolyQ[25]
Myelination status	Decrease in myelin content[26]	Decrease in myelin content[27]	Decrease in myelin content[28]	Decrease in myelin content[29]
Autophagy	Impaired[30]	Impaired[31]	Impaired[32]	Impaired[33]

Apoptosis	Activated[34]	Activated[35]	Activated[36]	Activated[37]

AD – Alzheimer's disease, ALS – Amyotrophic Lateral Sclerosis, PD – Parkinson's disease, HD – Huntington's disease; pTau – phosphorylated Tau, TDP-43 – TAR-DNA-binding protein 43, SOD1 – Superoxide dismutase 1, FUS - Fused in Sarcoma RNA-binding protein, p62 – Sequestosome 1, PolyQ – Polyglutamine.

1.3 The role of reactive oxygen species (ROS) in neurodegeneration

Oxygen is vital for all aerobic organisms but can potentially disrupt cellular homeostasis[38]. The harmful effects of oxygen are associated with the damage done by ROS[39]. As their name suggests, ROS are highly reactive molecules /radicals that originate from diatomic oxygen e.g., peroxides, superoxide, singlet oxygen, nitric oxide (NOX), hydroxyl radical, etc[39]. Unpaired electron couple in their structure makes them highly reactive[40]. Thus, ROS are known to interact with a multitude of biomolecules, e.g., proteins, lipids, and nucleic acids causing their oxidation[39]. There are both exogenous and endogenous sources of ROS[40]. Exogenous stimulation of ROS production occurs upon exposure to several agents, e.g., heavy metals[41], tobacco[42], microplastics[43], xenobiotics[44] or ionizing radiation[45]. Endogenous ROS production is an intrinsic component of normal metabolism in mitochondria[46] and peroxisomes[47]. Historically, ROS have been associated with a detrimental impact on cellular metabolism[48]. However, extensive research has shown that aerobic organisms have evolved to take advantage of ROS by incorporating them into essential signalling pathways[39]. Hydrogen peroxide (H_2O_2) and superoxide radicals are the major ROS in normal physiologic conditions[49]. They are indispensable for the regulation of cell proliferation[50], differentiation[51], migration[52] and apoptosis[53]. Consequently, the complete abolishment of ROS generation is as detrimental to the cell as their overproduction[54]. To avoid an excessive production of ROS and subsequent damage to structural and regulatory biomolecules, cells have developed a highly

elaborate and complex antioxidant system[55]. This system is composed of vitamins, redox proteins, and enzymes[55]. Of particular interest to my project, antioxidant thiol proteins are especially important in maintaining ROS levels and in rejuvenating oxidized proteins[56]. This is mediated by electron donation from Cysteine residues in the active site of these proteins[57]. Mechanistically, these proteins neutralize the toxic products of protein, lipid, and DNA oxidation, e.g., peroxides, aldehydes, alcohols, ketones, cholesterol oxide, etc[55]. The adequate capacity of the antioxidant system maintains the equilibrium between oxidized and reduced biomolecules. This state is called redox balance[58]. Depletion of antioxidant capacity or overproduction of ROS results in a breakdown of redox balance otherwise known as oxidative distress[58].

Neuronal cells have naturally higher ROS production and lower antioxidant capacity compared to other cell types, e.g., astrocytes[59]. This feature underlies high susceptibility of the CNS to oxidative damage and neuronal cell death. A decline in cellular antioxidant capacity during aging further enhances oxidative damage in neurons and highlights oxidative distress as a key component of several neurodegenerative disorders, e.g., AD, PD, ALS, HD, etc[60]. An expanding body of literature indicates that excessive ROS production in CNS induces several key features of neurodegeneration such as accumulation of misfolded proteins, increase in intracellular free Ca^{2+}, release of excitatory amino acids, interruption of pro-survival autophagy and induction of apoptosis[60,61].

1.4 The evidence of oxidative distress in common neurodegenerative diseases

The main pathohistological features of AD are the accumulation of misfolded protein Amyloid-beta and intraneuronal neurofibrillary tangles composed of hyperphosphorylated cytoskeletal

protein Tau[62]. Oxidative distress is believed to have a more prominent role in the pathogenesis of AD compared to other neurodegenerative diseases[63].

Overproduction of ROS in AD results in increased levels of DNA oxidation products as evidenced by increased 8-hydroxydeoxyguanosine in the nucleus and mitochondria[64,65]. Enhanced protein oxidation is detected by an increased content of carbonylated proteins in post-mortem brain samples of patients with AD[66]. Additionally, high levels of oxidized, glycated and nitrated proteins are commonly detected in senile plaques[67,68], helical filaments[68] and cerebrospinal fluid (CSF)[68] from patients with AD. Mounting evidence suggests the presence of a vicious circle in the pathogenesis of AD where oxidative stress leads to enhanced Amyloid-beta production and Tau hyperphosphorylation, and, conversely, accumulation of structurally damaged proteins leads to the overproduction of ROS[69].

Protein oxidation by free radicals affects enzymatic pathways critical to neuron and glial metabolism. For instance, glutamine synthase, a redox-sensitive enzyme involved in the turnover of the excitatory neurotransmitter glutamate, is found to be oxidized in AD brain[70]. Loss of glutamine synthase activity in neural tissue results in alterations in glutamine metabolism and enhanced excitotoxicity, a well-known player in the pathophysiology of AD[70]. Another redox-sensitive enzyme commonly inactivated in AD is creatinine kinase[71]. Oxidation-dependent loss of creatinine kinase activity underlies brain hypometabolism in AD patients[71].

Hyperphosphorylation of Tau protein, a hallmark of AD pathology, is also shown to be oxidation-dependent and therefore accumulation of neurofibrillary tangles is also rooted in oxidative distress[69]. Thus, Tau oxidation is linked to oxidation through microtubule-associated protein kinase pathway[72] and through activation of JNK[73].

Amyloid-beta, another marker of AD pathology, is classified as metalloprotein. It is able to bind to transition metals due to the presence of three histidine and one tyrosine residue in its hydrophilic N-terminal[74]. Pro-oxidative milieu facilitates enhanced binding of soluble Amyloid-beta with Cu^{2+} and Fe^{3+} ions[74]. Upon interaction with these metals, soluble Amyloid-beta aggregates and forms toxic oligomers, polymers, and ultimately senile plaques[74].

Along with the activation of ROS-producing pathways, mounting evidence suggests a drastic reduction in the antioxidant capacity to be an indispensable component of AD pathogenesis. Thus, significant downregulation of glutathione (GSH)[75], thioredoxin (Trx)[76], peroxiredoxin (Prx)[77], catalase[78] and superoxide dismutase (SOD)[79] was identified in post-mortem brain samples from subjects with AD.

An excessive production of ROS associated with depletion of antioxidant capacity represents a crucial pathophysiological feature of ALS[80]. Mounting evidence has demonstrated increased oxidation of lipids, proteins and DNA in post-mortem neural tissue[81-83], CSF [84-87], plasma[88], and urine[89] collected from human subjects with ALS. However, there is no consensus on whether oxidative distress is the primary cause or the secondary consequence of this disorder[90]. Mutations in Superoxide dismutase 1 (SOD-1), an antioxidant enzyme that converts superoxide radicals into hydrogen peroxide, accounts for approximately 20% of ALS cases[91]. SOD-1 plays an important role in antioxidant protection, energy metabolism, and cell respiration[92]. To date, more than 180 mutations in the coding region of SOD-1 gene as well as several mutations located in non-coding regions were identified in patients with ALS[91,93]. The outcome of these mutations is generally heterogeneous including loss[86], maintenance[94] and gain[86,95] of activity compared to wild-type SOD-1. Interestingly, SOD-1 knockout in rodents does not mimic the ALS phenotype[95]. Additionally, there is no correlation between SOD-1 activity and the severity of the clinical

presentation of ALS in humans[96]. Therefore, it has been suggested that SOD-1 mutations are linked to the gain of toxic function rather than to the alteration of enzymatic activity[97]. In the majority of cases, mutant SOD-1 is prone to aberrant aggregation in the cytoplasm and is believed to disrupt ubiquitin/proteasome function, mitochondrial metabolism and mitophagy[98,99]. Protein misfolding in ALS is viewed as a consequence of redox dysregulation[100]. This specifically involves discrepancies in the thiol-reducing system that facilitates the reduction of Cysteine residues in protein molecules (e.g., Trx and GSH systems)[101]. In mutant SOD-1 molecules, disulfide bonds involve Cys6 and Cys111 and lead to pathological aggregation of the misfolded protein monomers in the cytoplasm[102]. Discrepancies in the GSH system are the common finding in post-mortem samples from humans with ALS[103]. Consequently, several studies demonstrated decreased GSH peroxidase activity and GSH content in spinal cord and cerebral cortex of ALS patients[104,105]. Further evidence for the involvement of oxidative distress has been shown by decreased GSH peroxidase activity in erythrocytes that positively correlates with disease progression in subjects with ALS and, hence is proposed as a promising prognostic marker[106]. Mutations in Trx reductase-1 (TrxR1), another key enzyme in thiol reduction, are also linked to the pathogenesis of familial ALS[107]. Such mutations are associated with an early age onset (decreased by 8 years compared to average)[107].

Similar to SOD-1, TDP-43 is another key component of protein aggregates in ALS. Cysteine oxidation and aberrant disulfide cross-linking have been linked to the pathophysiology of ALS[108]. In TDP-43 disulfide bond formation occurs within Cys173, 175, 198, and 244 of the RNA-recognition motifs[109,110]. Induced by dysregulation of the redox conditions, such aberrant linkage leads to misfolding and subcellular mislocalization of TDP-43[108]. Cytoplasmic accumulation of TDP-43 is viewed as a key event in the pathophysiology of ALS and is believed to have a negative

impact on cellular homeostasis in two ways[108]. First, via loss of its transcriptional control in the nucleus for more than 3000 genes including genes relevant to neurodegeneration[108], and secondly, via gain of toxic function since misfolded TDP-43 aggregates exhibit toxic properties[108]. Taken together, similar to other neurodegenerative disorders, redox imbalance in ALS potentiates protein oxidation, misfolding and aggregation and vice versa, protein aggregation propels oxidative distress[101].

The previous sections highlight the importance of cellular redox balance for normal cellular function. GSH and Trx systems are the major cellular thiols that are responsible for maintaining cellular proteins in their reduced state to ensure proper regulation of cellular signalling[111]. GSH has been extensively studied in CNS[112-115] and will not be discussed here; my thesis will specifically focus on the role of Trx-1 in neurons.

1.5 Trx system

Trxs are small antioxidant proteins with similar structures and functions[116]. The name "thioredoxin" originated from the molecular mechanism that underlies their redox function. Thus, two Cysteines in active site of the Trx molecule facilitate reduction of a single S-S group in their target proteins[57], resulting in Trx oxidation. The oxidized Trx must be then reduced by Thioredoxin reductase (TrxR1 or TrxR2), a specific FAD-containing enzyme, using electrons from NADPH [116].

Functionally, Trxs either play the role of electron donor for catalytic cycles of biosynthetic enzymes (e.g., ribonucleases, methionine sulfoxide and sulphate reductases) or regulate the intra- and intermolecular disulfide bonds in their protein targets in different conditions (**Figure 1.2**)[117].

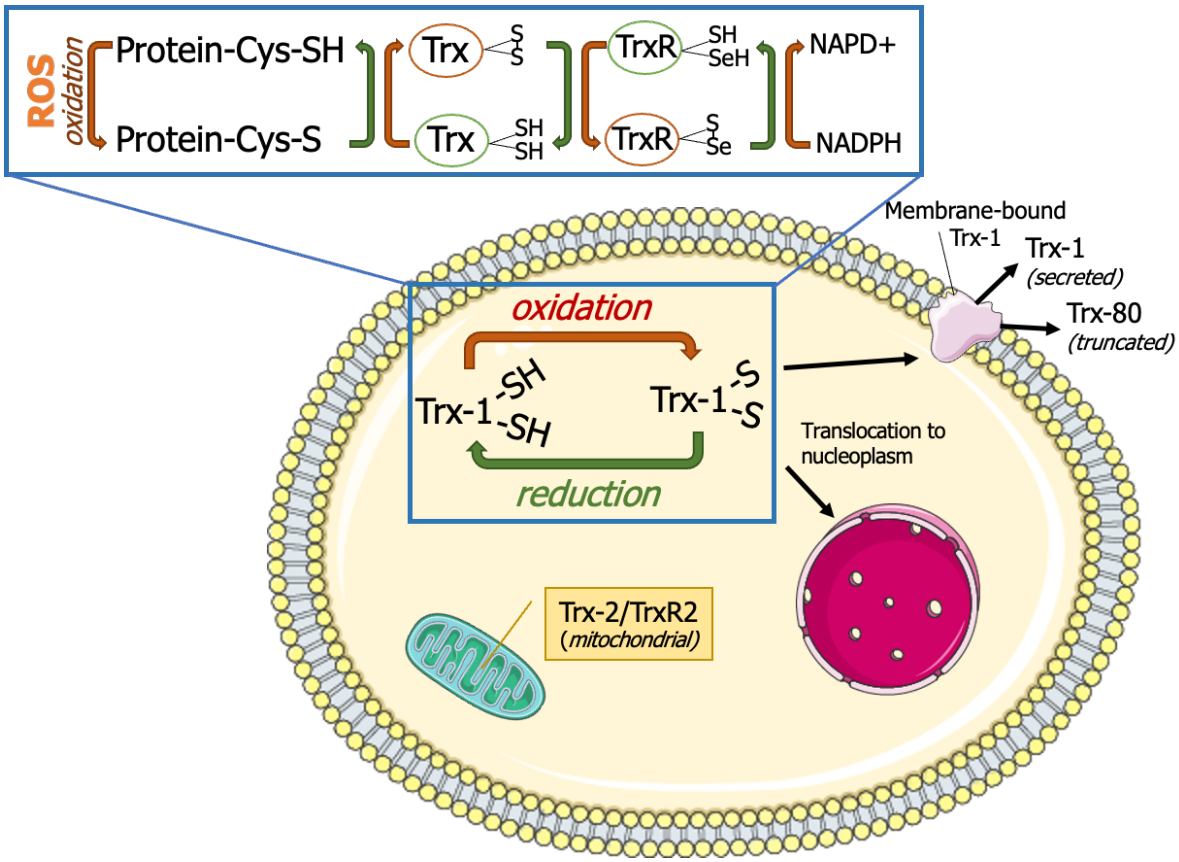

Figure 1.2 The principle of function of the Trx system

Thioredoxins (Trx) donate Hydrogen to resolve difulfide bonds (S-S) in protein Cysteines (Cys). Oxidized Trx is reduced by Thioredoxin reductases (TrxR) with the help of Reduced Nicotinamide Adenine Dinucleotide Phosphate (NADPH). Thioredoxin-1 (Trx-1) is typically localized in cytoplasm but can also undergo nuclear translocation, membrane binding or secretion. Thioredoxin-2 (Trx-2) and Thioredoxin reductase-2 (TrxR2) are localized in mitochondria.

The importance of protein disulfide reduction in overall cellular homeostasis is based on the abundance of cysteine-containing proteins in the mammalian proteome[116]. For instance, several

regulatory proteins form reducible disulfide bonds and are subjected to Trx-1 mediated reduction, e.g., insulin, human choriogonadotropin, several blood coagulation factors, and fibrinogen[118].

1.5.1 Isoforms of mammalian Trx

To date, three isoforms of Trx have been identified in mammals: Trx-1, Trx-2, and Trx-3. Trx-1 and Trx-2 are encoded by two separate genes (Txn1 and Txn2 respectively), while the Trx-3 protein is a result of genetic duplication of the Txn1 gene[119]. While Trx isotypes have a relatively similar structure with conserved disulfide active site sequence (Trp-Cys-Gly-Pro-Cys)[120], subcellular and tissue-specific localization are the factors that determine their specific functions. Thus, Trx isoforms could be divided into two subgroups: a) Trxs which are ubiquitously expressed in all cell types (Trx-1 and Trx-2); b) Trx expressed specifically in testes (Trx-3)[118].

Human Txn1 gene is located on chromosome 9[121]. Its expression is under the control of a ubiquitous promoter and also under an inducible promoter known as antioxidant response element (ARE)[122]. Stress-induced activation of Txn1 transcription is mediated by several transcription factors, i.e., nuclear erythroid 2-related factor (Nrf-2), cAMP response element-binding protein (CREB) or TATA-binding protein (TBP)[123,124].

Trx-1 protein is located in the cytoplasm of all cells and tissues. Aside from its typical localization, this Trx isoform is known to translocate to the nucleus in response to oxidative or nitrosative stress[125] or to be secreted extracellulary[126]. Both Trx-1 and its truncated form (Trx-80) are secreted by immune cells (e.g., monocytes, lymphocytes, and neutrophils). This is proven to have a role in

cell-to-cell communication and facilitation of chemotaxis[127]. This mechanism is specifically important in infection and inflammation as well as in neoplastic changes in the hematopoietic system[128].

The involvement of Trx-1 in vital cellular processes is discussed in the following sections.

1.5.2 The structure of Trx-1

Thioredoxin-1 (Trx-1) is the most studied isoform which was first isolated from *E. coli* in 1964[129]. Before that, it was reported under different names as a hydrogen donor for enzymes reducing methionine sulfoxide and sulphate by NADPH in yeasts[130].

The Trx-1 system is a redox system conserved across all botanic and animal species. Trx-1 crystal structure was described for yeasts (Saccharomyces cerevisiae, Schizosaccharomyces pombe) plants (Arabidopsis thaliana), bacteria (E. coli, M. tuberculosis), protozoa (T. vaginalis, P. falciparum, Dictyostelium discoideum), nematodes (Caenorhabditis elegans), and mammals (Rattus norvegicus, Mus musculus, Bos taurus, Equus caballus, Ovis aries, Sus scrofa, Homo sapiens)[118]. Despite being first discovered and described in yeasts, the structure and role of Trx-1 are now well-established in mammalian cells. The active site of Trx-1 molecule is conserved across all the species described to date and includes the following amino acid sequence: Trp-Cys-Gly-Pro-Cys[129]. Cys32 and Cys35 are traditionally associated with Trx-1 antioxidant function[116]. Interestingly, mammalian Trx-1 has a slightly different structure compared to other species[129]. In addition to Cys32 and Cys35 located in its active site, it contains three other Cysteine residues (Cys62, Cys69, and Cys73)[129]. To date, there is no clear opinion regarding the function of these additional cysteines, however, it has been shown that oxidation of cysteines localized outside of

the active site leads to loss of Trx-1 enzymatic activity[57]. While both Cys62 and Cys69 undergo only S-nitrosylation[131-133], Cys73 is a multi-modification site that undergoes dimerization[133], nitrosylation[134,135], gluthathionylation[136] or 4-hydroxy-2-nonenal modification[137]. These structural features make Trx-1 molecule more susceptible to stress-induced posttranslational modifications compared to Trx-2 isoform. While Trx-1 molecule contains three Cysteines located outside of the active site (4.8% Cys of total amino acid sequence), Trx-2 has only one Cysteine (Cys37) located outside of the active motif (1.8% Cys of total amino acid sequence)[129,138]. Structural and functional features of Trx isoforms are listed in **Table 1.2.**

Table 1.2 Characterization of Trx isoforms

	Trx-1	Trx-2	Trx-3
Tissue specificity	Ubiquitous[118]	Ubiquitous[139]	Male germ cells[119]
Subcellular localization	Cytoplasm[116] Nucleus[56] Extracellular matrix[140]	Mitochondria[139]	Golgi apparatus[141]
Structure (human)	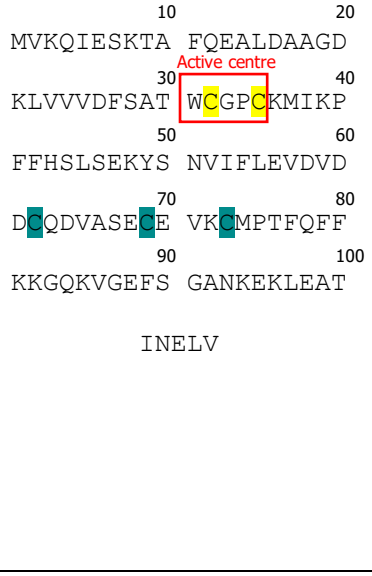	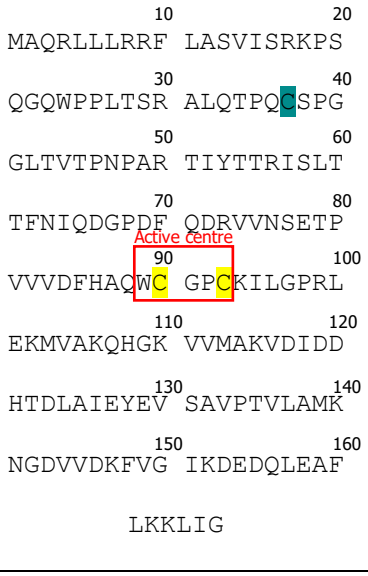	Similar to Trx-1

Cysteines located within the active center of Thioredoxin-1 (Trx-1), Thioredoxin-2 (Trx-2), and Thioredoxin-3 (Trx-3) are highlighted with yellow, Cysteines outside of the active centre are highlighted with Cyan.

1.5.3 General functions of Trx-1

Trx-1 is a structurally and functionally unique protein with multiple roles in cellular homeostasis. Due to its reducing capacity for Cysteine residues, it plays the role of redox switch in numerous vital cellular processes, i.e., cell proliferation, differentiation and migration, apoptosis, autophagy, inflammation, and metabolism[117]. The Trx-1/TrxR1 system was described in the 1960's and is currently a hot research topic due to the development of novel tools and techniques in the field of redox biology. Redox regulation of Trx-1 is mediated by its fast and transient protein-protein

interaction[116]. This rapid interaction enables Trx-1 to act like a concert conductor of the cellular protein orchestra.

In this chapter, I will discuss Trx-1 target proteins and the signalling pathways affected by such regulation.

1.5.3.1 Regulation of Cell Proliferation

Historically, the first role identified for Trx-1 in the cell was the donation of hydrogen/electron to ribonucleotide reductases (RNRs), enzymes that catalyze the conversion of ribonucleotides to deoxyribonucleotides for DNA synthesis[116]. For each conversion, the reduction of ribonucleotide is coupled with the formation of disulfide in the active site of RNR molecule[142]. Restoration of RNR conformation is reliant on an external thiol-dependant oxidant system, i.e., Trx-1/TrxR1[143]. These findings put Trx-1 inhibition as a prospective cancer treatment as uncontrolled cell proliferation is the key feature of neoplastic processes[144]. However, Trx-1 is not an exclusive reducing agent for RNR as it can also accept electrons from Glutaredoxin (Grx)[145], which is another dithiol donor. Accordingly, downregulation of the Trx-1/TrxR1 system does not result in a significant decrease in DNA synthesis and overall cell proliferation[146]. The GSH (GSH)/Grx system can reduce oxidized Trx-1 in the absence of TrxR1[147].

1.5.3.2 Antioxidant activity

Prxs are cellular peroxidases ubiquitously expressed in all cell types[148]. Similarly to Trxs, their role was first identified in yeasts and further confirmed in other systems including mammals[149]. The primary function of Prxs is the reduction of peroxides, for instance, H_2O_2, peroxynitrite or

lipid hydroperoxides[149]. In these reactions, Prxs require Trx-1 as a hydrogen donor and therefore establish a redox cascade that directs the electrons from NADPH to TrxR1 to Trx-1 to Prxs and, finally, to effector peroxide[150]. For most of the Prxs, Trx-1 is the main but not the only donor of Hydrogen[148]. Thus, it is speculated that the loss of Trx-1 might be partially equal to the loss of Prx system and result in ROS overproduction, specifically via increase in protein and lipid peroxidation[117]

Methionine and Cysteine are the two most susceptible to oxidation amino acids[151]. Similarly to Cysteine-rich proteins, the function of Methionine-rich proteins significantly depends on the capacity of antioxidant system[152]. There are three types of methionine reductases, i.e., Methionine sulforeductase A (MsrA), Methionine sulforeductase B (MsrB), and free methionine-R-sulfoxide reductase[153]. MsrA and MsrB are mechanistically linked to the Trx-1/TrxR1 system. Both of these reductases require hydrogen donated by Trx-1 to regenerate their redox-active catalytic center and regain their activity[154]. The physiological importance of this mechanism is dictated by the abundance of methionine-rich regulatory proteins in the mammalian proteome. For instance, Methionine oxidation/reduction is crucial for the activity of α-proteinase inhibitor[155], Ca^{2+}/calmodulin-dependent protein kinase[156], TDP-43[157]. However, the Trx-1/TrxR1 system is not the sole contributor to the reduction of MsrA and MsrB. Other thiol enzymes such as Thionein[154] and Grx are involved in the reduction of these enzymes and might be compensatory in Trx-1 deficient systems[158].

1.5.3.3 Regulation of apoptosis

Apoptosis is the classic form of programmed cell death, which is an indispensable component of normal development and elimination of defective cells[159]. This is identified by nuclear condensation and fragmentation[160]. Apoptotic cell death often does not involve the activation of immune cells[161]. However, hyperactivation of apoptosis is also a player in several pathologic processes, e.g., neurodegeneration[162-166], cardiomyopathies[167,168], viral infections[169], autoimmune disorders[170-172]. Activation of apoptosis occurs through either extrinsic or intrinsic pathways[160]. In the extrinsic pathway, pro-apoptotic changes in the cell are triggered by the extracellular environment, e.g., Tumor Necrosis Factor Alpha (TNF- α) secreted by immunocompetent cells[173]. The intrinsic pathway is otherwise known as mitochondrial as its activation occurs through primary damage to mitochondria[159]. Thus, loss of mitochondrial integrity results in release of Cytochrome C that triggers further pro-apoptotic cascade in cytoplasm[160]. Regardless of the initiation mechanism, downstream events are typically associated with activation of caspases, the executors of apoptosis, and subsequent cleavage of structural and regulatory components of the cell[159].
The growing body of evidence has also linked oxidative distress to initiation and execution of apoptosis[174,175]. Trx-1 is reported to be involved in the regulation of apoptosis via controlling the redox status of several molecules.

Trx-1 is linked to the activation of effector caspases. For instance, pharmacological inhibition of Trx-1 but not GSH system in SH-SY5Y cells (human neuroblastoma cells) induces activation of caspase-6[176]. In this work, restoration of the reduced Trx-1 pool was sufficient to prevent apoptotic cell death. Additionally, Trx-1 is reported to interact with a key determinant of apoptosis, caspase-

3. Thus, in Jurkat cells, transnitrosylation between Trx-1 and caspase-3 molecules prevents activation of apoptosis[177,178].

Another role of Trx-1 in redox regulation of apoptosis is mediated via reduction/oxidation of upstream pro-apoptotic molecules such as Apoptosis signalling kinase 1 (ASK-1)[179]. Under normal conditions, Trx-1 prevents the initiation of pro-apoptotic signalling via binding to ASK-1[174]. In case of Trx-1oxidation by ROS or after pharmacological/genetic downregulation of Trx-1 activity, ASK-1 is released from the bond[174]. Activated ASK-1 then conducts pro-apoptotic signals via p38 Mitogen-activated protein kinase (MAPK) or JNK[179].

Mammalian STE-20-like kinase-1 (MST1) is a ubiquitously expressed serine-threonine kinase involved in the regulation of cell proliferation, morphogenesis, senescence, and apoptosis. In response to different stressors including oxidative damage, MST-1 is activated by caspase-3 mediated cleavage of the autoinhibitory segment[180]. Upon activation, MST-1 translocates to the nucleus and induces apoptotic chromatin condensation and DNA fragmentation by phosphorylation of Histone H2AX[181]. Alternatively, MST-1 is activated via phosphorylation of Thr183 and Thr187 and itself becomes a caspase activator[182]. Thus, MST-1 can play a role as both an upstream or downstream kinase in apoptosis. Additionally, similar to most STE-20 group kinases, it can facilitate its pro-apoptotic effects via MAPK and JNK[183]. The potential role of Trx-1 in oxidative stress-induced activation of MST-1, is attributed to its ability to physically associate with this kinase and therefore prevent its phosphorylation, cleavage or homodimerization[184]. The bond between Trx-1 and MST-1 is lost upon the introduction of potent oxidative agents such as H_2O_2[184]. This is viewed as a potential trigger to MST-1 mediated activation of apoptosis.

1.5.3.4 Regulation of autophagy

Autophagy is a vital cellular mechanism required for the elimination of old or defective organelles, normal or damaged proteins, and other biomolecules[185]. This process allows proper degradation and recycling of biomaterial inside the cell[186]. The role of autophagy was first demonstrated in starving cells, which catabolize their structural and regulatory components via autophagy in order to produce the energy required for cell survival[186]. Autophagy is also crucial for normal embryonic development and implantation including elimination of paternal mitochondria from the zygote for maternal cytoplasmic inheritance[187]. Interruption of autophagy is reported in aging and is associated with the accumulation of damaged or dysfunctional cells in various organisms[188]. Consequently, autophagy deficits are implicated in a variety of age-dependent disorders, e.g., neurodegeneration[189], diabetes mellites (type 2)[190], and cataract formation[191]. As an example, in AD, accumulation of misfolded Amyloid-beta and hyperphosphorylated Tau (pTau) is attributed to deficits in autophagy[192]. It has been demonstrated that abnormalities in autophagy machinery precede the formation of these pathologic aggregates[192,193]. However, autophagy is not a strictly pro-survival mechanism and hyperstimulation of autophagy results in complete cell elimination, a cell-death mechanism called type II programmed cell death[194].

Mechanistically, the process of autophagy is tightly associated with lysosomal metabolism[186]. In short, a portion of cytoplasm including organelles and proteins is isolated with a newly formed membrane called phagophore that results in information of double-membrane vesicle otherwise known as autophagosome. The latter then fuses with lysosome and forms autolysosome which undergoes hydrolytic digestion[195]. Initiation of autophagy is dependent on the activity of the mammalian target of rapamycin (mTOR) kinase[196] or 5' adenosine monophosphate-activated

protein (AMPK) kinase[197]. These kinases have opposite effects on autophagy, with AMPK being a positive[197] and mTOR a negative regulator[196]. Master-regulator kinases trigger the downstream signalling cascade of proteins encoded by autophagy-related (ATG) genes[198]. To date, there have been identified thirty-six ATG proteins, eighteen of which are considered core autophagy machinery[199].

Autophagy is modified in response to various stimuli, e.g., growth factors, hypoxia[185] or oxidative stress[200]. Ans similar to other signalling pathways, several protein-regulators of autophagy are redox-sensitive molecules and therefore are subjects of redox signalling[201]. Trx-1 is implicated in the regulation of autophagy due to its ability to reduce disulfide bonds between oxidized Cysteine residues in proteins.

One such redox-regulated autophagy modulator is mTOR. Exposure to H_2O_2 results in mTOR oxidation at Cys1483 and results in the loss of its activity[202]. Oka et al. showed that knockout of Trx-1 in cardiomyocytes has a similar effect[202,203]. This group is the first to describe the direct interaction between Trx-1 and mTOR that is required for regulation of autophagy.

Normal progression of autophagy also requires interaction of Trx-1 with ATG-7[204]. ATG-7 is an important component of the pathway that contributes to autophagosome biogenesis[185]. Under oxidative conditions, ATG-7 undergoes transnitrosylation by Cys402 through the transfer of NO group from Trx-1 Cys73 with simultaneous dithiol-disulfide exchange[204]. This interaction is crucial for the restoration of ATG-7 enzymatic activity and therefore plays an important role in pro-survival autophagy in ischemic myocardium[204]. Evidence of Trx1 involvement in autophagy regulation has also been shown in human lens epithelial cells by induction of pro-survival

autophagy as shown by increased autophagy turnover (LC III B/A ratio)[205]. An ATG-4 interaction with Trx-1 has also been reported in yeast which is crucial for autophagy progression[206,207]. ATG-4 activity is regulated by the oxidation/reduction of Cys338 and Cys394. Perez-Perez et al. showed that the disulfide bond formed upon oxidation of these Cysteines is a subject of reduction by Trx-1[207]. The role of this interaction in mammalian systems remains to be investigated.

1.5.3.5 Cytoskeleton organization

Cytoskeleton is an intracellular multicomponent structure that determines cell shape and internal compartmentation[208]. In addition to mechanical support, it is involved in vital cellular functions, e.g., cell division or movement[209]. Structurally, the eukaryotic cytoskeleton is a coordination between several classes of filamentous proteins: microtubules, intermediate filaments and microfilaments (**Figure 1.3**)[208]. The ratio of these components as well as subtypes of proteins may vary across different cell types which is determined by functions specific to particular cell types, e.g., neurofilaments in neurons[173,210].

Microtubules are the largest elements of cytoskeleton that consist of protofilaments organized in hollow cylinders[211]. Microtubules facilitate the transport of organelles, e.g., mitochondria, across the cell compartments via interaction with specific transport proteins called dynein and kinesin[212]. The stability of microtubule structure is modulated by Tau proteins[213]. This is specifically relevant to cells with processes, e.g., neurons[214]. Thus, the expression of Tau proteins is significantly higher in neural tissues compared to other organs[213].

Intermediate filaments are rope-like structures characterized by high resistance to tension and compression[215]. They work in tandem with microtubules and provide support by reducing the mechanical impact on rigid and fragile tubulin structures[215]. Intermediate filaments are a heterogenous class of proteins with a number of cell type-specific variants, e.g., glial fibrillary acidic protein in astrocytes[216], neurofilaments light, medium and heavy in neurons[21], keratin in epithelial cells[217], and vimentin in mesenchymal cells[218]. Another subtype of intermediate filaments are nuclear Lamins, proteins involved in the maintenance of the three-dimensional structure of nucleus.[219] The roles of neuronal nuclear lamina and the involvement of Trx-1 in its protection is discussed along with other nuclear functions of Trx-1.

Microfilaments, also known as actin filaments, are assembled from linear polymers of G-actin, one of the most abundantly expressed proteins in eukaryotic cell[220]. These components of the cytoskeleton are flexible and relatively strong[208]. Microfilaments are involved in cellular movement and contractility and hence are highly organized in muscle cells, however in non-muscle cells, actin filaments are less organized and myosin expression is significantly lower[221].

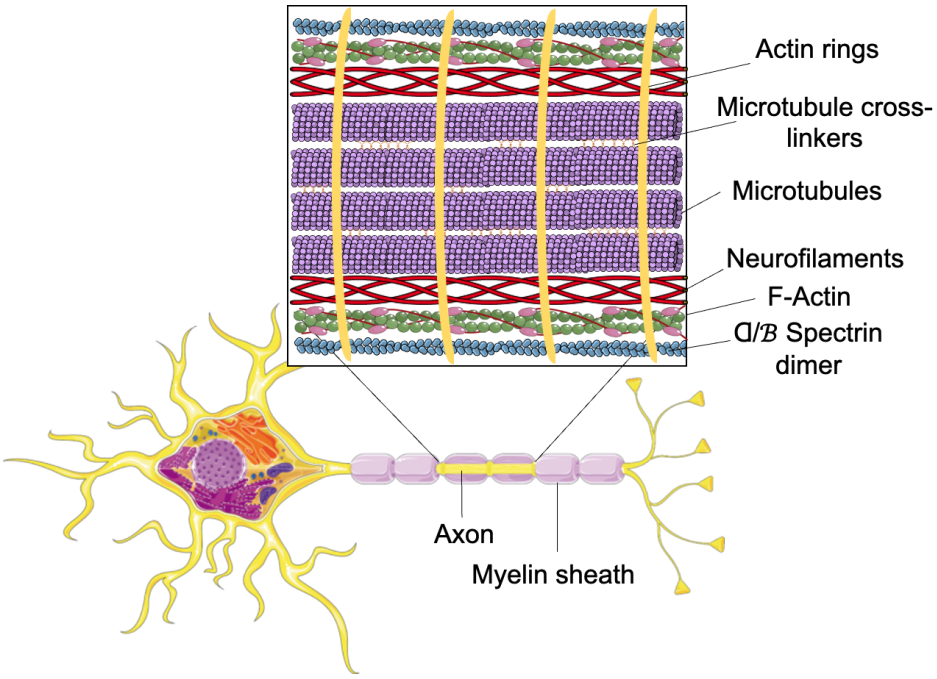

Figure 1.3 A simplified schematic of the axonal cytoskeleton
The axonal core is composed of a bundle of microtubules which are cross-linked by a variety of microtubule-associated proteins which includes Tau and sometimes neurofilaments. This core is surrounded by neurofilaments. The outermost layer has an array of periodically spaced rings composed of F-actin filaments. The actin rings are interconnected by α/β-spectrin tetramers, which are aligned along the axonal axis. F-actin is also localized outside of the acting rings. Image composed of stock templates available at Servier Free Medical Art (https://smart.servier.com/).

Cytoskeletal proteins are sensitive to changes in the redox state. Several studies have shown that redox balance affects cytoskeletal dynamics both *in vitro* and *in vivo* and directly modifies cell morphology[222,223]. For instance, porcupine cornea epithelial cells show signs of microtubule disintegration even after brief exposure to H_2O_2[223]. In this experiment, microtubule disassembly led to prominent changes in cell shape as well as loss of apical barrier junctions and overall barrier integrity of monolayer[223]. However, complete inhibition of ROS is almost as detrimental to cytoskeleton as their overproduction. Thus, suppression of ROS production via pharmacological inhibition of NOX leads to aberrant actin polymerization with consequent retardation of axon sprouting and cell polarization in neurons[224]. Mechanistically, redox regulation of the cytoskeleton

is mediated via Cysteine thiol groups in cytoskeletal proteins. After interaction with ROS, these sites can undergo reversible glutathionylation, nitrosylation and disulfide bond formation[225] or even irreversible carbonylation and sulfenic acid formation[222]. While irreversible changes to cytoskeleton organization are permanent, other modifications can be reversed through Trx[226-228], Grx[229] and Prx systems[230].

Trx-1/TrxR1 system is implicated in redox regulation of the cytoskeleton through interaction with several proteins.

For instance, Trx-1 contributes to the maintenance of microfilament stability by reducing Cys62 in Actin molecule[231]. This physical interaction is crucial for cytoskeleton protection under pro-oxidative conditions. For instance, Wang et al. showed that Trx-1 is capable of maintaining Actin in the reduced state even under severe oxidative distress induced by H_2O_2[231]. Loss of this interaction resulted in disorganization of the actin cytoskeletal system, and decreased cell viability due to apoptosis activation[231].

The role of the Trx-1/TrxR1 system in the redox regulation of microtubules was also demonstrated by Landino et al[226]. This group reported that peroxynitrite-induced disulfides in porcine brain tubulin can be repaired by the Trx-1/TrxR1 system (recombinant human Trx-1 (rhTrx-1), rat liver TrxR1 and NAPDH)[226]. The thiol-disulfide exchange between Trx-1 and Tubulin molecules was confirmed by western blotting[226]. Reduction of Tubulin by Trx-1/TrxR1 system restored normal Tubulin polymerization activity that was lost after peroxynitrite treatment. This suggests that the Trx-1 system is involved in cytoskeleton repair after ROS-induced microtubule disintegration. However, this mechanism remains to be explored using *in vitro* and *in vivo* systems.

1.5.3.6 Interaction with transcription factors

In basal conditions the highest concentrations of Trx-1 are found in the cytoplasm. However, several stressors including oxidative distress, UV radiation, cytokines and lipopolysaccharides induce Trx-1 translocation to the nucleus *in vitro* and *in vivo*[56,232,233]. It is considered a part of the general pro-survival strategy aimed to prioritize the preservation of redox equilibrium in the nucleus by translocating antioxidant molecules from cytoplasm[234]. Accordingly, it has been demonstrated that oxidative stress triggered by nutrient depletion affects cytoplasmic and mitochondrial components more than nuclear[234]. In this condition, cells sacrifice cytoplasmic antioxidant defence to protect the genetic information required to recover organelles and biomolecules damaged by ROS[125,235].

Interestingly, nuclear Trx-1 is functionally autonomous from cytoplasmic Trx-1. While the cytoplasmic function of Trx-1 is mainly mediated via Cysteine reduction in oxidized proteins, its nuclear function is tightly associated with transcription factors, e.g, Redox factor -1 (Ref-1), hypoxia-induced factor-1α (HIF-1α), nuclear factor kappa-light-chain-enhancer of activated B cells (NF- κB), p53, Activator protein (AP-1), Nrf-2, glucocorticoid and estrogen receptors, and others[56,234,236-239].

Nrf-2 is a transcription factor that participates in complex regulatory networks of metabolism, inflammation, autophagy, mitochondrial homeostasis, and proteostasis[240]. In basal conditions, Nrf-2 has predominantly cytoplasmic localization where it exists in association with Kelch-like-ECH-associated protein 1 (KEAP1) and Cullin 3 proteins[241]. These two proteins are responsible for prevention of nuclear translocation of Nrf-2. They mediate ubiquitination of Nrf-2 molecule, its

subsequent proteasomal degradation and recycling[242]. Thus, in normal conditions, half-life of Nrf-2 is only 20 min[243]. However, oxidative stress disrupts the association between Nrf-2 and KEAP1 by oxidation of critical Cysteine residues in KEAP1 molecule[244]. Non-bound Nrf-2 then accumulates in the cytoplasm and translocates to the nucleus. Inside the nucleus, it targets specific to ARE in the upstream promoter region of several pro-survival genes and initiates their transcription[242]. Numerous studies have linked nuclear translocation of Nrf-2 with upregulation of antioxidant proteins (i.e., Trx, Grx, and Prx families), energy metabolism, NADPH synthesis, cell detoxification mechanisms and protein turnover (e.g., p62)[118].

As discussed, Cysteine oxidation is crucial for the regulation of Nrf-2 activity. The dominant role in the maintainance of Nrf-2/KEAP1 association belongs to the GSH family of antioxidants[245]. Downregulation of this redox system has the most significant effect on KEAP1 oxidation (by Cys257, Cys 273, Cys 288, and Cys 287) and subsequent release of Nrf-2[245]. Trx-1 in its turn is crucial for the proper DNA binding of Nrf-2. Thus, it prevents oxidation of critical cysteine residue (Cys506) in DNA-binding domain of Nrf-2[245]. Hansen et al. demonstrated that loss of Trx-1 activity is associated with lower expression of ARE proteins while overexpression of Trx-1 has opposite effects as evidenced by enhanced transcription of target genes[245].

Nuclear Trx-1 is involved in the regulation of AP-1 function via reduction of Cysteine residues crucial for its DNA-binding properties[246]. Overexpression of Trx-1 in COS-7 cells results in potentiation of AP-1 transcriptional activity, while introduction of redox-inactive Trx-1 has an opposite effect[246].

AP-1 is a transcription factor assembled through heterodimerization of c-Fos and c-Jun subunits[247,248]. Similar to other transcription factors, AP-1 is involved in the regulation of various intracellular processes from cell growth and differentiation to apoptosis[249]. AP-1 assembly requires phosphorylation of c-Jun protein by JNK[247]. JNK in its turn functions as a sensor to various stimuli, e.g., oxidative stress, heat, ionizing radiation, DNA damage, cytokines as well as growth factors[250]. Activation of this pathway is reported to have different outcomes for cell survival and metabolism. Thus, an increase in c-Fos and c-Jun expression along with the enhanced transcriptional activity of AP-1 dependent genes is observed in apoptosis[251]. However, the AP-1 function is indispensable for cell proliferation and growth. For instance, AP-1 activity is upregulated upon stimulation with growth factors, e.g., Transforming growth factors alpha and beta[252]. In such conditions, AP-1 upregulates the expression of proliferative markers associated with cell cycle regulation, e.g., Cyclin D1 and E2F[252,253].

Another function of the JNK/AP-1 pathway is regulation of cytoskeleton stability. For instance, both c-Jun and JNK are shown to be activated by microtubule disarray[254,255]. Upon activation, JNK can modify the properties of cytoskeleton components via transcriptional regulation, phosphorylation of Tau, intermediate filaments, and tubulins[256,257]. JNK-mediated Tau phosphorylation at Ser 202/Thr205, Ser 396, and Ser 422 is an early event in Tauopathy, e.g., AD[258-260]. A study by Ruff et al. used a knockout approach to show the roles of cJun and JNK in axonal regeneration[261]. Thus, lack of either cJun or JNK activity in motoneurons resulted in delayed axonal regeneration after axotomy with a significantly decreased number of neurons reconnected with their targets[261]. Consequently, this translated into reduced functional recovery

and significantly decreased signal conductivity[261]. Taken together, JNK/AP-1 axis participates in the sensing of cytoskeletal alterations and provides support in its stabilization after injury.

1.5.3.7 The role of Trx-1 in maintenance of nuclear lamina integrity

Our lab recently reported the involvement of Trx1 in nuclear integrity[176]. Nuclear lamina is a protein network at the interface of the nuclear envelope and chromatin[262,263]. Nuclear lamina is composed of polymerized type V intermediate filaments called Lamins[262]. To date two types of Lamins have been identified: type A and type B[263,264]. Type A includes Lamins A and C which are the products of alternative splicing of a single gene called Lamin A[219]. Due to their similar origin and functions, these two Lamins are often described as a complex named Lamin A/C[265,266]. In contrast, type B Lamins, Lamins B1 and B2 are encoded by different genes[265,267].

Previous studies showed that the composition of nuclear lamina differs in a cell-type specific manner[265,267]. Thus, type B Lamins are expressed in most cell types independently of their differentiation stage, while type A Lamins are restricted to mature cells[219]. Neuronal tissue is almost devoid of Lamin A while both neurons and astrocytes express Lamin C[268]. Type B Lamins are abundantly expressed in neuronal tissues including neurons, astrocytes, microglial cells, and mature and immature oligodendrocytes[268]. It has been shown, that Lamin B1 stability is more important for neuronal nuclear lamina integrity compared to other Lamins[269].

The structure of nuclear lamina dictates its functions. For instance, its mesh-like structure permits the placement of nuclear pores and proteins that link nucleoplasm with cytoplasm[270], e.g., Nesprins

and SAD1/UNC-84 homology (SUN) proteins that associate nuclear lamina with microfilaments and microtubules[271-274] or nuclear envelope transmembrane proteins that penetrate through nuclear lamina to interact with chromatin[275-277]. Lastly, nuclear lamina provides chromatin docking sites required for proper chromatin arrangement during different stages of the cell cycle[270,275]. **Figure 1.4** highlights the structural and functional features of nuclear lamina.

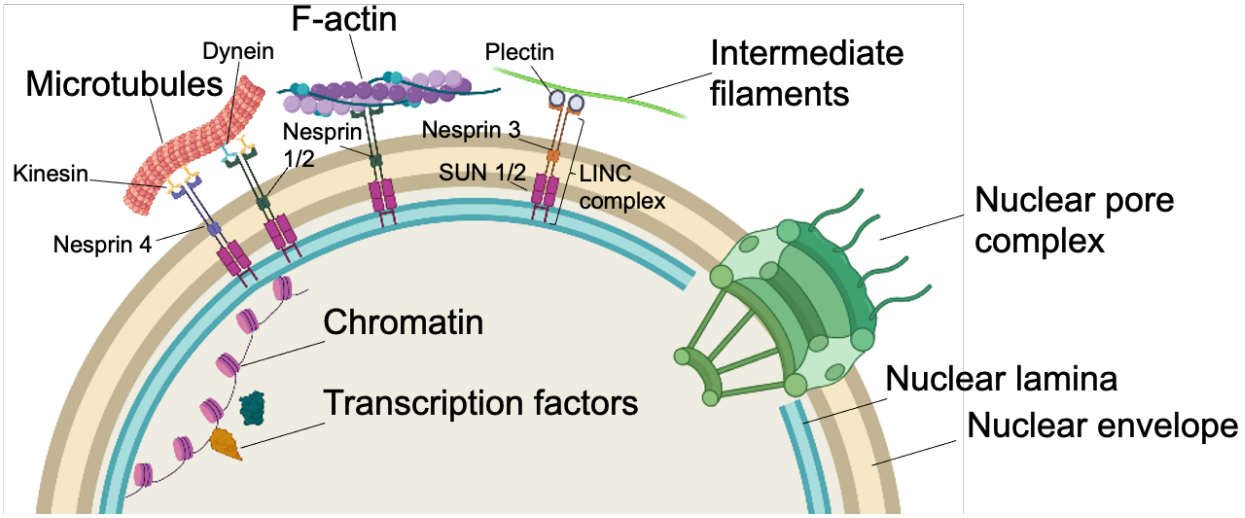

Figure 1.4. Schematic overview of nuclear envelope proteins involved in cytoskeleton/nucleoskeleton coupling
Interaction of cytoskeletal elements (actin filaments, intermediate filaments, microtubules) with nuclear lamina is mediated via Nesprin proteins on the outer nuclear membrane. SUN domain proteins on the internal nuclear membrane connect Nesprins with nuclear lamina. Additional proteins such as Linker of Nucleoskeleton and Cytoskeleton (LINC) complex proteins and lamins are involved in anchoring the nuclei and transmitting forces between the nucleus and cytoskeleton. Image composed of stock templates available at Servier Free Medical Art (https://smart.servier.com/).

The plethora of nuclear lamina functions determines its importance for cellular homeostasis, including embryonic development[278,279] and differentiation[280,281], DNA replication and repair[282,283], cell migration[280,284,285] as well as apoptosis[176,286]. Nuclear lamina disorganization

consequential to mutations of Lamins has been recognized as the main pathological feature of several hereditary diseases called laminopathies such as Emery–Dreifuss muscular dystrophy[287], restrictive dermopathy[288], Charcot-Marie-Tooth disease type 2B[289], Autosomal dominant leukodystrophy[290], Autosomal and premature ageing disorder (Progeria)[282,291]. Additionally, laminopathy is involved in the pathophysiology of AD[292,293], PD[294], cancers[284,295-297], ageing[298-301], etc.

The role of Trx-1 system in maintenance of nuclear lamina integrity was previously shown by Islam et.al[176]. This work highlights the antiapoptotic properties of Trx-1. Specifically, it shows that Trx-1 is indispensable for the prevention of Caspase-6 activation[176]. Nuclear Lamins are the subjects of Caspase-6 mediated cleavage, which results in nuclear lamina damage and subsequent imbalance in its functions, e.g., gene expression or transport between cytoplasm and nucleoplasm[176]. Trx-1 depletion and Caspase-6-mediated nuclear lamina damage are also found in post-mortem samples from AD patients as well as a classic mouse model of this neurodegenerative disorder, 3xTg mice[292,293].

The regulatory functions of Trx-1 are listed in **Table 1.3.**

Table 1.3 Trx-1 mediated redox regulation

Subcellular localization	Cell Function	Target	Cell type	Reference
Cytoplasm	***Antioxidative defence***	Oxidized proteins	All	Bertini et al.[127], Ueno et al.[302], Liu et al.[303], Hwang et al.[304], Akterin et al.[305], Nakamura et al.[140], Tao et

				al.[132], Arner et al.[116]
	Apoptosis	ASK-1	Mv1Lu (Mink Lung Epithelial Cells), L929 (mouse fibroblast cell line) and 293 (mouse fibroblast cell line)	Saitoh et al.[306]
		MST-1	MEF (murine embrionic fibroblasts)	Chae et al.[184]
		Casp-6	SH-SY5Y (human neuroblastoma cells)	Islam et al.[176]
		Casp-3	Jurkat (immortalized human T-lymphocytes)	Mitchell et al.[177]
	Autophagy	mTOR	Rat cardiomyocytes	Oka et al.[307]
		ATG7	Rat cardiomyocytes	Nagarajan et al.[204]
		ATG4	Yeast Saccharomyces cerevisiae	Perez et al.[207]
		LC III-B	HLE-B3 (human lens epithelial cells)	Hu et al.[205]
	Cytoskeleton organization	Actin	SH-SY5Y (human neuroblastoma cells)	Wang et al.[231]
		Tubulin	Purified porcine tubulin	Landino et al.[226]
		CRMP-2	Embryonic DRG neurons from Sprague-Dawley rats	Morinaka et al.[308]
		NGF	PC-12 (adrenal phaeochromocytoma cells)	Bai et al.[309]
	Signalling transduction	AKT and PTEN	Neuroblastic neoplasms, and neuroblastoma cells lines	Sartelet et al.[310]

	Inflammation	Monocyte chemoattractant protein-1 (MCP-1)	Trx-1 Overexpressing/ knockdown EA.hy 926 and bovine aortic endothelial cells	Chen et al.[311]
	Immunomodulatory	Regulatory T-cells	Tregs (regulatory T-lymphocytes)	Mougiakakos et al.[126]
Nucleus	***Gene regulation***	NFκ-B, AP-1, and Ref-1	L929 (mouse fibroblast cell line), HeLa (cervical cancer cells) COS-7 (African green monkey kidney fibroblast-like cells)	Chen et al.[311], Schenk et al.[236]
		HIF-1α	HeLa (cervical cancer cells)	Naranjo-Suarez et al.[312]
		Oct-4	Embryonic stem cells	Guo et al.[313]
		HDAC4	Cardiac myocytes	Ago et al.[314]
	DNA-bindning	NRF-2	HeLa (cervical cancer cells)	Hansen et al.[245]
	Transportation to nucleus	Glucocorticoid receptor	COS7 and CV-1 (African green monkey kidney fibroblast-like cells), HeLa (cervical cancer cells)	Makino et al.[239]
		Estrogen receptor	MCF-7 (breast cancer cells)	Rao et al.[315]
Cell membrane	***Immunomodulatory***	Complement deposition	HUVEC (human umbilical vein endothelial cells)	King et al.[316]
Extracellular matrix	***Chemokine-like***	Chemoattraction	human monocytes, PMNs, leucocytes	Bertini et al.[127], Nordberg et al.[317]

1.5.4 Neuron-specific functions of Trx-1

Aside from the previously discussed general cytoprotective effects of the Trx-1 system, it has specific functions in specialized cells. The neuron-specific functions of Trx-1 have been demonstrated in several *in vitro* and *in vivo* studies. This chapter focuses on the regulation of functions specific to neuronal cells by Trx-1.

1.5.4.1 The role of Trx-1 in neuronal differentiation

The regulatory role of Trx-1 has been shown through potentiating the effect of the nerve growth factor (NGF) which is crucial for neuronal development, survival, and function[318]. In cholinergic neurons, NGF additionally enhances Trx-1 mRNA and protein expression via CREB causing nuclear translocation of Trx-1 with subsequent transcriptional effects mediated through Nrf-2 and AP-1[319].

Administration of exogenous Trx-1 is also beneficial in cases of neurodegenerative, ischemic, and chronic stress conditions, promoting neuronal regeneration and speeding up recovery[320-322]. Tian et al. investigated the role of Trx-1 in ischemia-induced hippocampal neurogenesis by subjecting adult mice to bilateral common carotid artery occlusion and rhTrx-1 administration before reperfusion[322]. The rhTrx-1 treated mice had enhanced neuronal proliferation and differentiation in their dentate gyrus. Functionally, rhTrx-1 treated animals recovered faster compared to non-treated controls as shown by their better performance in the Morris water maze and probe trail test. The authors associated the pro-neurogenic effect of Trx-1 with the activation of extracellular signal-regulated kinases 1 and 2 (ERK 1/2) pathway as demonstrated by enhanced ERK 1/2 phosphorylation after rhTrx-1 administration[322].

Another study showed the role of Trx-1 in recovery from chronic stress[321]. They subjected adult mice to 14 consecutive days of restraint stress. Neural progenitor cells (NPCs) isolated from the dentate gyrus of these animals were treated with rhTrx-1. Such treatment increased the number of proliferating cells as well as the total count of Tuj+ neurons indicating increased neurogenesis. Mechanistically, these changes were linked to an increase in phospho-ERK1/2, and nuclear β-catenin. Interestingly, the treatment also increased the expression of β2-adrenergic receptors (β2-AR). The possible role of Trx-1 and β2-AR interaction was investigated by the introduction of butaxamine, a selective β2-AR inhibitor, into the rhTrx-1-treated NPC culture. Such conditions abolished rhTrx-1-induced hippocampal neurogenesis suggesting the physiological effect of this interaction in chronic stress recovery.[321]

1.5.4.2 Trx-1 in axonogenesis and regeneration

Axon sprouting, elongation and establishing synaptic connections are crucial events in the establishment of neuronal functions. In addition to its functions in modulation of cytoskeletal proteins, Trx-1 is shown to have a specific role in regulation of axonal development and regeneration.

Trx-1 is involved in regulation of axon elongation through redox control over Semaforin 3A (Sema 3A)/Collapsin response mediator 2 (CRMP2) pathway. Sema 3A is a signalling molecule involved in the inhibition of axonal growth by repulsive guidance of growth cones[323].

Trx-1 is also shown to participate in NGF-mediated stimulation of neurite outgrowth. Bai et al. investigated the impact of Trx-1 on neurite outgrowth in PC12 cells[309]. In this work, the downregulation of Trx-1 activity resulted in the abolishment of NGF signalling and consequent suppression of neurite elongation in these cells[309].

An indispensable role for Trx-1 in axonal regeneration has been suggested in an *ex-vivo* model of axotomized DRG neurons with peripheral nerve attached. Inhibition of Trx-1 retrograde axonal transport using Cyclopentenone prostaglandins administration in medium halted axonal growth from the transected nerve[324]. This study highlights the indispensable role of Trx-1 in the regulation of axonal regeneration in traumatic condition[324].

Further evidence of Trx-1 protective role for axons in inflammatory conditions is suggested by its ability to prevent optic nerve degeneration in a model of intravitreal administration of TNF-α. The degenerative effect of TNF-α was mitigated by rhTrx-1 through inhibition of inflammatory cytokines such as IL-1b[325].

1.5.4.3 Trx-1 functions in synaptic terminals

Signal transmission is a unique feature of neuronal cells facilitated in synaptic terminals of axons and dendrites. Synapse homeostasis is impaired in various neurological disorders including epilepsy, autism spectrum disorder, schizophrenia, bipolar disorder, and dementia[326].

To date, the role of the Trx-1/TrxR1 system in synaptic function remains to be the subject of detailed investigation. Available data suggest the possible implication of this antioxidant system

in the regulation of synaptic function ant the neuromuscular junction. Stemme et al. and LoPachin et al. showed evidence of anterograde and retrograde axonal transport of Trx-1 and TrxR1 in stressed rat sciatic nerves[327,328]. According to the authors, this transport may be important for thiol reactions required for modulation of synaptic functions, e.g., membrane pore formation via regulation of redox state in Cysteines that modulate regulatory proteins[328]. These findings are indirectly supported by the evidence of high sensitivity of synaptic processes to modifications in nucleophilic sulfhydryl groups by different electrophilic neurotoxicants, e.g., methylmercury or acrylamide[327].

Pirazzini et al. discovered that both Trx-1 and TrxR1 are present on synaptic vesicles[329]. Their work suggested that the Trx-1/TrxR1 thiol reduction system is involved in the reduction of interchain disulfides in botulinum toxin serotypes A, C, and E. Inhibition of Trx-1/TrxR1 system prevented paralysis of impulse transmission in neuromuscular junction upon exposure to botulinum toxin. This study proposed inhibitors of the Trx-1/TrxR1 system as effective and non-toxic candidates for preventive and therapeutic medication for human botulism[329]. The involvement of Trx-1 in the redox regulation of other synaptic proteins remains to be investigated.

1.5.4.4 Dysregulation of Trx-1 system in neurological diseases

The evidence of dysregulation of Trx-1 system in neurological disease is shown by numerous studies. The findings are summarized in **Table 1.4**.

Table 1.5.4.4 The status of Trx-1 in neurological diseases

Neurological disease	Sample type	Cell type	Trx-1 expression	Reference
Alzheimer's disease	Brain (post-mortem)	Neurons (frontal cortex, hippocampus, amygdala)	↓	Lovell et al.[76], Akterin et al.[305]
	Brain (post-mortem)	Astrocytes in white matter	↑	Asahina et al.[330]
	Blood and CNS from AD patients		↑	Arodin et al.[331]
Amyotrophic lateral sclerosis	Spinal cord (post-mortem)		↑ (mRNA)	Malaspina et al.[332]
Multiple sclerosis	Blood and CSF from MS patients		↑	Pennisi et al.[333]
Huntington's disease	Blood from HD patients	Erythrocytes	↓	Sánchez-López et al.[334]
Schizophrenia	Schizophrenia	Plasma	↑	Zhang et al.[335], Owe-Larsson et al.[336]
Autism spectrum disorder	Blood from ASD patients	Blood from ASD patients	↑	Zhang et al.[337]
Bipolar disorder	Blood from patients with BD (maniac phase)		↓	Genc et al.[338]

↑ - upregulated, ↓ - downregulated

The role of Trx-1 is most studied in context of AD. In post-mortem brain samples of AD patients, decrease in Trx-1 content coincides with accumulation of Amyloid-ß aggregates[76,233,339]. Decrease in Trx-1 expression in these samples is observed in brain regions primarily affected in AD, i.e., CA1 of hippocampus and frontal cortex[305]. SH-SY5Y cells treated with Amyloid-ß exhibit early time-dependent oxidation of Trx-1 molecule, while overexpression of Trx-1 rescues these cultures

from Amyloid-ß toxicity[76,340]. Guo et al. showed that overexpression of Trx-1 in diabetic mice with AD-like pathology reverses activation of hippocampal neurodegeneration and apoptosis as well as improves spatial learning and memory[341]. Data from our laboratory demonstrates that downregulation of Trx-1 in SH-SY5Y cells leads to activation of caspase-6 mediated nuclear lamina cleavage[176], a common finding is post-mortem AD samples[292,293].

Less is known about the role of Trx-1 system in the etiology and pathogenesis of ALS. Mitchell et al. discovered mutations of TrxR1 gene in several cases of familial ALS. These mutations were associated with early-onset and more severe course of the disease[107]. This study highlights the importance of Trx-1 system and thiol-redox regulation in the pathogenesis of ALS. However, the matter of mutations in Trx-1 gene and their relation to ALS pathology remains to be investigated.

1.6 Hypothesis and Research objectives

Rationale: Impaired redox regulation is a well-established component of neurodegenerative diseases. Neurons are comparatively more sensitive to oxidative stress. Neuronal homeostasis heavily relies on cellular antioxidant systems. Dysregulation of Trx-1 system is a common finding in post-mortem samples of various neurologic disorders. Reports from several research groups including ours have demonstrated the detrimental neurodegeneration-relevant effect of Trx-1 depletion in neuronal cells. Despite extensive *in vitro* data that proves the importance of Trx-1 system for neuronal homeostasis, there is no animal model of neuron-specific Trx-1 knockout.

The overall goal of my M.Sc. thesis is to explore the effect of neuron-specific Trx-1 depletion in rodents and to investigate whether the outcomes of this mutation have neurodegeneration-specific features.

Hypothesis: Trx-1 neuronal depletion is sufficient for induction of neurodegenerative changes associated with these diseases.

Specific research aims:

Aim 1) Characterization of molecular and histological changes associated with Trx-1 depletion in neurons.

Aim 2) To investigate the histopathological changes associated with neuronal Trx-1 depletion in glial cells.

2. Materials and Methods

2.1 Generation and maintenance of Trx-nKO mice colony

Generation of Trx-nKO mice was performed by Dr. Peter F Vitiello's laboratory (University of Oklahoma, Oklahoma City, USA).

To generate mice with conditional neuron-specific deletion of Trx-1, gRNA sequences were selected based on the distance to the modification site and predicted off-target profile. gRNAs were designed to insert loxP sequences into Trx-1 at intron 1 (5'-ACTCACGCTGGAGGCCAACATGG-3') and downstream of the 3' UTR (5'-

GAAATACAATGTCCCACTCCAGG-3') with the PAM sequence underlined. A surveyor assay (Transgenomic North America, Omaha NE) using N2A cells transfected with Trx-1 gRNAs cloned into the Cas-9 co-expression vector pBT-U6-Cas9-2A-GFP confirmed NHEJ frequencies of 14.8% and 22% for Trx1 5' and 3' gRNAs respectively. Homology-directed repair occurred following the injection of guide RNA molecules and qualified Cas-9 mRNA into the cytoplasm of C57Bl/6 embryos which were implanted into surrogate CD1 mice (Applied StemCell, Milpitas CA). Floxed Trx-1 mice (Trx-1 fl/fl) were bred with Syn1-Cre^{pos} (strain 003966) mice with C57BL/6J background obtained from The Jackson Laboratory (Bar Harbor ME) which express Cre recombinase under the expression of the rat Synapsin 1 (Syn-1) promoter for neuron-targeted recombination[342]. Syn-1 is a neuronal phosphoprotein located on the cytoplasmic surface of synaptic vesicles[343]. Syn-1 expression is restricted to neuronal cells and is identified in excitatory and inhibitory neurons in CNS and PNS, as well as bipolar and horizontal cells in retina[344]. It is also detected in neuroendocrine cells of the gastrointestinal tract and Leydig cells in testes[344]. Syn-1 expression in CNS is detectable at E12[345].

The Syn-Cre^{pos} mice were crossed with Trx-1$^{fl/fl}$ to produce Trx-1$^{fl/WT}$Syn-Cre^{pos} female mice. The latter was crossed back with Trx-1$^{fl/fl}$ Syn-Cre^{neg} male to generate Trx-1$^{fl/fl}$ Syn-Cre^{pos} animal (further referred as Trx-nKO). Usage of Syn-Cre^{pos} male breeders was avoided to prevent Cre recombination in testes[346]. Trx-1$^{fl/WT}$Syn-Cre^{neg} littermates were used as controls in all the experiments.

Mice were maintained under standard housing conditions with a 12-hour light/dark cycle. Water and food were provided ad libitum. All the experiments were conducted under the protocols

approved by the Sanford Research Institutional Animal Care and Use Committee (protocol number 142-03-21E) and the University of Manitoba Animal Care Committee (protocol number 19-036). Sanford Research has an Animal Welfare Assurance on file with the Office of Laboratory Animal Welfare (A-4568-01) and is a licensed research facility under the authority of the United States Department of Agriculture (46-R-0011). All animal experiments at the University of Manitoba Animal Care Facility were performed in accordance with the Canadian Council on Animal Care guidelines and policies.

Animal subjects were deeply anesthetized with Isoflurane (20% v/v Isoflurane in propylene glycol) and euthanized by cervical dislocation at defined time points or when morbidity parameters were apparent (acute loss of body condition, impairment of mobility influencing feeding/drinking).

The significantly reduced lifespan of Trx-nKO mice (mean lifespan of 58 days) dictated the **time points** for our studies. Thus, we used 4 weeks (adolescents) and 8 weeks old (young adult) mice for our experimental purposes (behavioral and physical assessments, western blotting, immunohistochemistry (IHC), and enzymatic assays. The investigator was blind to the genotype of animals.

2.2 Genotyping procedures

DNA digestion was performed by boiling ear punches in lysis buffer (25mM NaOH, pH 12) for 1 hour and subsequent addition of neutralization buffer (40mM Tris-HCl, pH 5). Next, 5µl of obtained genomic DNA was mixed with 20µl of MasterMix (2.5 µl of ThermoPol Reaction buffer (New England BioLabs #B9004S), 0.5µl of dNTP mix (New England BioLabs #N0447S), 0.5µl

of forward primer, 0.5µl of reverse primer (manufactured by IDT), 0.125µl of TaqDNA Polymerase (New England BioLabs #M0267L), 15.875 of µl RNAse-free water) in DNAse/RNAse free PCR tubes. In this study two sets of primers were used: 1) for Trx-1 flox genotyping: mTrx-1 3'LoxP forward sequence (CCA CTT TAT GTG GTT GCT TTG GA; Tm: 55.9°C) and mTrx-1 3'LoxP reverse sequence (TCT GGG GCC AAA GGT TCA AAT CCC A; Tm: 62.8°C); 2) for Syn-Cre genotyping: Syn-Cre forward sequence (GCC TGC ATT ACC GGT CGA TGC AAC GA; Tm: 65°C) and Syn-Cre reverse sequence (GTG GCA GAT GGC GCG GCA ACA CCA TT; Tm: 67.8°C). The samples were then subjected to PCR in Thermocycler (Bio-Rad MyCycler 563BR) with the following settings: cover: 103°C; volume: 25µl; 35 thermocycles (95°C for 3 min, 95°C for 15s, 62°C for the 30s, 72°C for 45°C, 72°C for 5 min) and final dwell temperature 4°C (forever). Following the PCR, 4µl of 6x DNA loading dye (ThermoFisher #R0611) was added to each tube and 20µl of each sample was loaded in 3% agarose (ThermoFisher #BP160-500) gel with RedSafe™ Nucleic Acid Staining Solution (Intron Biotechnology #21141), 5µl of 100 bp DNA ladder (Gene Dire X #DM001-R500) were loaded for reference. The gel was electrophoresed in Horizontal Electrophoresis System (BioRad) in TAE buffer (pH 8.3). Trx-1 flox bands were detected at 473 and 513 bp for Trx-1 wild-type and Trx-1 flox respectively. Syn-Cre band was observed at 726 bp.

2.3 Trx-nKO phenotype characterization

To provide a complete assessment of the Trx-nKO phenotype, we investigated several morphological parameters.

2.3.1 Body weight

Body weight was monitored weekly starting from week 6. The results are reported for males and females combined with no regard to sex-dependent differences in body weight.

2.3.2 Hindlimb circumference

To examine the differences in muscle mass, I measured the circumference of two hindlimb segments. Femoral circumference was measured at the point equally distanced from femoral and knee joints perpendicularly to the femur axis. Tibial circumference was measured at the point equally distanced from the knee and ankle joint perpendicularly to the tibial axis[347].

2.3.3 Racine scale for seizure activity assessment

Seizure activity was assessed using modified Racine scoring[348]. Animals were observed daily from 4 weeks of age till death (approximately 8-9 weeks). The most severe seizure episode was used for scoring **(Table 2.1).**

Table 2.1 Modified Racine scale for seizure scoring

Grade	Behavioral stage
1	Stiffness and rigid posture
2	Head nodding
3	Partial forelimb clonus
4	Continuous severe whole-body seizure
5	Falling, forelimb clonus, jumping (general motor convulsions)

2.4 Tissue collection and processing

Mice were deeply anesthetized in a glass drop jar with Isoflurane (20% v/v Isoflurane in propylene glycol). When used for IHC, mice were perfused transcardially with cold phosphate-buffered saline (PBS) (pH 7.4) followed by cold 4% paraformaldehyde. Brains, spinal cords, and sciatic nerves were further dissected and immersed in 4% paraformaldehyde at 4˚C overnight and then cryoprotected by gradually increasing concentrations of sucrose (10% and 20% respectively). Tissues were then embedded in OCT and stored at -80°C for further use. Tissue blocks were serially sectioned (thickness 20 μm) using a cryotome (Leica CM 3050 S) and mounted on Superfrost Plus microscope slides (FisherBrand). Obtained slides were either immediately used for staining or stored at -80°C.

For Lamin B1 staining, not fixed tissues were directly embedded in OCT, snap-frozen on dry ice, serially sectioned, and post-fixed in ice-cold 100% Methanol (12 min for brains, 8 min for spinal cords) followed by permeabilization in cold Acetone (3 brief dips).

Protein extraction for western blot was performed on snap-frozen brain tissue using lysis buffer containing 50mM Tris-HCl (pH 8.0), 150 mM NaCl, 5 mM EDTA, 1% v/v NP-40, 1x Halt™ Protease and Phosphatase inhibitor (ThermoFisher #78442). Tissues were first mechanically homogenized with a handheld tissue homogenizer and then sonicated (3 x 10s) on ice. Samples were then centrifuged at 16,200 g for 30 min at 4°C. Supernatants were subjected to protein estimation by Bradford protein assay (bovine serum albumin (BSA) was used as standard) and immediately used for the preparation of western blot samples. Western blot samples of equal protein concentration were prepared with the addition of Laemli loading buffer and subsequent denaturation at 95°C for 10 min.

For cell fractionation, brain cortex tissue was first mechanically homogenized in cytosolic buffer (20mM HEPES (pH 7.4), 250mM sucrose, 10mM KCl, 1.5mM EDTA, 1mM EGTA, 1x Halt™ Protease and Phosphatase inhibitor (ThermoFisher #78442) and then centrifuged at 1000g for 30 min at 4°C. The supernatant was collected as the cytosolic fraction. Pellet was further washed with cytosolic buffer and centrifuged at 1000g two times to remove residing cytoplasmic proteins. Next, the pellet was resuspended in RIPA buffer (50mM Tris HCl (pH 8.0), 150mM NaCl, 1mM EGTA, 1% NP-40, 0.1% SDS, 1% Triton X-100, 5% glycerol, 1x Halt™ Protease and Phosphatase inhibitor (ThermoFisher #78442) and then sonicated (3 x 10s) followed by 1-hour centrifugation at 21,000 g at 4°C. Obtained supernatants were collected as the nuclear fraction. Both protein fractions were then subjected to Bradford assay and boiled for 10 min after the addition of Laemli buffer.

2.5 Immunohistochemistry

Sections (thickness 20 μm; block advance 100 μm) were defrosted at room temperature for 5 min and then rehydrated with phosphate-buffered saline for 1 min. Next, sections were permeabilized and blocked in 0.3% Triton X-100, 10% v/v normal goat serum, 0.5% BSA, and 0.3% glycine in phosphate-buffered saline for 2 hours at room temperature in a humidified chamber. Sections were incubated with primary antibody (**Table 2.3**) solution diluted in PBS containing 0.01% Triton X-100, 5% goat serum, and 0.01% BSA overnight at 4°C. The following day, sections were washed in PBS three times and incubated with Alexa-Fluor-tagged secondary antibodies in PBS containing 1% goat serum for 2 hours. The sections were then washed with PBS three times and incubated

with DAPI (1:50,000 in PBS) for 8 minutes for nuclear counterstain. Lastly, the slides were coverslipped with Mowiol and dried in dark chambers overnight at room temperature.

To perform spinal cord diameter measurements, 20 μm sections distanced 200μm from each other obtained from the lumbar spinal cord (starting from the level of L1) were stained with hematoxylin and eosin according to routine staining procedures. Sections were first fixed in 50% ethanol and then stained in fresh hematoxylin solution for 3 min followed by 10 min wash in double distilled water. Next, they were immersed in eosin for 1 min and washed with 95% and 100% ethanol two times each. Sections were then cleared in two changes of Xylene and coverslipped with Permount. Slides were dried in a fume hood overnight at room temperature.

FluoroJade C staining was performed using the kit supplied by Biosensis. Double labelling was done in accordance with the protocol provided by the manufacturer. The sections were first stained with NeuN primary and AlexaFluor 568 secondary antibodies as described previously. Next, the slides were dried in the oven (at 55°C for 40 min) and incubated with FluoroJade C solution (1:10,000) for 20 min. The slides were then washed with double distilled water three times and stained with DAPI (1:50,000 in PBS) for 10 min. Slides were then dried on a slide warmer at 50-60°C for at least 5 min, cleared by brief immersion (3 min) in xylene in the dark, and coverslipped with Permount.

2.6 Image acquisition and quantitative analysis

Images were acquired with Carl Zeiss LSM 7.0 confocal laser scanning microscope, Carl Zeiss Axio Observer 2.1 and Carl Zeiss Axio Imager M2 LED, and Leica Aperio VERSA digital slide scanner (Buffalo Grove IL) fluorescence microscopes using 2.5x, 10x, 20x, 40x and 63x (oil) objectives. Identical acquisition parameters were used for all sections within a single set of experiments. The region of interest was first localized using low magnification and then images were acquired using high magnification (40x or 63x, oil). Image analysis was performed on 3-4 serial sections per animal.

Spinal cord diameter was measured with ZEN Blue software using the circumference tool. Measurements from equal distances from L1 were compared between Trx-nKO and Cntl mice.

Corpus Callosum thickness was measured in two specific areas, i.e., body and lateral parts. For this purpose, obtained image of the corpus callosum was divided into 4 equal parts. Measurements from the median (body) and equally distanced lines from the left and right hemispheres were taken for further analysis (**Figure 2.1**).

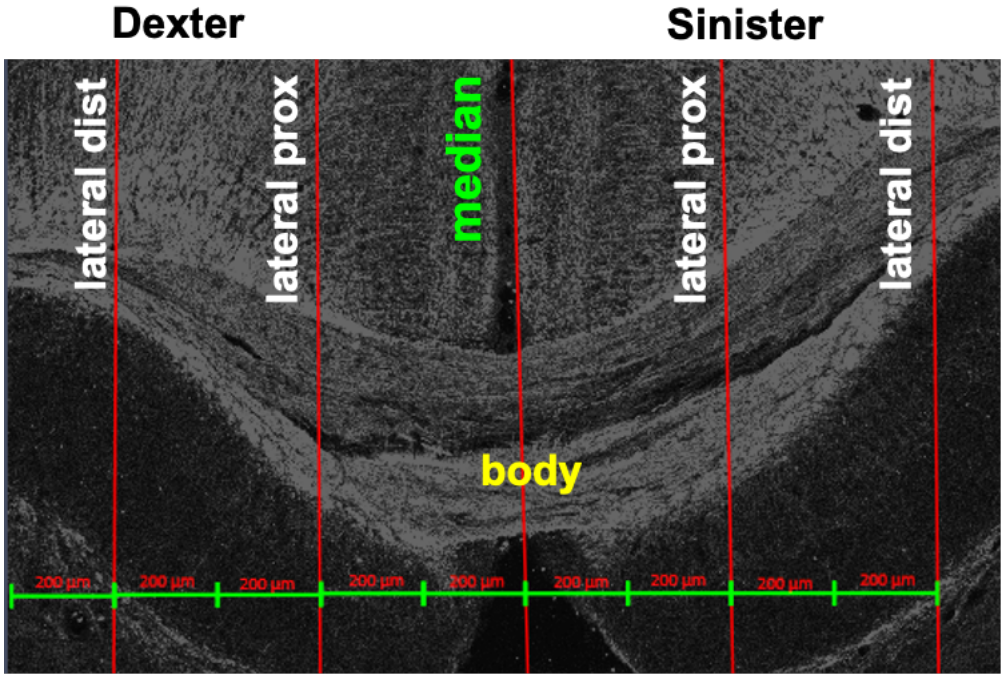

Figure 2.1 Quantification of corpus callosum thickness

ImageJ program (Cell Counter plugin by Kurt De Vos, University of Sheffield) was used for cell type quantifications. The number of cells in 1 mm^2 was counted and the average per mouse was represented.

Axon Ferret diameter was measured using the ImageJ program as described by Dolapchieva et al[349]. First, an equal Threshold was applied to the images to remove the background. Then we used the "Analyze particles" tool in ImageJ to estimate the Ferret diameter of axons. The measurement was performed on 4 sections per animal distanced 100 µm from each other, the average per animal is represented.

The Myelination index (overlap coefficient between MBP and NFH signals) was estimated using the ImageJ Colocalization Finder plugin by Christophe Laummonerie and Jerome Mutterer, CNRS, Strasbourg, France. The colocalization coefficient was measured between the axon-specific protein NFH and myelin-spicific protein MBP[350,351].

To determine the degree of nuclear lamina invaginations, we created a scale based on analysis of over 100 nuclei imaged from both Trx-nKO and Cntl cortex sections. The scale included 4 degrees of nuclear lamina damage: 0 – no obvious changes in nuclear lamina structure; 1 – minor invaginations that do not affect circularity of nuclear lamina; 2 – medium invaginations less than ½ of nuclear diameter in length that moderately affect nuclear circularity; 3 deep nuclear invaginations, folds, ruptures more that ½ of nuclear diameter in length, deformed nuclei (**Table 2.2**). The high-magnification confocal images acquired from similar areas of the brain cortex and spinal cord grey were used for quantification in accordance with the scale described above.

Table 2.2 Nuclear lamina structure scale

0 – no invagination	1 – minor invagination(s)	2 – medium invagination(s)	3 – severe invagination(s)
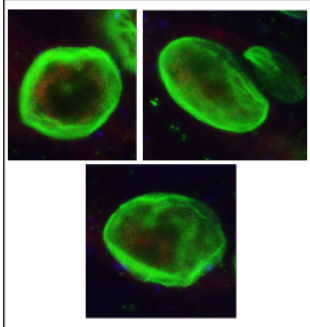	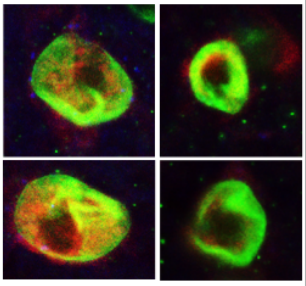	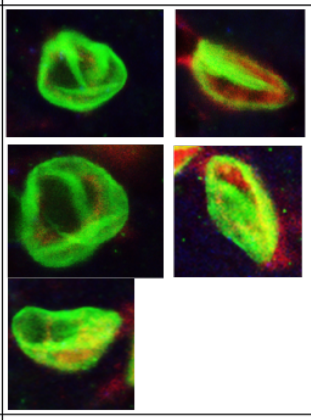	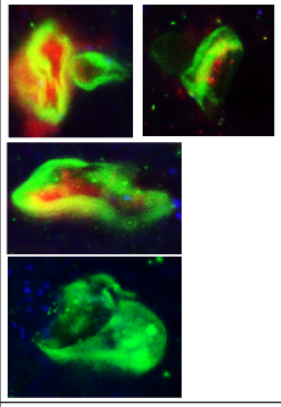
Circular shape No visible folds	Circular shape No deep folds	Minor loss of circularity Folds no more than ½ diameter of nuclei Multiple folds Long folds that cover the whole surface	Major loss of circularity Folds more than ½ diameter of nuclei Multiple deep folds Nuclear lamina rupture

TDP-43 intracellular compartmentation was estimated using the ImageJ Colocalization Finder plugin by Christophe Laummonerie and Jerome Mutterer, CNRS, Strasbourg, France. The colocalization coefficient was measured between the TDP-43 signal and the nucleus (DAPI).

2.7 Western Blot

The same volume of samples was loaded in SDS-PAGE gel (15% gel for Trx-1; 13% gel for MBP, Iba1; 12% gel for pTDP-43, JNK 1/2, pJNK 1/2, AT8, AT180, pTau (Ser 296); 10% gel for MAG, GFAP), electrophoresed (BioRad MiniProtean Tetra System) and transferred into methanol-activated PVDF membrane using semi-dry quick-transfer method (BioRad Trans-Blot Turbo 690BR; BioRad Trans-Blot Turbo RTA Mini 0.2 µm PVDF Transfer Kit #170472). Membranes were blocked by 5% skim milk or 5% BSA (for detection of phosphorylated proteins) in TBST for

1-2 hours and incubated in primary antibodies (**Table 2.3**) diluted in 1% skim milk or 1% BSA respectively overnight at 4°C with constant agitation. The following day, membranes were washed with TBST 3 times 6 minutes each and incubated with secondary HRP-conjugated antibody diluted in 1% skim milk for 2 hours with constant agitation at room temperature. After washes, ECL (BioRad Clarity Western ECL Substrate #1705061) was used to detect the protein band signal through Micro-Chemi 4.2 (DNR Bio-Imaging Systems). The membranes were then incubated with GAPDH HRP-conjugated antibody (loading control) for 3 hours at room temperature. ImageJ was used for semi-quantitative analysis of protein bands.

To detect protein carbonylation in cortex tissue, we used the OxiBlot kit supplied by Cell Biolabs, INC (#STA-308). in accordance with the manufacturer's recommendations. Regular western blot samples were subjected to electrophoresis in 13% SDS-PAGE gel. After the regular gel transfer procedure, the membrane was immersed in 100% methanol for 15s and then dried for 5 min at room temperature. Next, the membrane was equilibrated in TBS containing 20% Methanol for 5 min followed by a 5 min wash in 2N HCl solution. The membrane was then incubated with Dinitrophenylhydrazine (DNP) (diluted in 2N HCl) for exactly 5 min, washed with 2N HCl 3 times (5 min each), and blocked in 5% skim milk for 1 hour. Subsequent steps included incubation with primary anti-DNP antibody, secondary HRP-conjugated antibody, and image acquisition as described above.

Table 2.3. List of antibodies used in experiments

Procedure	Antigen	Source	Manufacturer	Catalog number	Concentration
Western blot	GFAP	Mouse	Sigma Aldrich	G3893	1:1000
	Lamin A/C	Mouse	Santa Cruz	SC-376248	1:1000
	MAG	Mouse	Santa Cruz	SC-166849	1:1000
	MBP	Rabbit	Sigma Aldrich	G3893	1:1000
	pTDP-43	Rabbit	Proteintech	80007-1-RR	1:1000
	Trx-1 (mouse-specific)	Mouse	IMCO	ATRX-06	1:1000
	TrxR1	Mouse	Santa Cruz	SC-28321	1:1000
	Iba1	Rabbit	FUJIFILM Wako Pure Chemical Corporation	019-19741	1:1000
	TNF-α	Rabbit	Cell Signalling Technology	3707	1:1000
	JNK 1/2	Mouse	Santa Cruz	SC-7345	1:1000
	pJNK 1/2	Mouse	Santa Cruz	SC-6254	1:1000
	AT8	Rabbit	Invitrogen	MN1020B	1:1000
	AT180	Rabbit	Invitrogen	MN1040	1:1000
	PFH-1	Mouse	Santa Cruz	SC-32279	1:1000
	tTau 46	Mouse	Santa Cruz	SC-K0518	1:1000
	pH2.AX	Rabbit	Cell Signalling Technology	2577	1:1000
	GAPDH HRP-conjugated	Mouse	Santa Cruz	SC-166574	1:4000
	Mouse HRP-conjugated	Goat	Thermofisher Scientific	31430	1:2500
	Rabbit HRP-conjugated	Goat	Cell Signalling Technology	7074S	1:2500
IHC	ChAT	Goat	Sigma Aldrich	AB144P	1:200
	GFAP	Mouse	Sigma Aldrich	G3893	1:200
	Iba1	Rabbit	FUJIFILM Wako Pure Chemical Corporation	019-19741	1:200
	Lamin B1	Rabbit	Abcam	ab16048	1:200
	MBP	Rat	Sigma Millipore	MAB386	1:200
	NeuN	Mouse	Sigma Aldrich	MAB377	1:200
	NFH	Mouse	Sigma Aldrich	N0142	1:200
	TDP-43	Rabbit	Cell Signalling Technology	3448S	1:200
	Trx-1	Rabbit	Cell Signalling Technology	2429S	1:200
	Alexa Fluor 647-conjugated anti-rabbit	Goat	Invitrogen	A21244	1:500
	Alexa Fluor 647-conjugated anti-mouse	Goat	Invitrogen	A21236	1:500
	Alexa Fluor 647-conjugated anti-goat	Donkey	Invitrogen	A21447	1:500
	Alexa Fluor 568-conjugated anti-rat	Goat	Invitrogen	A11077	1:500
	Alexa Fluor 568-conjugated anti-rabbit	Goat	Invitrogen	A11036	1:500
	Alexa Fluor 568-conjugated anti-mouse	Goat	Invitrogen	A11031	1:500

2.8 Trx-1 activity assay

Snap-frozen mouse brain tissues were dissolved in 50mM MES lysis buffer (50mM MES, 250mM NaCl, 2mM EDTA), pH 6.5 with Halt™ Protease and Phosphatase inhibitor (ThermoFisher #78442). Tissues were first mechanically homogenized with a handheld tissue homogenizer and then sonicated (3 x 10s) on ice. Samples were then centrifuged at 16,200 g for 30 min at 4°C. Supernatants were subjected to protein estimation by Bradford protein assay (BSA was used as

standard). Trx1 activity was determined by using the FKTRX-02-V2 kit (IMCO Corporation Ltd AB) as described by Islam et al.[176] following the manufacturer's protocols.

In brief, 10 µg of protein was incubated with β-NADPH and TrxR at 37 °C for 30 min. Then, 20 µl of Eosin-labeled insulin was added to the reaction mixture and further incubated for 5 min. The fluorescence was measured kinetically at excitation 520 nm and emission 545 nm wavelengths using Synergy H1 Hybrid microplate reader (BioTek Instruments, USA). Trx-1 specific activity was calculated as follows: Trx-1 specific activity = [Absorbance/min(V_{max})]/mg protein.

2.9 Behavioral assessments

Behavior testing was performed during the daytime (10 a.m. – 2 p.m.) under dim light conditions. Both male and female mice were used in experiments and the ages were as follows: 4 weeks old mice (adolescents) for hindlimb clasping, RotaRod, sensory-motor, gate, ledge, and Y-Maze tests; 8 weeks old mice (young adults) for hindlimb clasping, RotaRod, sensory-motor, gate, ledge, Y-Maze and novel object recognition tests. To reduce the impact of stress on behavioral outcomes, we started with less stressful tests and continued to perform other tests as follows: Y-Maze, NOR, sensory-motor, gate, ledge, RotaRod, and hindlimb clasping tests. To minimize anxiety-like behavior, mice were allowed to acclimate to the test room for at least 1 hour before each test. Indirect low lightning was used during our assessments to prevent the stress of white light in mice. Temperature and humidity were similar to housing conditions. All mice were previously habituated to handling by the investigator. The video camera was placed directly overhead of the apparatuses

to provide an optimal view of exploration. After behavioral assessments, mice were used in other experiments (IHC, western blotting, etc.).

2.9.1 Hindlimb clasping test

Mouse was gently grasped by the base of the tail and lifted to clear off all surrounding objects. Hindlimb position was observed for 10s. If the hindlimbs were consistently extended away from the abdomen, a mouse received a score of 0. Score 1 was assigned if one of the hindlimbs was retracted toward the abdomen for more than ½ of the time observed. If both hindlimbs were partially retracted toward the abdomen for more than ½ of the time observed, a mouse received a score of 2. If the hindlimbs were completely retracted to the abdomen and were touching, a mouse was assigned a score of 3. Mouse was returned to the home cage after testing.

2.9.2 RotaRod

Mice were removed from their home cage and placed on the rod (diameter 5 cm; with non-slip coating) rotating with increasing speed from 5 to 40 rpm for 5 min. Each mouse was subjected to 3 trials. The time mouse remained on the rod was recorded for each trial. If a mouse spent 5 min on RotaRod without falling, it was removed from the apparatus by the investigator and received a maximum score (300s). The apparatus was cleaned with 70% ethanol and wiped dry after each mouse. The results are represented with latency to fall (time elapsed on RotaRod averaged for 3 three trials).

2.9.3 Sensory-motor test ("adhesive removal" test)

Three-four mm square pieces of laboratory tape were applied on either forelimb in random order. Equal pressure applied to stick a tape was maintained among all the animals tested. Mouse was then placed in a transparent cage under video registration. The time when the animal first noticed the tape (touch) was recorded as a sensory component, and the time elapsed from first touch to complete removal was registered as a motor component. The maximum time allowed for either component was the 30s. The cage was cleaned with 70% ethanol and wiped dry after each mouse.

2.9.4 Novel object recognition test

Two pairs of mouse-size (or slightly larger) objects with a similar degree of complexity (texture, color pattern, and brightness) made of non-breakable material were selected. For the main arena, we used a square chamber (40cm x 40 cm x 40 cm) made from white non-porous plastic. Mice were trained two days prior to test. On the first training day, mice were allowed to explore the empty arena for 5 min. On the second training day, two identical objects were placed in opposite quadrants of the arena. Mouse was returned to the home cage after 5 min of exploration. The test was performed 4 hours after training. One of the objects was replaced by a novel object of a different shape and color. Mouse was allowed to freely explore for 10 min. The first 5 min of recorded exploration were scored, however, if the mouse did not meet the minimum exploration time of the 20s for both objects, scoring was continued past 5 min until the total exploration time exceeded 20s. The arena was cleaned with 70% ethanol and wiped dry after each mouse. Discrimination and preference indexes were calculated as follows: Discrimination index = [(Time

spent exploring novel object) – (Time spent exploring familiar object)] / [Total exploration time]; Preference index (%) = [(Time spent exploring novel object) / (Total exploration time)] x 100.

2.9.5 Y-Maze

The white non-porous plastic maze consisted of three arms (length 35cm; width 4 cm; height 15 cm). Each of the three arms was extended from the center at 120° angles. To reduce anxiety-like behavior, mice were habituated to the maze for 5 min 3 days before testing. On the day of the experiment, mice were removed from their home cage, placed in the middle of the maze, and allowed to freely explore for 5 min under video registration. The maze was cleaned with 70% ethanol and wiped dry after each mouse. The spontaneous alternation was calculated as follows: Spontaneous alternation (%) = [(number of spontaneous alternations) / (total number of arm entries – 2)] x100.

2.10 Mouse magnetic resonance imaging (MRI)

8 weeks old Trx-nKO (n=4) and Cntl (n=3) mice were used for MRI experiments using MRS PET/MRI Scanner (MR S3000 – MRSPET802, MR Solutions Ltd.). Experiments were conducted under general anesthesia (1-2% Isoflurane, 0.8-1.0 L/min O_2), and mice were restrained. The mice were placed in an MR-compatible cradle and inserted in an MR probe. The brain was localized and imaged with a 17-cm bore. T2-weighted images were acquired with the following parameters: FOV 30 × 30 mm, matrix 256 × 238, slice thickness 0.3 mm, TR 5,000 ms, and TR 45 ms. Two averages were acquired. Measurements were performed in Weasis v4.03 software using the

Polygon measurement tool. For better visualization of high-density (e.g., corpus callosum) vs low-density (e.g., brain ventricles) structures Cardiac filter was applied.

2.11 Statistical analysis

Statistical analysis was performed using GraphPad Prism 9.0 software. Results are represented as means of ±SEM. Student's t-test and two-way ANOVA with multiple comparisons and Tukey's posthoc corrections were used for comparisons between groups. Statistical significance was defined as $P \leq 0.04$.

3. Results

3.1 Confirmation of Trx-1 neuron-specific knockout

Knowing the role of Trx-1 in neuronal homeostasis, I aimed to investigate the functional, histopathological, and molecular outcomes of neuron-specific Trx-1 knockout in mice.

Developmental depletion of neuronal Trx-1 in mice was performed by Dr. Peter Vitiello (The University of Oklahoma Health Sciences Center) using Cre-LoxP recombination. Trx-$1^{fl/fl}$ was crossed with Synapsin-1 Cre (Syn-Cre) animal (C57B/L background) as shown in **Fig. 3.1A**. Trx-$1^{fl/fl}$ Syn-Cre^{pos} animal is further referred to as **Trx-nKO**. Trx-$1^{fl/WT}$ Syn-Cre^{neg} heterozygous mice were used as controls (Cntl). The representative genotyping procedure is shown in **Fig. 3.1B**.

To confirm the Trx-1 knockout, I performed confirmatory western blotting on cortex tissue homogenates derived from animals of 4 and 8 weeks of age (**Fig. 3.1 C** & **D**). Significant decrease (~60%) in Trx-1 expression was observed at both time points. Residual expression of Trx-1 is attributed to other cells present in neural tissue (e.g., astrocytes, oligodendrocytes, immune cells, etc.). Further confirmation of Trx1 deficiency was assessed by measurement of Trx-1-like Insulin reducing activity, which was also significantly decreased in Trx-nKO cortices at 8 weeks of age (**Fig. 3.1 E**). Immunohistochemical examination of Trx-1 expression in Trx-nKO CNS tissues showed a prominent decrease in Trx-1 signal in cortices, dentate gyri, and lumbar spinal cord grey. However, there was no statistically significant decrease in CA1 of the hippocampus (**Fig. 3.1 F, G**).

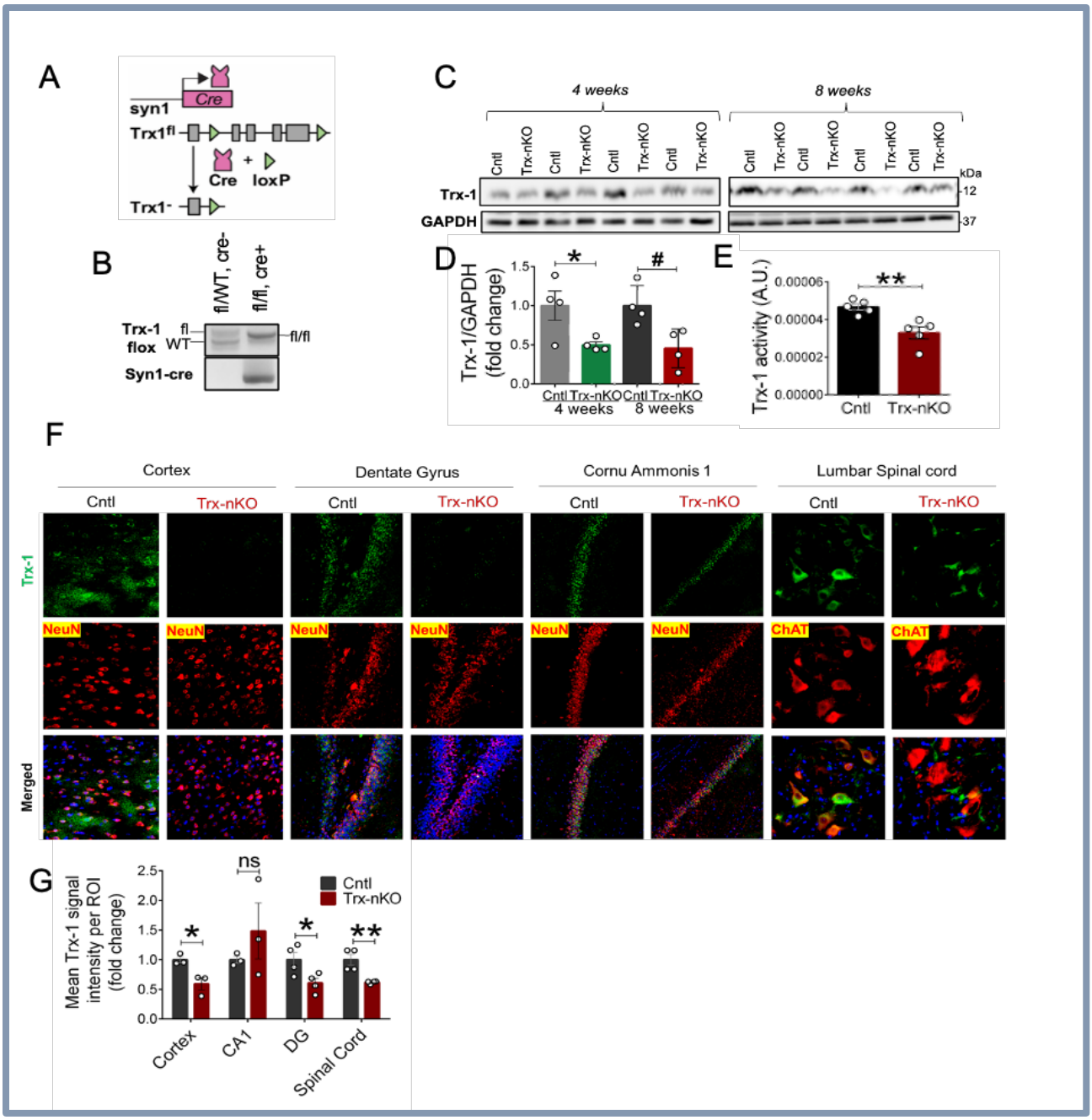

Figure 3.1 Generation and confirmation of Trx-1 neuron-specific knockout in mice

A. Schematic represents the Cre-recombination approach used for the excision of the Trx-1 gene in neurons.

B. Representative Trx-nKO mice genotyping. For Trx-1 gene, the top band represents floxed allele, the bottom band stands for wild type Trx-1. Heterozygous (Trx-1 fl/WT) and homozygous (Trx-1 fl/fl) animal subjects are shown. Syn-Cre band represents the presence of Cre recombinase in the genome.

C. Confirmatory western blot performed on cortical tissues derived from 4- and 8-week-old animals depicts Trx-1 protein levels.
D. Semiquantitative densitometry shows a **significant reduction in Trx-1 protein content at both 4- and 8- weeks of age**. n=4, males and females. Protein level is normalized to loading control (GAPDH) and expressed in fold change to control. Statistical analysis: Student t-test, the graph shows Mean ±SEM, * and # $p<0.04$.
E. Trx-1-like activity is significantly reduced in Trx-nKO cortices at 8 weeks. n=5, males and females. Statistical analysis: Student t-test, the graph shows Mean ±SEM. **$p<0.01$
F. Immunohistochemical characterization of Synapsin-Cre mediated Trx-1 knockout shows **differential efficacy of Trx-1 downregulation across different CNS regions** (no prominent decrease was observed in CA1 of the hippocampus). n=4, males and females, 8 weeks.
G. Quantification performed on images acquired from Trx-nKO and Cntl brains and lumbar spinal cords shows a significant reduction in Trx-1 signal intensity in Trx-nKO cortices, DG and spinal cords but not in CA1. Quantification was performed on 3 images acquired from 3 equally distanced sections (block advance 100 μm) per animal. The graph depicts the mean signal intensity in fold change to control. n=4, 8 weeks, males and females. Statistical analysis: Student t-test, the graph shows Mean ±SEM, *$p<0.04$, **$p<0.01$, ns - not significant.

3.2 Phenotypical characterization of Trx-nKO mice

Global Trx-1 knockout results in death at early stages of embryonic development[352]. Rodents with organ-specific depletion of Trx-1 in heart[353], liver[354] and lung[355] have significantly reduced lifespan with prominent functional deficits. Similarly, Trx-nKO mice have significantly shortened lifespan (mean lifespan of 58 days) as depicted in **Fig. 3.2A**. These animals develop a significant reduction in body weight by 6 weeks of age (**Fig. 3.2 B**) and exhibit reduced muscular mass as evidenced by hindlimb circumference measurements (**Fig. 3.2 C**). Trx-nKOs are prone to handling-induced seizures with onset at 7 weeks of age. These seizures first appear as nodding and partial forelimb clonus and freezing and then develop into generalized convulsions and jumping (**Fig. 3.2 D**).

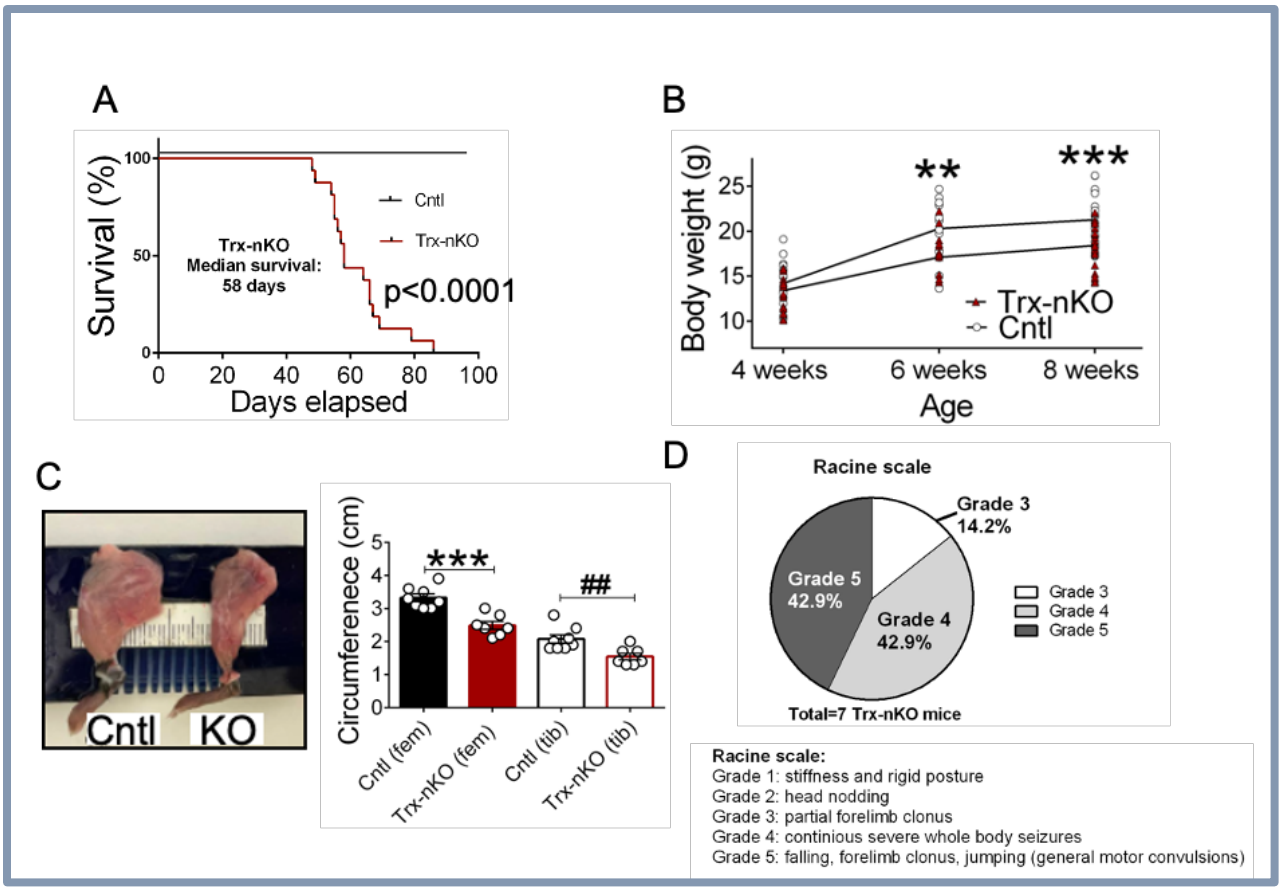

Figure 3.2 Phenotypical characterization of Trx-nKO mice

A. Trx-nKO mice have a significantly reduced lifespan, median survival of 58 days. n=16, males and females. Statistical analysis: Log-rank (Mantel-Cox) test.
B. Significant reduction in body weight is observed from week 6 for both sexes. n=16, males and females. Student t-test, the graph shows Mean ±SEM, **p<0.01, ***p<0.001.
C. Significant decrease in the femoral and tibial diameter of the hindlimb is observed at 8 weeks of age. Measurements were performed at the point equally distanced from joins (femoral and knee or knee and ankle respectively), perpendicularly to the bone axis. n=7, males and females. Statistical analysis: Student t-test, the graph shows Mean ±SEM, ##p<0.01, ***p<0.001.
D. The pie chart depicts the **Racine seizure severity scale in Trx-nKO mice**. Mice were observed daily and habituated to handling starting from week 4. Seizure occurrence and type were recorded. The most severe episode is used for analysis per each animal subject. n=7, males and females.
Racine scale: Grade 1: stiffness and rigid posture; Grade 2: head nodding; Grade 3: partial forelimb clonus: Grade 4: continuous severe whole-body seizure; Grade 5: falling, forelimb clonus, jumping (general motor convulsions).

3.3 Sensory and motor behavioural assessments reveal severe motor deficits in Trx-nKO mice.

Behavioural assessment highlights the prominent **motor dysfunction** in these animals. The mice demonstrate a significantly higher incidence of hindlimb clasping at 4 and 8 weeks of age (**Fig 3.3 A**). Hindlimb clasping is used as an indication of neurodegeneration and is often observed in other murine models of neurodegeneration[356]. Motor impairment is also highlighted by poor performance in the Rotarod test observed at both 4 and 8 weeks of age (**Fig. 3.3 B**). Discrepancies in sensory and motor functions of the CNS are illustrated by the increased time required to perform sensory and motor components of the "sticky tape" sensory-motor test at both time points (**Fig. 3.3 C**).

To our surprise, the two-month-old mice showed no significant deficits in cognitive tests as assessed by novel object recognition (**Fig. 3.3 D**) and Y-maze behavioural tests (**Fig. 3.3 E**). The Trx-nKO animals did not show any differential preference for novel objects and behaved similarly in the Y-maze test that assesses their willingness to explore new environments. However, the total number of entries in Y-maze arms was significantly decreased in Trx-nKOs (**Fig. 3.3 E)** which might be associated with the observed motor deficits or ataxia and higher susceptibility to stress. Normal cognitive function of Trx-nKO shown by behavioral testing might be associated with the heterogenous efficacy of Trx-1 depletion in the hippocampus of these animals (previously shown in **Fig. 3.1 F**), the center of memory formation and maintenance.

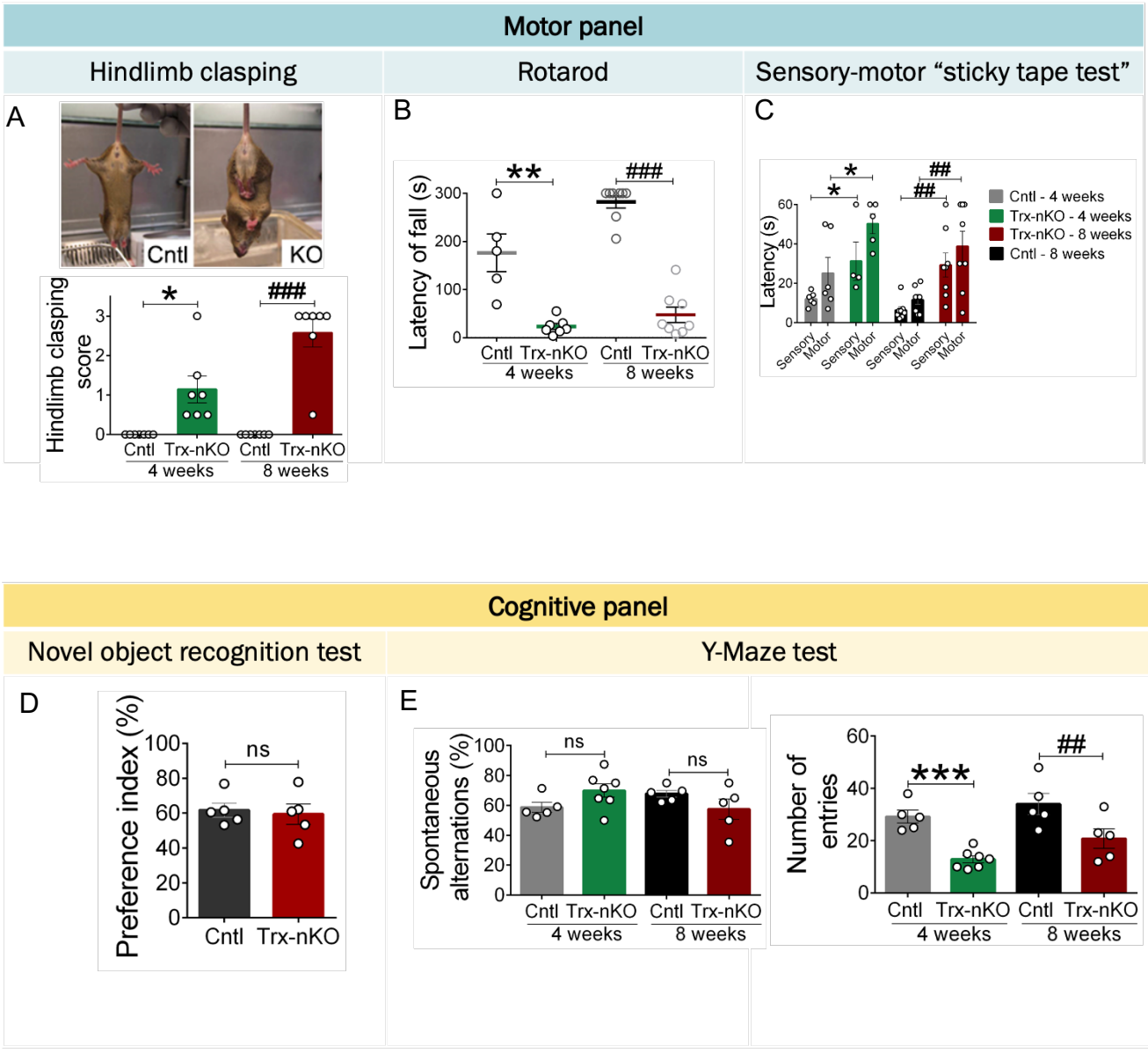

Figure 3.3 Behavioral assessments reveal severe motor deficits in Trx-nKO mice

Motor panel:

A. Trx-nKO mice exhibit classic signs of motor dysfunction depicted by the hindlimb clasping test. n=6 – 4 weeks, males and females; n=7 – 8 weeks, males and females. Statistical analysis: Student t-test, the graph shows Mean ±SEM, *p<0.04, ###p<0.001.

B. Trx-nKO mice fail to perform the Rotarod challenge at both 4 and 8 weeks of age. n=8, males and females. Statistical analysis: Student t-test, the graph shows Mean ±SEM, **p<0.01, ###p<0.001.

C. Both sensory and motor components of the sensory-motor ("sticky tape") test are affected in Trx-nKO animals. Significant increase in time elapsed before sensing and complete removal of a

tape stuck to the animal's forelimb is observed at both 4 and 8 weeks of age. n=6 – 4 weeks, n=8 – 8 weeks, males and females. Student t-test, the graph shows Mean ±SEM, *p<0.04, ##p<0.01.

Cognitive panel:
D. Trx-nKO mice do not show any deviations in short-term memory compared to healthy littermates as shown by the novel object recognition test (NOR). No significant difference is observed in the novel object preference index. n=5 – 8 weeks, males and females. Student t-test, the graph shows Mean ±SEM, ns – not significant.
E. No significant difference is observed in patterns of exploratory behavior as evidenced by % of spontaneous alternations in the Y-maze test. An overall decrease in motor activity is illustrated by a significantly reduced total number of entries in Y-maze arms at both 4 and 8 weeks of age. n=7 – 4 weeks, n=5 – 8 weeks, males and females. Student t-test, the graph shows Mean ±SEM, ***p<0.001, ##p<0.01, ns – not significant.

3.4 Trx-1 neuronal knockout results in changes in CNS morphology and cellular organization

Trx-nKOs demonstrate a slight but significant reduction in whole brain size as evidenced by MRI measurements (**Fig. 3.4 A**). Significant differences are also observed in the cerebellum size but not in the cortex or hippocampus. A significant decrease in Trx-nKO spinal cord diameter is observed by serial tissue sectioning starting from vertebra L1 with subsequent H&E staining and quantification (**Fig. 3.4 B**). I further asked if these changes are associated with a decrease in the number of neurons. Although, the neuronal count did not reveal a decrease in NeuN-positive (marker of mature neurons) neurons in cortex (**Fig. 3.4 C, D**), a significant reduction of motoneurons was observed in the lumbar spinal cord grey matter (**Fig. 3.4 C, E)**. Western blotting also did not show any significant decrease in the expression of NenN protein in Trx-nKO cortices (**Fig. 3.4 F, G**). Evidence of decreased synaptic density was detected by a significant decrease in the expression of synaptic marker PSD95 protein by western blotting, indicating possible neurodegenerative changes in these mice (**Fig. 3.4 F, H**).

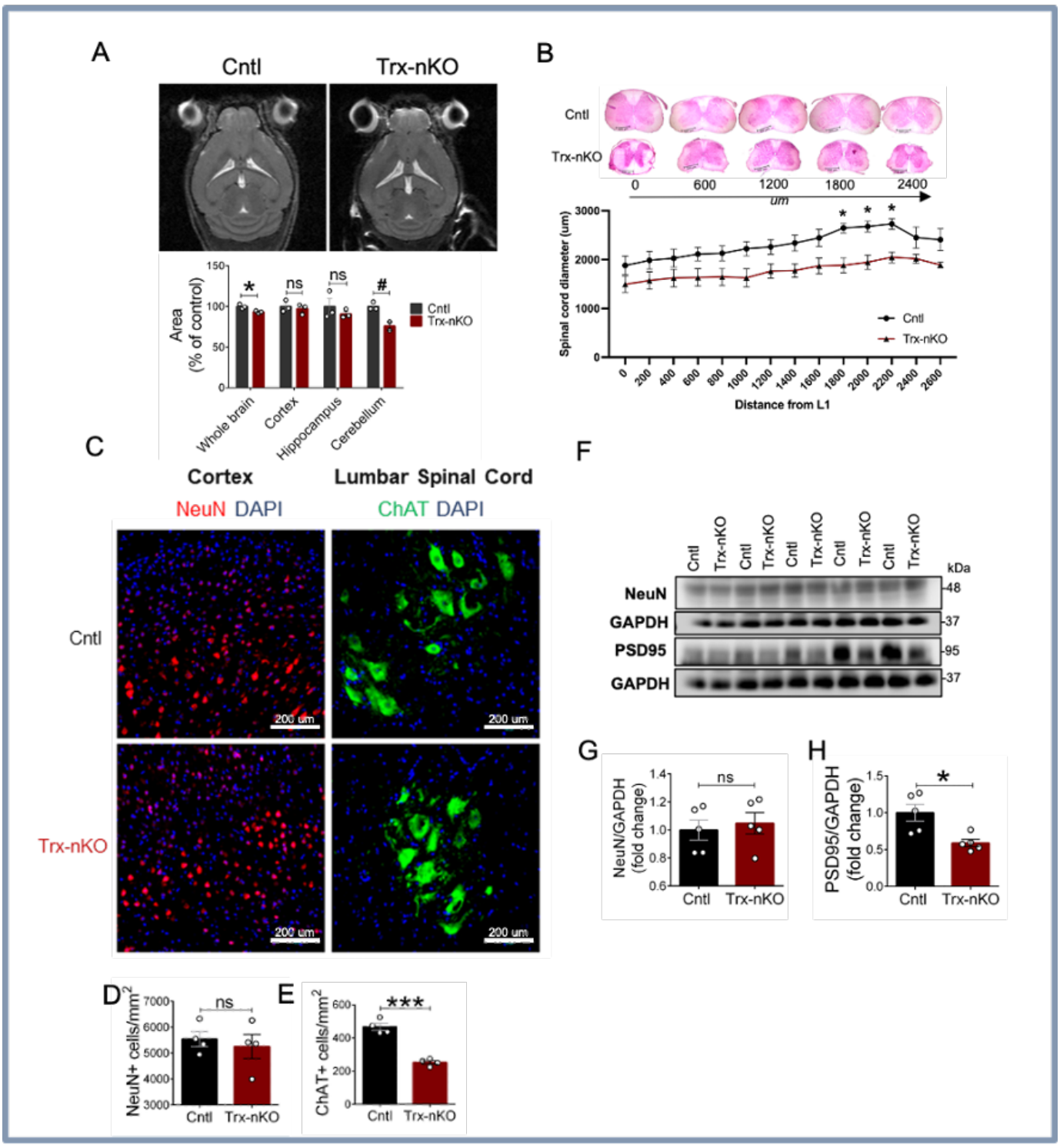

Figure 3.4 Trx-1 neuronal knockout results in changes in CNS morphology and cytoarchitectonics

A. Coronal T2-weighted sections acquired with magnetic resonance imaging compare brain morphology of Trx-nKOs with Cntls. Measurements of the whole brain and specific brain regions

(cortex, hippocampus, cerebellum) were performed with Weasis DICOM medical viewer. **A slight but significant reduction is detected in the whole brain area and cerebellum. No significant difference in hippocampal and cortical areas.** n=3, 8 weeks, males and females. Statistical analysis: Student t-test, graph compares the measurements obtained from Trx-nKOs with Cntls, values are expressed in % of control (Mean ±SEM), * and # $p<0.04$, ns – not significant.

B. A significant reduction in Trx-nKO spinal cord diameter is observed in the lumbar region. Serial sectioning starting from the L1 vertebra was performed on PFA-fixed spinal cords. Sections distanced 200 μm from each other were stained with H&E and used for measurements. n=4, 8 weeks, males and females. Statistical analysis: Student t-test, the graph shows Mean ±SEM, *$p<0.04$.

C. Immunofluorescent staining of the cortex and lumbar spinal cord with neuron-specific markers (NeuN – mature neurons in the cortex; ChAT – motor neurons in spinal cords).

D. Neuronal count performed on images acquired from the cortex show no significant difference between Trx-nKOs and Cntls. Quantification was performed on 3 images acquired from 3 equally distanced images (block advance 100 μm) per animal. The graph depicts the number of NeuN+ cells per 1 mm^2. n=4, 8 weeks, males and females. Statistical analysis: Student t-test, the graph shows Mean ±SEM, ns – not significant.

E. Quantification performed on images acquired from lumbar spinal cord grey matter shows a significant reduction in the number of motoneurons in Trx-nKO. Quantification was performed on 3 images acquired from 3 equally distanced images (block advance 100 μm) per animal. The graph depicts the number of ChAT+ cells per 1 mm^2. n=4, 8 weeks, males and females. Statistical analysis: Student t-test, the graph shows Mean ±SEM, ns - not significant.

F. Western blot performed on cortex tissue homogenates demonstrate the levels of NeuN (a marker of mature neurons) and PSD95 (synaptic marker).

G. Semiquantitative densitometry shows no significant difference in NeuN protein content in cortices between Trx-nKO and Cntl groups. Protein level is normalized to loading control (GAPDH) and expressed in fold change to control. n=4, 8 weeks, males and females. Statistical analysis: Student t-test, the graph shows Mean ±SEM, ns – not significant.

H. Semiquantitative densitometry shows a significant decrease in PSD95 protein content in cortices of Trx-nKOs compared to Cntls. Protein level is normalized to loading control (GAPDH) and expressed in fold change to control. n=4, 8 weeks, males and females. Statistical analysis: Student t-test, the graph shows Mean ±SEM, *$p<0.04$.

3.5 Trx-1 knockout in neurons is associated with white matter deficits

Axonal dieback is an important component in pathophysiology of degenerative, inflammatory and traumatic neurological diseases[357]. In neurodegeneration, axonal damage is often linked to severe

oxidative distress[357]. This is explained by high susceptibility of cytoskeletal proteins to oxidation by ROS[358]. Thus, enhanced oxidation of cytoskeletal proteins in neurons leads to irreversible modification of their mechanical properties, e.g., changes in rigidity, elasticity, and extent of polymerization[358]. Knowing the contribution of Trx-1 to disulfide homeostasis in cytoskeletal proteins[231], I investigated the impact of Trx-nKO on white matter.

Filtered T2 weighted coronal sections acquired with MRI showed a significant reduction in corpus callosum area in Trx-nKOs compared to Cntls (**Fig. 3.5 A**). Histological assessment of the major white matter pathways (**Fig. 3.5 B)** showed profound deficits in axonal morphology and quantity. Indicating that Trx-nKOs have significantly thinner corpus callosum (**Fig. 3.5 C**), a significantly lower number of neurons in dorsal spinal cord white matter (**Fig. 3.5 D**), with significantly reduced axon diameter in dorsal spinal cord and sciatic nerve (**Fig. 3.5 E**). Of note, to assess the myelination efficiency, the signal intensity of neurofilament was divided by MBP staining and presented as NFH/MBP ratio[350,351]. My assessment suggests no apparent differences in myelination between the Trx-nKO mice and their wildtype littermates. (**Fig. 3.5 F**).

Discrepancies in axonal structure in Trx-nKOs are associated with decreased myelin content as evidenced by quantitative western blotting (**Fig. 3.5 G, H, I**). Thus, I detected almost a 50% reduction in myelin basic protein (MBP) and myelin-associated glycoprotein (MAG).

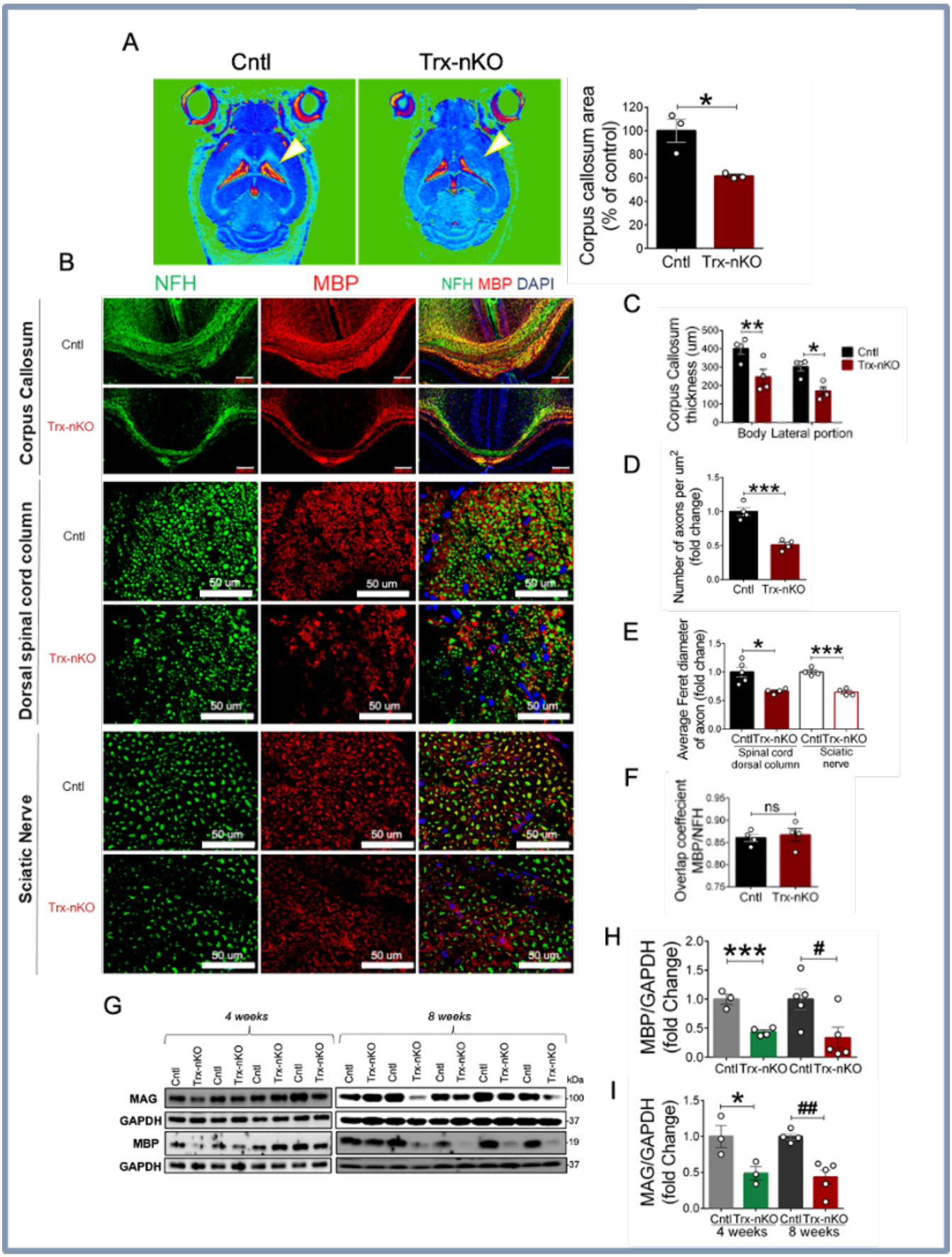
A
Cntl
Trx-nKO
Corpus callosum area (% of control)
120
100
80
60
40
20
0
*
Cntl
Trx-nKO
B
NFH
MBP
NFH MBP DAPI
Corpus Callosum
Dorsal spinal cord column
Sciatic Nerve
Cntl
Trx-nKO
50 um
C
Corpus Callosum thickness (um)
500
400
300
200
100
0
**
*
Cntl
Trx-nKO
Body
Lateral portion
D
Number of axons per um2 (fold change)
1.5
1.0
0.5
0.0
***
Cntl
Trx-nKO
E
Average Feret diameter of axon (fold chane)
1.5
1.0
0.5
0.0
*
***
Cntl
Trx-nKO
Cntl
Trx-nKO
Spinal cord dorsal column
Sciatic nerve
F
Overlap coeffecient MBP/NFH
0.95
0.90
0.85
0.80
0.75
ns
Cntl
Trx-nKO
G
4 weeks
8 weeks
Cntl
Trx-nKO
kDa
MAG
GAPDH
MBP
GAPDH
100
37
19
37
H
MBP/GAPDH (fold Change)
2.0
1.5
1.0
0.5
0.0
***
#
Cntl
Trx-nKO
Cntl
Trx-nKO
I
MAG/GAPDH (fold Change)
1.5
1.0
0.5
0.0
*
##
Cntl
Trx-nKO
Cntl
Trx-nKO
4 weeks
8 weeks

Figure 3.5 Trx-1 knockout in neurons is associated with white matter deficits

A. Significant reduction in Trx-nKO corpus callosum area. Filtered (red – low density (liquid), blue – high density) coronal T2-weighted sections acquired with magnetic resonance imaging compare brain morphology of Trx-nKOs versus Cntls[359]. Measurements of the corpus callosum were performed with Weasis DICOM medical viewer. n=3, 8 weeks, males and females. Statistical analysis: Student t-test, graph compares the measurements obtained from Trx-nKOs with Cntls, values are expressed in % of control (Mean ±SEM), *p<0.04, **p<0.01.

B. Histological assessments of the principal conductive pathways. Neurofilament heavy (NFH) and Myelin Basic Protein (MBP) was used to stain axons and myelin sheath.

C. Significant reduction in corpus callosum thickness observed in Trx-nKO animals. Corpus callosum thickness measurement performed on images acquired with 5x objective. Quantification was performed on 3 images acquired from 3 equally distanced images (block advance 100 μm) per animal. Per each image, 3 measurements were taken as follows: body (through the median of the central fissure) and left and right lateral parts (distanced 400 μm from the median). n=4, 8 weeks, males and females. Statistical analysis: Student t-test, the graph shows Mean ±SEM, ***p<0.001.

D. Significantly decreased axonal count in Trx-nKO lumbar spinal cord dorsal white matter. Measurement performed on images acquired with 20x objective. Quantification was performed on 3 images acquired from 3 equally distanced images (block advance 100 μm) per animal. ImageJ was used to quantify the number of axons. Values expressed in fold change to control. n=4, 8 weeks, males and females. Statistical analysis: Student t-test, the graph shows Mean ±SEM, *p<0.04, ***p<0.001.

E. Axon Feret diameter measurements performed on Trx-nKO dorsal spinal cord white matter and sciatic nerves demonstrate a significant decrease. Measurement was performed on images acquired with 63x objective (oil). Quantification was performed on 3 images acquired from 3 equally distanced images (block advance 100 μm) per animal. ImageJ was used to quantify the Feret diameter of axons[349]. Values expressed in fold change to control. n=4, 8 weeks, males and females. Statistical analysis: Student t-test, the graph shows Mean ±SEM.

F. No change in MBP/NFH overlap coefficient was observed in Trx-nKO white matter compared to Cntls. Measurement was performed on images acquired with 63x objective (oil). Quantification was performed on 3 images acquired from 3 equally distanced images (block advance 100 μm) per animal. The colocalization finder plugin in ImageJ was used to quantify the overlap coefficient between NFH and MBP signals[350,351]. n=4, 8 weeks, males and females. Statistical analysis: Student t-test, the graph shows Mean ±SEM, ns-not significant.

G. Western blotting performed on cortex tissues derived from 4- and 8-weeks old animals using myelin-specific antigens (myelin basic protein (MBP) and myelin associated glycoprotein (MAG).

H. Semiquantitative densitometry shows significant reduction in MBP content in cortices between Trx-nKO and Cntl groups. Protein level is normalized to loading control (GAPDH) and expressed in fold change to control. n=4 – 4 weeks, n=5 - 8 weeks, males and females. Statistical analysis: Student t-test, the graph shows Mean ±SEM, ***p<0.001, #p<0.04.

I. Semiquantitative densitometry shows significant reduction in MAG content in cortices of Trx-nKO group. Protein level is normalized to loading control (GAPDH) and expressed in fold change to control. n=3 – 4 weeks, n=5 - 8 weeks, males and females. Statistical analysis: Student t-test, the graph shows Mean ±SEM, *p<0.04, ##p<0.01.

3.6 Trx-1 deficiency in neurons is associated with nuclear lamina damage

Our laboratory has previously shown a specific role of Trx-1 depletion in nuclear lamina damage[176].

Trx-nKO mice exhibit a significantly higher incidence of nuclear lamina invaginations in cortices and spinal cords compared to control littermates (**Fig. 3.6 A, B, C**). For instance, in the cortex, more than 25% of nuclei were ruptured or severely damaged (**Fig. 3.6 B**). The reference scale for assessment of nuclear lamina damage is shown in Matherials and methods section (**Table 2.2**).

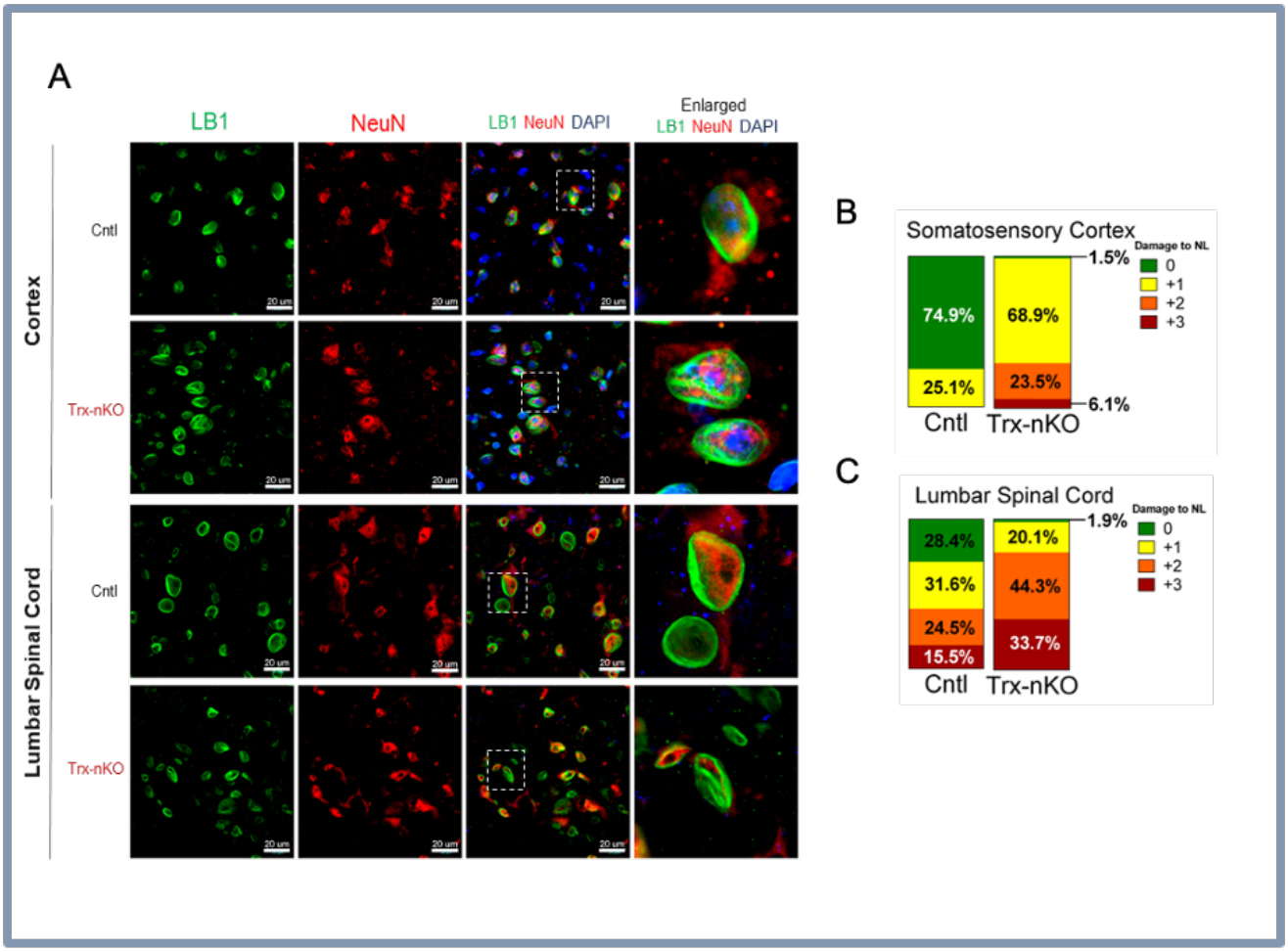

Figure 3.6 Trx-1 deficiency in neurons is associated with and nuclear lamina damage

A. **Immunofluorescent staining** demonstrates nuclear lamina structure in Trx-nKO and Cntl cortices and spinal cords. Lamin B1 is used as a nuclear lamina marker in neurons.

B. **Quantification depicts a higher percentage of moderate and severe damage to nuclear lamina in Trx-nKO cortices compared to the control.** Assessments were performed on images acquired with 63x objective (oil). 3 images acquired from 3 equally distanced sections (block advance 100 µm) were used per each animal. Each neuronal cell in the field received a nuclear lamina damage score as follows: Grade 1: circular shape, no visible folds; Grade 2: Circular shape, single shallow folds, no deep folds; Grade 3: Minor loss of circularity, folds no more than ½ diameter of nuclei, multiple folds, long folds that cover the whole visible surface of nuclear lamina; Grade 4: Major loss of circularity, folds larger than ½ diameter of nuclei, multiple deep folds, nuclear lamina rupture. n=4, 8 weeks, males and females.

C. Quantification depicts a higher percentage of moderate and severe damage to nuclear lamina in Trx-nKO cortices compared to the control. n=4, 8 weeks, males and females.

3.7 Trx-1 depletion in neurons is associated with increased neurodegeneration

Although the cortex did not show any overall decrease in neuronal numbers, I asked whether Trx-1 depletion may be associated with neuronal damage. FluoroJade C is a dye used for the detection of degenerating neurons regardless of the specific mechanism of neurodegeneration[360]. The number of FluoroJade C-positive neurons was significantly higher in Trx-nKO cortices and spinal cords compared to Cntls (**Fig. 3.7 A, B**). Interestingly, the percentage of degenerating neurons in spinal cord was considerably higher than in the cortex.

A recent study has reported that spontaneous Trx-1 loss-of-function mutations in midbrain neurons result in epilepsy[361]. This group showed that ENU-mutagenesis in Trx-1 gene locus (Chr 5: 75,159,000 to 76,708,000) resulted in loss of Trx-1 function and induced a transient model of epilepsy[361,362]. Our Trx-nKO mice also developed a severe form of epilepsy during the last two weeks of their lifespan and showed signs of epileptic death. While our animals showed evidence of neurodegeneration the shortened life span prevented them from developing a full-blown neurodegenerative phenotype.

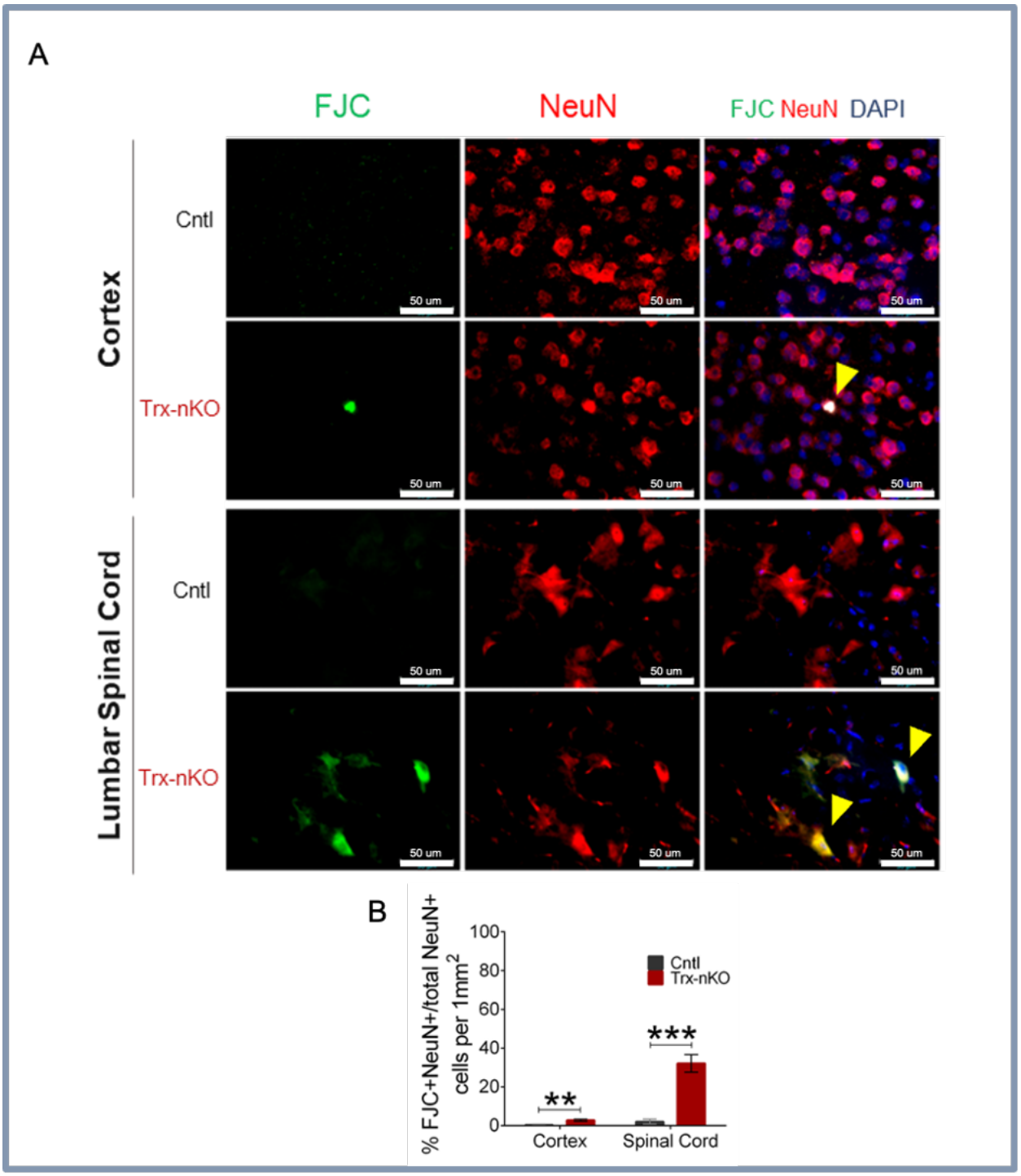

Figure 3.7 Trx-nKO pathology includes elements of neurodegeneration

A. Immunofluorescent staining performed on cortices and lumbar spinal cords detects FlouroJade C-positive neurons in Trx-nKOs but not Cntls. 3 images acquired from 3 equally distanced sections (block advance 100 μm) were used per each animal. n=4, 8 weeks, males and females.

B. Quantification performed on images acquired from Trx-nKO and Cntl cortex and lumbar spinal cord shows a significant increase in FJC+ neurons in Trx-nKOs. Quantification was performed on 3 images acquired from 3 equally distanced images (block advance 100 μm) per animal. The graph depicts the % of FJC+/NeuN+ out of total NeuN+ per 1 mm^2. n=4, 8 weeks, males and females. Statistical analysis: Student t-test, the graph shows Mean ±SEM, **p<0.01; ***p<0.001.

3.8 Trx-nKOs exhibit increased Tau phosphorylation.

Several studies have described nuclear lamina damage as a downstream event after cytoskeleton changes[363,364]. It has also been shown that impaired nuclear lamina structure is associated with increased Tau phosphorylation and microtubule disassembly[363,365]. Our lab showed that Trx-1 depletion/inactivation results in nuclear lamina damage. Additionally, Trx-nKOs have prominent signs of impaired cytoskeleton organization. Tau phosphorylation can happen secondary to initial cytoskeletal disorganization[366]. To investigate the relation of these events to a possible increase in Tau phosphorylation in Trx-nKOs, I investigated the status of Tau in Trx-nKO CNS. Interestingly, Trx-1 is a known regulator of JNK activity, a stress response kinase which is involved in Tau phosphorylation[258]. In neural stem cells, Trx-1 depletion is shown to activate JNK pathway through Prx-1/Oct-4 pathway[313,367]. JNK activation in these cells inhibits differentiation and promotes stemness via acceleration of cell proliferation and growth[367].

I, therefore, used western blotting to examine the status of JNK activation. Using both cortex and hippocampal tissue homogenates, I examined the level of p-JNK/t-JNK. JNK molecules are fully activated by phosphorylation at a Thr-Glu-Tyr motif, specifically at Thr183 and Tyr185[368]. Phosphorylation of JNK was detected using antibody raised against a sequence of JNK molecule containing Thr183 and Tyr 185. **Trx-nKO animals demonstrate significant activation of JNK pathway in hippocampi as shown in Fig. 3.8. A-E** JNK-mediated phosphorylation of Tau protein

(AT8: Ser 199, Ser 202 and Thr 205; PFH1: Ser 396 and Ser 404) has been reported as an early event of tauopathy in AD[369]. No significant activation of JNK pathway is observed in Trx-nKO cortex (**Fig. 3.8 G**). pTau is predominantly localized in perivascular areas and not in neuronal cell bodies as evidenced by immunofluorescent staining (**Fig. 3.8 H**). These data suggest that Trx1 depletion may be critical player in induction of neurodegenerative pathology in hippocampus.

Additionally, histone γH2A.X is a known target of JNK-mediated phosphorylation[370]. This event is typically observed upon oxidative DNA damage[370]. Evidence of DNA oxidation was observed in hippocampal homogenates in Trx-nKO mice.

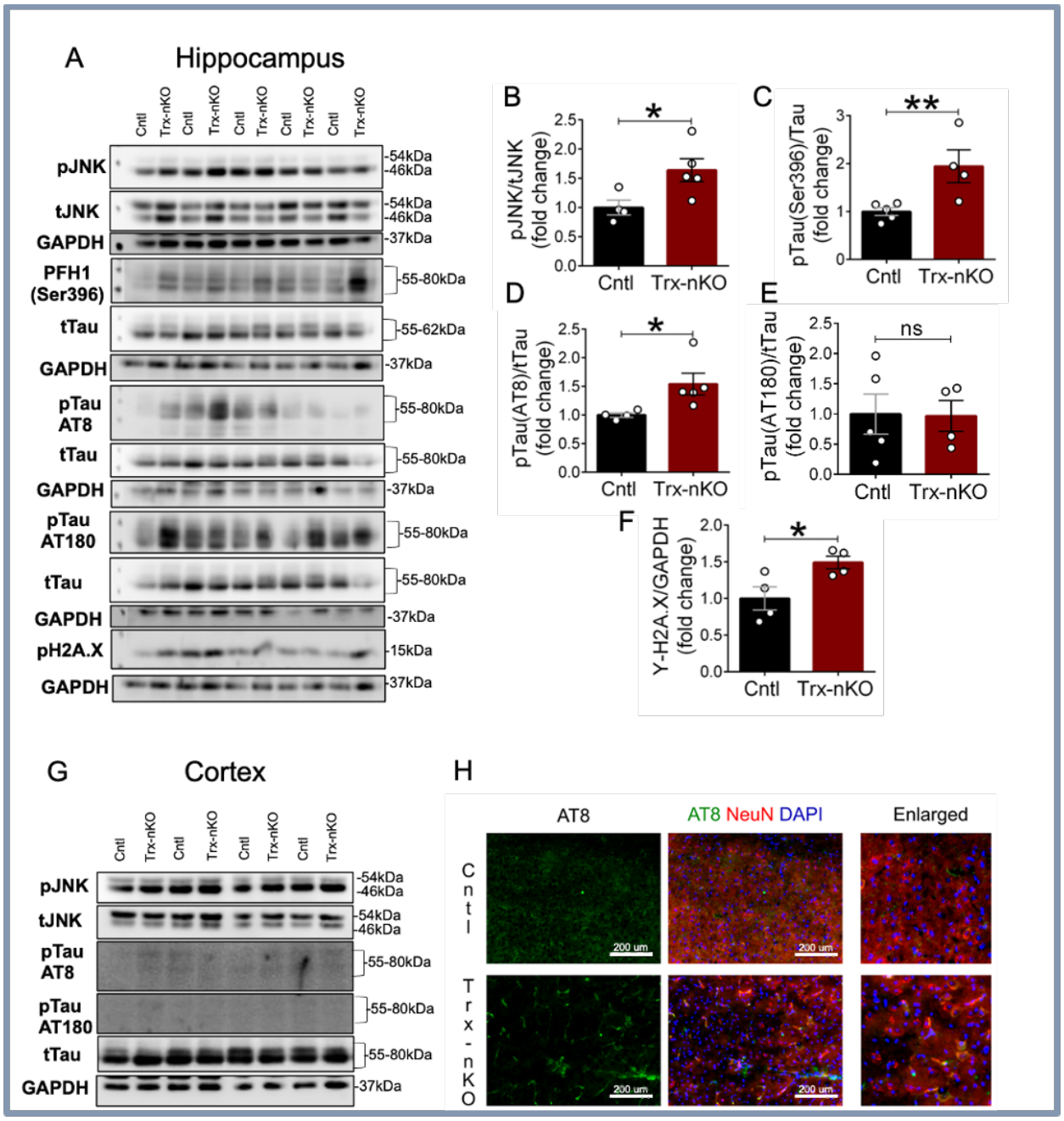

Figure 3.8 Trx-1 knockout in neurons is associated with activation of stress-related kinase JNK

- **A.** Western blotting shows depicts the levels of pJNK, tJNK and substrates for JNK-mediated phosphorylation, AT8, PFH-1 AT180, and γH2A.X in Trx-nKO and Cntl hippocampi.
- **B.** Semiquantitative densitometry shows significant increase in JNK activation in Trx-nKO hippocampi as evidenced by increased pJNK/tJNK ratio. n=5, 8 weeks, males and females. Protein level expressed in fold change to control. Statistical analysis: Student t-test; the graph shows Mean ±SEM, *p<0.04.

C. Semiquantitative densitometry demonstrates significant increase in Tau phosphorylation by Ser 396 (PFH-1) in Trx-nKO hippocampi as shown by PFH-1/tTau ratio. n=4, 8 weeks, males and females. Protein level in fold change to control. Statistical analysis: Student t-test; the graph shows Mean ±SEM, **p<0.01.

D. Semiquantitative densitometry demonstrates significant increase in Tau phosphorylation by Ser 199, Ser 202, and Thr 205 (AT8) in Trx-nKO hippocampi as shown by AT8/tTau ratio. n=5, 8 weeks, males and females. Protein level expressed in fold change to control. Statistical analysis: Student t-test; the graph shows Mean ±SEM, *p<0.04.

E. Semiquantitative densitometry shows no significant difference in Tau phosphorylation by Thr 231 (AT180) in Trx-nKO hippocampi as shown by AT180/tTau ratio. n=5, 8 weeks, males and females. Protein level expressed in fold change to control. Statistical analysis: Student t-test; the graph shows Mean ±SEM, ns – not significant.

F. Semiquantitative densitometry shows significant increase in y-H2A.X in Trx-nKO hippocampi. n=4, 8 weeks, males and females. Protein level is normalized to GAPDH and expressed in fold change to control. Statistical analysis: Student t-test; the graph shows Mean ±SEM, *p<0.04.

G. Western blotting shows depicts the levels of pJNK, y JNK, AT8, and AT180 in Trx-nKO and Cntl cortices. No significant difference detected. n=4, 8 weeks, males and females.

3.9 Trx-1 depletion results in disruption of intracellular transport

Nuclear lamina integrity is indispensable for proper nucleus-cytoplasm transport[264]. Defects in nuclear lamina were shown to disrupt nuclear pore function and lead to leakage of nuclear proteins and DNA[371]. To test whether nuclear lamina damage in Trx-nKO is associated with any disturbances in the exchange between cytoplasm and nucleoplasm, I examined the status of nucleus-specific proteins.

TDP-43 is a multifunctional transcriptional regulator[108]. In basal conditions, it is predominantly localized in the nucleus. Cytoplasmic inclusions containing the TDP-43 are considered a pathological hallmark of ALS and other neurodegenerative disorders[108]. TDP-43 pathology impacts neuronal homeostasis via: a) loss of function in the nucleus (loss of control over pre-

mRNA splicing, nucleocytoplasmic transport, modulation of mRNA stability and translation); b) gain of function (post-translational TDP-43 modifications in the cytoplasm, e.g., phosphorylation, cleavage or acetylation, leading to the formation of toxic aggregates)[108]. Interestingly, the peak expression of this protein in neurons coincides with neuronal differentiation and axonogenesis[372]. To investigate whether TDP-43 mislocalization is happening in Trx-nKO neurons, I examined the status of TDP-43 in cortex and spinal cord tissues. Histological assessment showed a significant decrease in nuclear TDP-43 in neurons compared to the control group (**Fig. 3.9 A, B**). Western blot performed on cytoplasmic and nuclear fractions derived from Trx-nKO and Cntl cortices shows a significant increase in phosphorylated TDP-43 in the cytoplasm compared to Cntl (**Fig. 3.9 C, D**). This further indicate the key role of oxidative stress and specifically Trx-1 depletion in pathophysiology of neurodegenerative diseases.

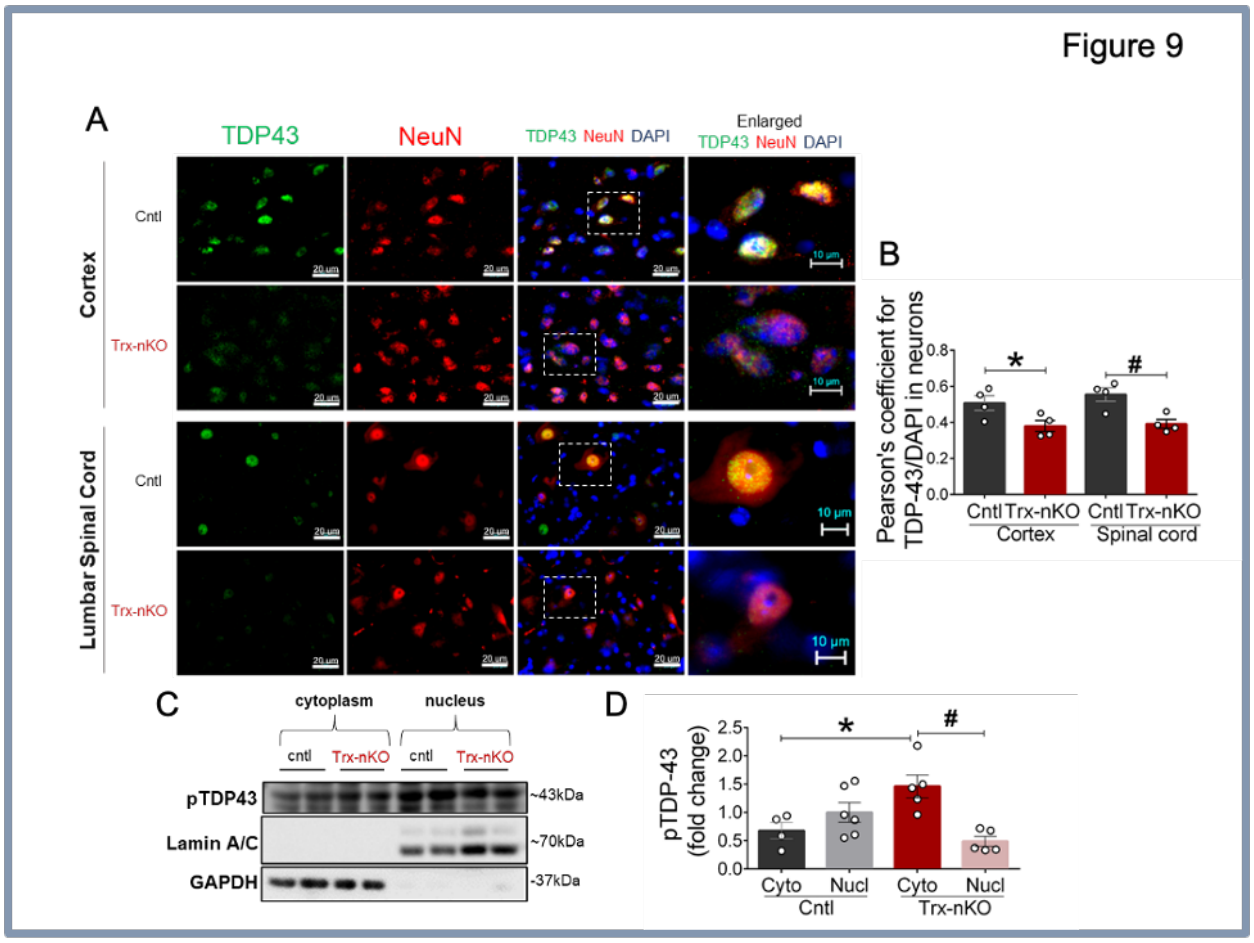

Figure 3.9 Trx-1 deficiency in neurons is associated with TDP-43 proteinopathy

A. Immunofluorescent staining of cortices and lumbar spinal cords depicts intracellular localization of TDP-43 in neurons.

B. Significant depletion in nuclear TDP-43 is shown by decreased colocalization with DAPI (nuclear marker). Quantification was performed on images acquired with 63x objective (oil). 3 images acquired from 3 equally distanced sections (block advance 100 μm) per animal were used. The colocalization finder plugin in ImageJ was used to quantify Pearson's colocalization coefficient between TDP-43 and DAPI signals. n=4, 8 weeks, males and females. Statistical analysis: Student t-test, the graph shows Mean ±SEM, * and # $p<0.04$.

C. Western blot performed on cytoplasmic and nuclear fractions derived from cortex tissue depicts intracellular localization of phosphorylated TDP-43.

D. Semiquantitative western blot densitometry shows a significant increase in pTDP-43 in the cytoplasm compared to the nucleus in Trx-nKO cortices. Accumulation of pTDP-43 in Trx-nKO cytoplasm is significantly higher compared to Cntls. n=5, 8 weeks, males and females. Protein level is normalized to loading control (cytoplasmic fraction –

GAPDH; nuclear fraction – Lamin A/C) and expressed in fold change to nuclear fraction of Cntls. Statistical analysis: Two-way ANOVA with multiple comparisons, Tukey's posthoc corrections; the graph shows Mean ±SEM, * and # $p<0.04$.

3.10 Trx-1 depletion results in accumulation of neurofilaments and axonal deformation

A recent article by Briese et al. showed that TDP-43 knockdown in motoneurons is detrimental to axon health[373]. They have demonstrated that depletion of TDP-43 in primary motoneurons negatively affects axonal morphology with an apparent decrease in the synthesis of axon-specific proteins. According to Briese et al., loss of TDP-43 function might be a major contributor to axonal pathology in ALS[373]. Interestingly, the peak expression of this protein in neurons coincides with neuronal differentiation and axonogenesis[372].

To investigate whether nuclear TDP-43 depletion in Trx-nKOs is associated with defective axonal structure, I stained cortical and spinal cord tissues with Neurofilament Heavy (NFH), an intermediate filament specific to axons. This protein is typically equally distributed evenly throughout the axonal length[374]. The antibody detects only phosphorylated form of NFH and has no reactivity with phosphorylated neurofilaments according to the manufacturer[375]. Intriguingly, in Trx-nKO cortices and spinal cords, NFH is accumulated in the perikaryal area and shows a prominent reduction of signal in axons (**Fig. 3.10**). Similar defects are typically found in motoneurons in post-mortem samples from ALS patients[20,376].

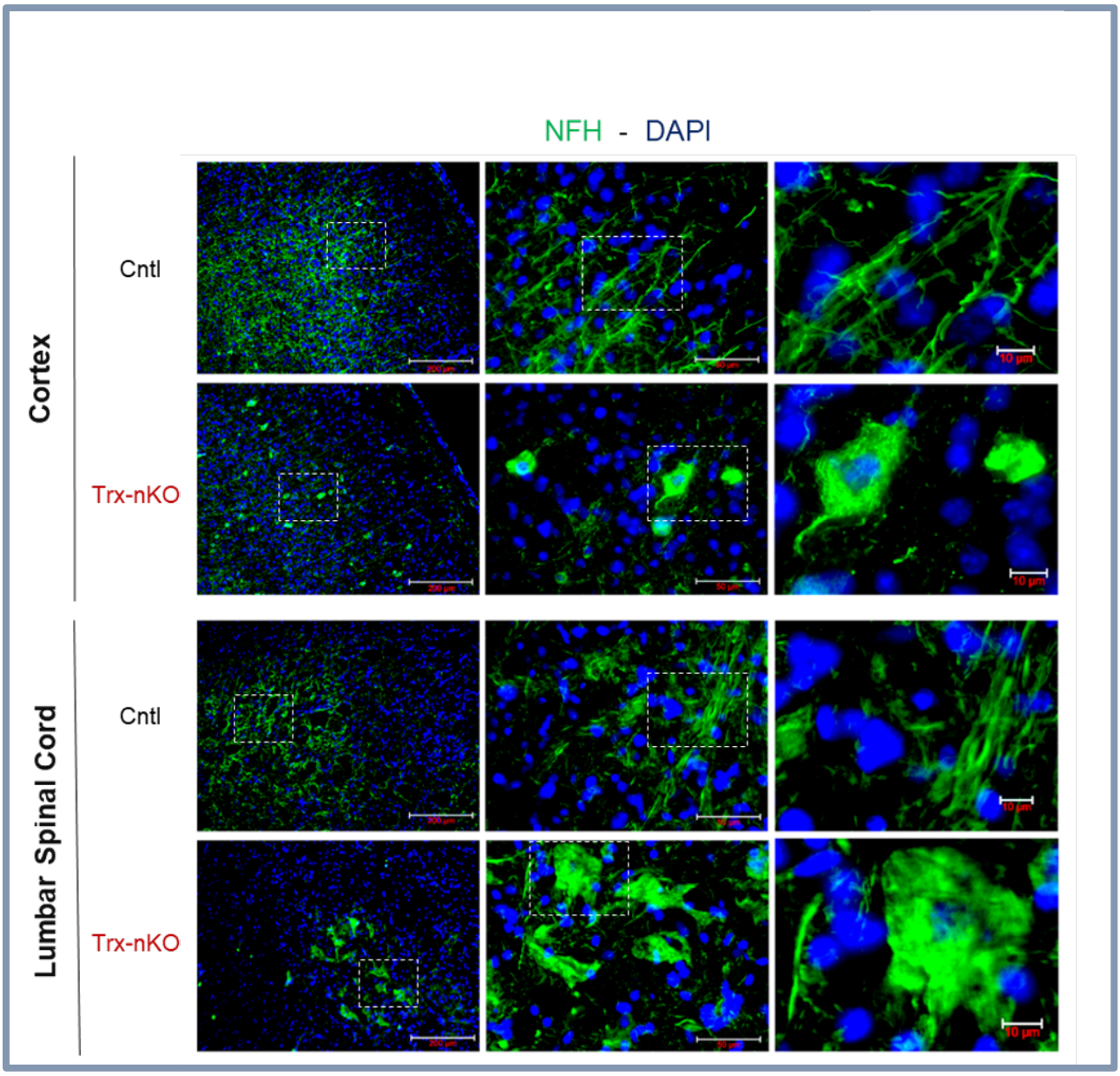

Figure 3.10 Trx-nKOs exhibit changes in axonal morphology along with decrease in myelin content

Immunofluorescent staining with axon-specific marker neurofilament heavy (NFH) highlights impaired axonal morphology in Trx-nKOs. Abnormal perinuclear accumulations of NFH in Trx-nKO cortices and lumbar spinal cord grey with low expression in axons. Cntls demonstrate even distribution of NFH across axons.

3.11 Trx-1 depletion in neurons is associated with increased protein oxidation.

Knowing the role of Trx-1 in the regulation of protein oxidation/reduction, I aimed to identify the extent of protein oxidation caused by Trx-1 depletion in neurons. Protein carbonylation assay is an indirect indicator of protein oxidation. Using the OxiBlot™ kit, I observed a significant increase in the content of carbonylated proteins in cortex (**Fig. 3.11 A**) but not in hippocampus (**Fig. 3.11 B**),. No prominent effect on protein oxidation in hippocampus might be related to comparatively lower Trx-1 knockout efficacy in CA1.

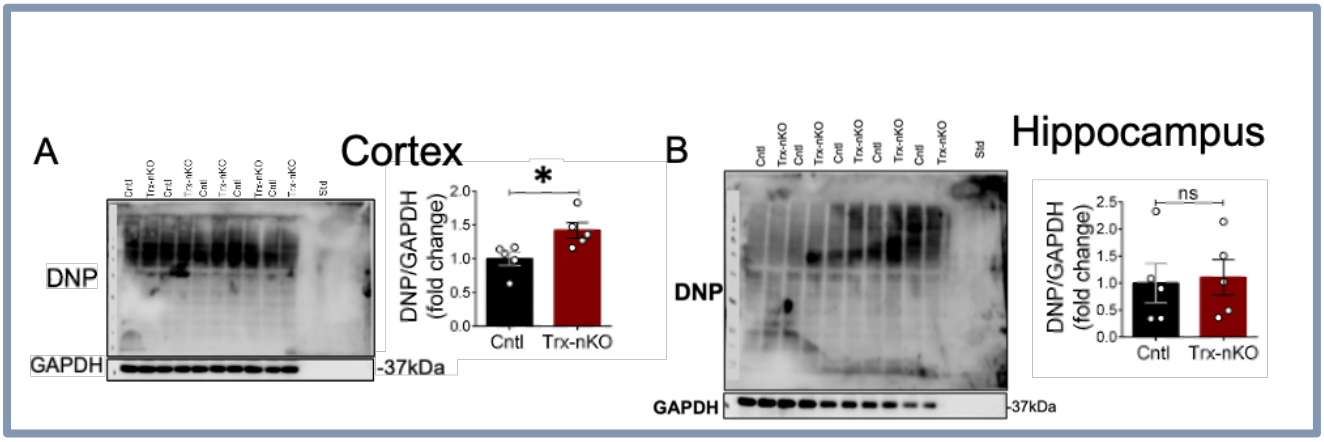

Figure 3.11 Trx-1 depletion enhances protein oxidation in neurons

A. OxiBlot™ was performed on cortex tissue homogenates as an indirect assessment of protein oxidation by the extent of protein carbonylation. Semiquantitative densitometry demonstrates a **significant increase in carbonylated proteins** (sites of Dinitrophenylhydrazine (DNP) binding) at 8 weeks of age. n=5, males and females. DNP level is normalized to loading control (GAPDH) and expressed in fold change to control. Statistical analysis: Student t-test, the graph shows Mean ±SEM, *p<0.04.

B. OxiBlot™ was performed on hippocampus tissue homogenates. Indirect assessment of protein oxidation by the extent of protein carbonylation. Semiquantitative densitometry showed **no change in protein carbonylation** (sites of Dinitrophenylhydrazine (DNP) binding) at 8- weeks of age. n=5, males and females. DNP level is normalized to loading control (GAPDH) and expressed in fold change to control.

Statistical analysis: Student t-test, the graph shows Mean ±SEM, ns – not significant.

3.12 Trx-1 depletion in neurons evokes glial responses

Glial cells are responsible for maintaining tissue homeostasis through interaction with neurons, amongast each other as well as the immune cells. Hence, evidence of glial activation has been shown in all neurodegenerative diseases. To examine the involvement of astroglia in pathologic processes in Trx-nKO neuronal tissues, we performed immunofluorescent staining of cortex and spinal cord sections with GFAP marker. (**Fig. 3.12 A**). Quantitative analysis revealed a significantly increased number of astrocytes in Trx-nKO CNS compared to control mice (**Fig. 3.12 B**). However, these cells have no morphological signs of reactivation (e.g., swollen cell body). At the protein level, GFAP overexpression in the Trx-nKO brain is observed at both 4 and 8 weeks of age (**Fig. 3.12 C, D**).

Microglia activation is an indispensable component of all neurodegenerative and myelin diseases, e.g., in AD or multiple sclerosis[377]. Taking into account a significant decrease in myelin content, I investigated the potential involvement of inflammatory pathways in Trx-nKO pathology. Histological assessment of Trx-nKO cortices did not show significant changes in the number (**Fig. 3.12 E, F**). or morphology of Iba1+ microglial cells. Quantitative western blotting showed no significant differences in Iba1 protein content as well as in the expression of pro-inflammatory cytokine TNF-α (**Fig. 3.12 G, H)**. These findings suggest that at the time of tissue extraction (8 weeks) neuroinflammation may not be fully developed.

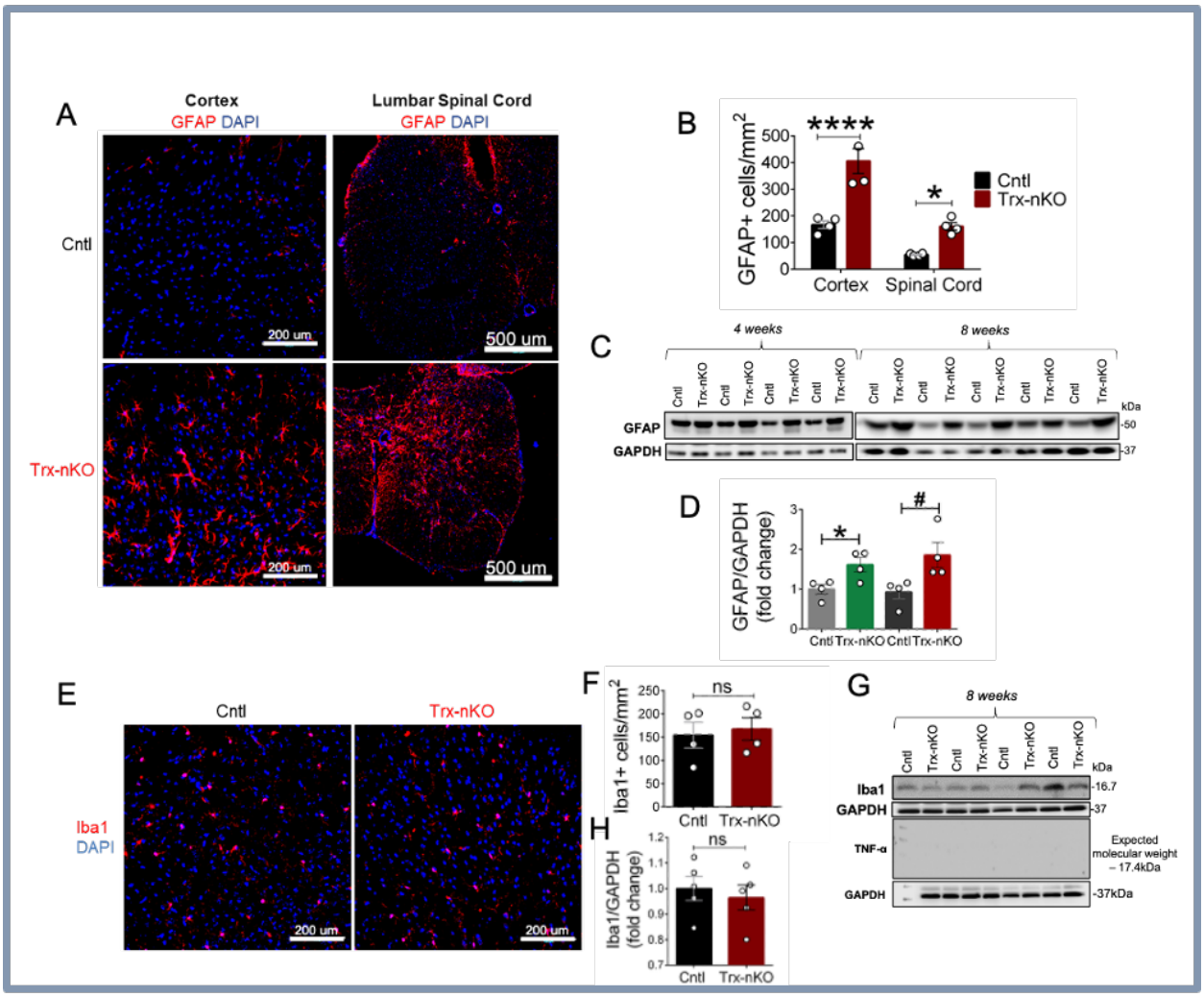

Figure 3.12 Trx-1 depletion in neurons evokes glial responses

A. **Immunofluorescent staining** performed on the cortex and lumbar spinal cord grey demonstrates the **signs of astrogliosis**. Astrocytes are labeled with GFAP.

B. **Quantification of the astroglia population performed on images acquired from the cortex shows a significant increase in the number of GFAP+ cells in Trx-nKO cortices and spinal cords.** Quantification was performed on 3 images acquired from 3 equally distanced sections (block advance 100 μm) per animal. The graph depicts the number of GFAP+ cells per 1 mm^2. N=4, 8 weeks, males and females. Statistical analysis: Student t-test, the graph shows Mean ±SEM, *p<0.04, ****p<0.0001.

C. **Western blotting** was performed on cortex tissue homogenates of 4- and 8-week-old animals.

D. **Semiquantitative densitometry showed a significant increase in GFAP protein expression at both 4- and 8- weeks of age.** n=4, males and females. Protein level is

normalized to loading control (GAPDH) and expressed in fold change to control. Statistical analysis: Student t-test, the graph shows Mean ±SEM, * and # $p<0.04$.

E. Immunofluorescent staining of cortex tissues reveals no morphological signs of microglia activation as evidenced by Iba1 staining.

F. **Quantification of the microglia population performed on images acquired from the cortex show no change in the number of Iba1+ cells in Trx-nKO cortices.** Quantification was performed on 3 images acquired from 3 equally distanced sections (block advance 100 μm) per animal. The graph depicts the number of Iba1+ cells per 1 mm^2. N=4, 8 weeks, males and females. Statistical analysis: Student t-test, the graph shows Mean ±SEM, ns – not significant.

G. **Western blotting** performed on cortex tissue homogenates demonstrate the levels of Iba1 (microglia-specific marker) and TNF-α (a pro-inflammatory cytokine).

H. **Semiquantitative densitometry shows no significant difference in Iba1 protein content in cortices between Trx-nKO and Cntl groups**. Protein level is normalized to loading control (GAPDH) and expressed in fold change to control. N=4, 8 weeks, males and females. Statistical analysis: Student t-test, the graph shows Mean ±SEM, ns – not significant.

4. Discussion

In the current study, I have demonstrated the role of Trx-1 in maintaining neuronal structure and function and its impact on CNS in an *in vivo* model of neuron-specific Trx-1 knockout. This gene deletion is associated with a dramatically reduced lifespan, increased seizure susceptibility, and prominent sensory and motor deficits. These features of Trx-nKO phenotype were associated with decreased number of motoneurons in the spinal cord and dramatic deficits in white matter across various levels of CNS. Detailed examination of molecular and histological features of Trx-nKO pathology revealed elevated expression of neurodegeneration-specific markers, i.e., nuclear lamina damage, Tau hyperphosphorylation, TPD-43 mislocalization and phosphorylation. Additionally, these findings were associated with impaired axonal morphology and reduced myelin content. Neurodegenerative changes in Trx-nKO neurons were confirmed by increased positive FluorojadeC staining. This study is the first report of the novel Trx-nKO mouse model. My work

describes Trx-1 protein as an important contributor to the maintenance of neuronal morphology and function. This proposes that therapeutic approaches for Trx-1 functional replacement and/or overexpression might be useful in the prevention and treatment of neurodegeneration.

4.1 Variable efficacy of Syn-Cre recombination underlies the mosaic pattern of Trx-nKO across the brain regions.

Syn-1 is one of the most frequently used neuron-specific transcriptional promoters used for pan-neuronal knockouts. Synapsin-1 protein is located at the cytoplasmic surface of synaptic vesicles in both peripheral and CNS neurons[378]. According to the official strain characterization report, Syn-Cre expression is limited to mature neurons and spares non-neuronal cells and neuroblasts[379]. The neuron-specific expression of Syn-1 was previously confirmed using IHC and western blotting[380]. However, several reports suggest the variability of Syn-Cre expression across different regions of CNS. and question the reliability of Syn-Cre recombinase as a pan-neuronal knockout tool. Immunohistology and quantitative PCR performed by Denroche et al. identified robust efficacy of Syn-1 mediated Cre recombination in the brainstem, cortex, hypothalamus, and spinal cord, with a lack of significant effect in the hippocampus and olfactory bulb[381]. More detailed report on Syn1-Cre expression in the hippocampus was provided by Zhang et al[382]. According to this group, the Syn-Cre effectively knocked out the target protein in NeuN-positive DG granular neurons at postnatal day 7[382]. Significant downregulation of the targeted protein in CA3 was observed by 14th postnatal day [382]. Of particular importance to my work, the authors showed that Cre-recombination in CA1 neurons was not as effective as in DG and CA3[382]. He et al. performed microdissection and western blotting to explore the effects of Syn-Cre mediated recombination[383].

In this work, CA1 tissue lysate showed no change in expression of the target protein compared to CA3 and DG[383]. Similar to the previously discussed findings, I observed a differential pattern of Syn-Cre-mediated Trx-1 knockout across different CNS regions. For instance, I detected a significant downregulation of this protein in brain cortex, DG of the hippocampus and lumbar spinal cord, but not in CA1 of the hippocampus. Consequently, the heterogeneous efficacy of Trx-1 downregulation in the hippocampus may reflect the lack of cognitive deficits in these mice.

4.2 Trx-1 neuron-specific pan-neuronal depletion triggers epileptogenesis

Epileptic activity can originate from different brain regions including hippocampus, frontal, temporal and olfactory cortex, amygdala, and midbrain[384]. Temporal lobe epilepsy is the most common form of epilepsy in humans[385]. The pathogenesis of this form includes trauma/degeneration or other neuropathologic changes in hippocampal neurons[386]. Aberrant impulses from such neurons underlie the seizure generation and subsequent spreading to neighbouring temporal cortex[386].

In Trx-nKOs I have identified several pro-epileptogenic changes in hippocampus and temporal cortex (e.g., impaired axonal structure[387] and increased astrocyte density[388]). Even though, it is likely that these changes are predisposing these animals to enhanced seizure susceptibility, other brain regions involved in epileptogenesis (i.e., midbrain and amygdala) must be studied to determine the origin of seizure activity in Trx-nKO mice. The role of astrocytes in epileptogenesis and overall neuropathology should be further investigated.

4.3 Trx-1 is essential for normal nucleo- and cytoskeleton morphology

Mounting evidence has linked damage to nuclear envelope to several neurodegenerative disorders[270]. We and others have shown the invagination of nuclear lamina in post-mortem samples of patients with AD[292,293]. It is viewed as a consequence of mechanical impact exerted by neurofibrillary tangles[363]. The applied pressure causes substantial morphological changes in nucleoskeleton and subsequent dysregulation of the chromatin organization[293]. Nuclear lamina invagination has been linked to oxidative distress. Thus, downregulation of Lamin B1 leads to loss of its interaction with Oct-1, a transcription factor involved in regulation of genes that encode antioxidant proteins[389]. Even though Lamin B1 depletion is a component of normal ageing, it is reported to be exacerbated in AD[390]. This is one of the possible explanations for oxidative distress in both conditions. Ultrastructural examination of post-mortem brain samples from patients with common neurodegenerative diseases, i.e., AD, FTD and HD identified nuclear lamina irregularities and invaginations[365]. This work highlights nuclear lamina damage as a common pathomorphological sign of neurodegeneration.

Our laboratory has recently discovered the induction of nuclear lamina damage upon pharmacologic inhibition of Trx-1 and genetic ablation of TrxR1[176]. These changes were associated with activation of Caspase 6[391]. Importantly, upregulation of Caspase 6 is observed in early stages of AD[391], and its inhibition results in improvement of cognitive functions in 5xFAD mice[392]. These data suggest a mechanistic link between oxidative distress and nuclear lamina damage in the context of AD.

Damage to nuclear lamina can also be mediated by mechanical pressure applied by pathologically rigid elements of the cytoskeleton. Thus, Paonessa et al. showed that cytoplasmic aggregates of hyperphosphorylated Tau in human neural stem cells caused abnormal microtubule movement and grossly deformed nuclear lamina[393]. Autosomal-dominant mutations in Tau protein cause an inherited form of Frontotemporal dementia[16]. Cortical neurons derived from patients with this disorder have high incidence of nuclear lamina damage providing a link between Tau-mediated nuclear envelope dysfunction and pathogenesis of FTD/ALS[393]. Another research group led by Frost et al. described Tau-mediated nuclear lamina damage as a common pathomorphological finding in post-mortem brain samples from subjects with AD[293]. In their experimental work, damage to nucleoskeleton was acquired through aberrant nucleoskeleton/cytoskeleton coupling that further resulted in heterochromatin relaxation and cell death[363].

Tau hyperphosphorylation is a common finding in several neurological diseases, e.g., AD[258], Frontotemporal dementia[393] or Down's syndrome[394]. ROS-mediated oxidation of Tau protein enhances phosphorylation and ultimately leads to formation of neurofibrillary tangles[395]. Oxidative stress itself activates stress-response kinases that can phosphorylate several amino acid residues in Tau molecule[250,396]. Trx-1 is involved in regulation of the stress response kinase JNK ½ commonly hyperactivated in neurodegeneration[397]. JNK-specific phosphorylation of Tau protein (AT8: Ser 199, Ser 202 and Thr 205; PFH1: Ser 396 and Ser 404) has been reported as an early event of tauopathy in AD[369].

Despite lower knockout efficacy, Trx-1 neuronal depletion in hippocampi was sufficient to induce JNK1/2 pathway activation at 8 weeks of age. This might be due to robust Trx-1 depletion and

CA3 even in the absence of significant effect on Trx-1 expression in CA1. Observed Tau hyperphosphorylation in JNK-specific sites highlights the importance of redox regulation in cytoskeleton stability. This pathological event is associated with increased evidence of nuclear lamina invaginations in Trx-nKO cortices. Current data available from the literature, suggests that nuclear lamina damage is mediated by Tau hyperphosphorylation, however, my data shows that depletion of Trx-1 protein reducing activity is sufficient to induce both Tau hypersphosphorylation and nuclear damage. The relevance of these findings in neurodegeneration remains to be examined.

FJC staining detected higher percentage of degenerating neurons in Trx-nKO spinal cords compared to cortices. This might be explained by robust decrease in the number and thickness of descending axons. Thus, cortical motoneurons connect monosynaptically with motoneurons in anterior horn of spinal cord[357]. Loss of axonal input from cortical neurons is shown to be detrimental to motor neurons in spinal cord and to trigger anterograde degeneration via[398]. Such mechanism is implicated in "dying-forward" hypothesis of ALS pathogenesis[357]. A similar principle could be applied to enhanced degeneration of spinal cord motor neurons in Trx-nKOs.

4.4 *Trx-nKO recapitulates the features of TDP-43 pathology*

Nuclear membrane plays an important role in the maintenance of the proper balance between nucleoplasm and cytoplasm. Aside from providing structural integrity for the nuclear envelope, nuclear lamina anchors to the nuclear pore complex[264,399]. Proper placement of the nuclear pore is crucial for cytoplasm/nucleoplasm shuttling[400]. This is particularly important for nucleoplasm-

specific proteins, e.g., TDP-43 and FUS[401]. Being a transcriptional regulator for over 3,000 proteins, TDP-43 is predominantly localized in the nucleoplasm. However, it is also a crucial component of the transport of mRNA granules that deliver the mRNAs to the sites of protein synthesis. Disruption of the nuclear pore transport system is ultimately associated with TDP-43 leakage from the nucleoplasm. It is unknown whether damage to nuclear envelope precedes or follows the pathological modification of TDP-43. According to Coyne et al., TDP-43 depletion in nucleoplasm is induced upon induction of damage to nuclear envelope[402]. On the other hand, as reported by Chou et al., aggregates of mutated TDP-43 can themselves disrupt nuclear pore function[403]. In Tau-mediated Frontotemporal dementia, destabilized microtubules were shown to induce nuclear invaginations and caused subsequent TDP-43 leakage to the cytoplasm[393]. While there is no consensus on the origin of TDP-43 leakage, there is an extensive amount of data on subsequent events in TDP-43 pathology. Thus, TDP-43 mislocalization impacts cellular homeostasis in two ways: a) through loss of function, i.e., loss of transcriptional control over a multitude of proteins; b) gain of toxic functions due to post-translational modifications in the cytoplasm (e.g., phosphorylation, acetylation, cleavage, etc.)[108,401]. Experimental data show that formation of toxic TDP-43 aggregates in the cytoplasm is not the ultimate component of TDP-43-mediated neuronal damage[404]. Only nuclear TDP-43 depletion is sufficient to induce ALS-like pathology[404].

Depletion of functional TDP-43 in the cell also has a detrimental effect on the transport of mRNA[405]. This process is particularly important for cells with extended processes, e.g., neurons. In neuronal cells mRNA granules contain mRNAs that encode axonal (e.g., neurofilaments, tubulins, actin) and synaptic proteins are transported along with TDP-43[373]. TDP-43 is important for the stabilization of granules and mediates phase separation and droplet formation[406]. Loss of

TDP-43 is sufficient to impair mRNA transport and is known to cause disruption in axonal synaptic structure evidenced by decreased axonal length and diameter as well as a lower number of functional synapses[373,405]. In these models, mRNAs that encode axon-specific proteins cannot be transported to the designed places of translation along the axonal axis[373]. This leads to aberrant protein synthesis and accumulation of axonal proteins, e.g., neurofilaments in perinuclear spaces[373]. Such findings are also typically found in post-mortem samples from patients with ALS[376,407,408].

My findings in the Trx-nKO perfectly show the signs of TDP-43 pathology. As such, Trx-nKOs have significantly reduced levels of TDP-43 in the nucleus and an increase of pTDP-43 accumulation in the cytoplasm. Additionally, Trx-nKOs demonstrate significant impairments in axonal structure and depletion of axon-specific proteins along the axonal axes with an accumulation of neurofilaments in perinuclear space. These findings link Trx-nKO to TDP-43-mediated pathology commonly found in ALS and AD, further suggesting the importance of Trx-1 in neuronal health.

5. Conclusion

In summary, my thesis uncovered novel aspects of redox neurobiology. Although decades of neurodegeneration research have already proven the key role of oxidative distress in induction and modulation of pro-neurodegenerative pathways, my project pioneered the characterization of the novel rodent model of neuron-specific Trx-1 knockout. I demonstrated that developmental neuron-specific knockout of Trx-1 in mice is associated with functional, morphological and molecular

abnormalities that are shared with neurodegenerative diseases. The severity of Trx-nKO phenotype emphasized the importance of Trx-1 antioxidant system in the maintenance of neuronal homeostasis and prevention of pro-neurodegenerative changes. Further investigation of this phenotype might open opened an avenue for novel approaches in diagnostics, prevention, and treatment of neurodegenerative diseases.

6. Limitations and Future Directions

The use of the developmental knockout approach in the study is an important caveat in my studies. Although Synapsin-1 Cre-recombinase driver is specific to mature neurons, its expression is observed as early as E12 and is reported to coincide with neuronal maturation. Therefore, it is not possible to exclude the contribution of developmental changes induced by Trx-1 knockout in this phenotype.

While general Trx-1 knockout leads to early embryonic lethality, pan-neuronal Trx-1 is associated with premature death. Multilevel pathology induced by Trx-1 knockout and consequent premature death at the stage of a young adult is a limiting factor to the development of full-blown neurodegenerative phenotype. Most neurodegenerative diseases are known to be age-dependent and are commonly studied on senile rodents. This enables closer recapitulation of neurodegenerative phenotype. The dramatically reduced lifespan of Trx-nKO mice is the main limiting factor in the investigation of age-dependent phenotype dynamics and therefore questions its relevance as a suitable model of neurodegeneration. To generate a more neurodegeneration-relevant model that can combine the effects of knockout with physiological aging, future

investigations should use inducible Cre-recombinase carriers such as Tamoxifen-inducible Cre-recombinase to include the use of senile animals to induce the mutation.

This work describes the effects of pan-neuronal Trx-1 knockout in cortex, hippocampus and spinal cord. Despite several neuropathologic findings identified in these regions of CNS, it is not possible to determine the reason of rapid premature death in these mice. Even though, based on my behavioural observations, the animals in most cases die from sudden epileptic death after several consecutive generalized seizures, there is a need to investigate the histopathology of other brain regions, especially those involved in the regulation of vital functions, e.g., brainstem. This will enable a better understanding of the cause of such rapid and premature death in Trx-nKO.

Differential efficacy of pan-neuronal Synapsin-1 Cre-recombinase expression is another limiting factor that disables the investigation of Trx-nKO effects in specific CNS regions. To enable the region-specific investigation of Trx-1 functions, further research could use stereotaxic injections of Cre-recombinase viral vector in Trx-1 floxed animals. This approach may yield to generation of more disease-relevant models.

This work also does not describe the impact of Trx-nKO on other antioxidant systems, e.g., GSH, Grxs which share functional similarities and are known to be upregulated to compensate for downregulation of other thiol enzymes. The extent of this protective antioxidant response is not investigated in my work and remains to be studied.

In this work, I showed a significant increase in number of astroglia in several brain regions. This coincides with increased expression of astrocyte-specific protein GFAP. However, I haven't investigated the functional role of these cells in Trx-nKO pathology, i.e., whether these astrocytes have pro-inflammatory or anti-inflammatory phenotypes. In neurodegenerative diseases, impaired glial metabolism results in excitotoxicity. The glutamate content as well as the proteins involved in production, metabolism, transportation and reception of this neurotransmitter remains to be studied. Overall, further investigations are needed to fully describe the functional outcome of glial activation in Trx-nKO.

7. References

1. Lamptey RNL, Chaulagain B, Trivedi R, et al. A Review of the Common Neurodegenerative Disorders: Current Therapeutic Approaches and the Potential Role of Nanotherapeutics. International Journal of Molecular Sciences 2022;23(3):1851, doi:10.3390/ijms23031851
2. Dugger BN, Dickson DW. Pathology of Neurodegenerative Diseases. Cold Spring Harbor Perspectives in Biology 2017;9(7):a028035, doi:10.1101/cshperspect.a028035
3. Chang E-S, Kannoth S, Levy S, et al. Global reach of ageism on older persons' health: A systematic review. PLOS ONE 2020;15(1):e0220857, doi:10.1371/journal.pone.0220857
4. 2023. Available from: https://www.healthdata.org/sites/default/files/files/country_profiles/GBD/ihme_gbd_country_report_canada.pdf.
5. NEURODEGENERATIVE DISEASE COSTS EXCEED $655 BILLION A YEAR IN MEDICAL EXPENSES AND ECONOMIC LOSSES | Keeping Education ACTIVE | Partnership to Fight Chronic Disease. 2023. Available from: https://www.fightchronicdisease.org/latest-news/neurodegenerative-disease-costs-exceed-655-billion-year-medical-expenses-and-economic.
6. Pandya VA, Patani R. Region-specific vulnerability in neurodegeneration: lessons from normal ageing. Ageing research reviews 2021;67(101311, doi:10.1016/j.arr.2021.101311
7. Winner B, Winkler J. Adult Neurogenesis in Neurodegenerative Diseases: Figure 1. Cold Spring Harbor perspectives in biology 2015;7(4):a021287, doi:10.1101/cshperspect.a021287
8. Wilson DM, Cookson MR, Van Den Bosch L, et al. Hallmarks of neurodegenerative diseases. Cell 2023;186(4):693-714, doi:10.1016/j.cell.2022.12.032
9. Rahman MM, Lendel C. Extracellular protein components of amyloid plaques and their roles in Alzheimer's disease pathology. Molecular Neurodegeneration 2021;16(1), doi:10.1186/s13024-021-00465-0
10. Brion JP. Neurofibrillary Tangles and Alzheimer's Disease. European neurology 1998;40(3):130-140, doi:10.1159/000007969
11. Okamoto K, Mizuno Y, Fujita Y. Bunina bodies in amyotrophic lateral sclerosis. Neuropathology 2008;28(2):109-115, doi:10.1111/j.1440-1789.2007.00873.x
12. Hughes AJ, Daniel SE, Lees AJ. Improved accuracy of clinical diagnosis of Lewy body Parkinson's disease. Neurology 2001;57(8):1497-1499, doi:10.1212/WNL.57.8.1497
13. Arrasate M, Finkbeiner S. Protein aggregates in Huntington's disease. Experimental Neurology 2012;238(1):1-11, doi:10.1016/j.expneurol.2011.12.013
14. Meneses A, Koga S, O'Leary J, et al. TDP-43 Pathology in Alzheimer's Disease. Molecular Neurodegeneration 2021;16(1), doi:10.1186/s13024-021-00503-x
15. Mackenzie IR, Rademakers R. The role of transactive response DNA-binding protein-43 in amyotrophic lateral sclerosis and frontotemporal dementia. Current Opinion in Neurology 2008;21(6):693-700, doi:10.1097/wco.0b013e3283168d1d
16. Strong MJ, Donison NS, Volkening K. Alterations in Tau Metabolism in ALS and ALS-FTSD. Frontiers in neurology 2020;11(doi:10.3389/fneur.2020.598907
17. Sheng Y, Chattopadhyay M, Whitelegge J, et al. SOD1 Aggregation and ALS: Role of Metallation States and Disulfide Status. Current Topics in Medicinal Chemistry 2013;12(22):2560-2572, doi:10.2174/1568026611212220010

18. Marrone L, Drexler HCA, Wang J, et al. FUS pathology in ALS is linked to alterations in multiple ALS-associated proteins and rescued by drugs stimulating autophagy. Acta Neuropathologica 2019;138(1):67-84, doi:10.1007/s00401-019-01998-x
19. Gal J, Ström A-L, Kilty R, et al. p62 Accumulates and Enhances Aggregate Formation in Model Systems of Familial Amyotrophic Lateral Sclerosis. Journal of Biological Chemistry 2007;282(15):11068-11077, doi:10.1074/jbc.m608787200
20. Kondo A, Iwaki T, Tateishi J, et al. Accumulation of Neurofilaments in a Sporadic Case of Amyotrophic Lateral Sclerosis. Psychiatry and Clinical Neurosciences 1986;40(4):677-684, doi:10.1111/j.1440-1819.1986.tb03184.x
21. Khalil M, Teunissen CE, Otto M, et al. Neurofilaments as biomarkers in neurological disorders. Nature Reviews Neurology 2018;14(10):577-589, doi:10.1038/s41582-018-0058-z
22. Stefanis L. -Synuclein in Parkinson's Disease. Cold Spring Harbor Perspectives in Medicine 2012;2(2):a009399-a009399, doi:10.1101/cshperspect.a009399
23. Zhang X, Gao F, Wang D, et al. Tau Pathology in Parkinson's Disease. Frontiers in neurology 2018;9(doi:10.3389/fneur.2018.00809
24. Schulte J, Littleton JT. The biological function of the Huntingtin protein and its relevance to Huntington's Disease pathology. Curr Trends Neurol 2011;5(65-78
25. Xiao G, Fan Q, Wang X, et al. Huntington disease arises from a combinatory toxicity of polyglutamine and copper binding. Proceedings of the National Academy of Sciences 2013;110(37):14995-15000, doi:10.1073/pnas.1308535110
26. Papuć E, Rejdak K. The role of myelin damage in Alzheimer’s disease pathology. Archives of Medical Science 2020;16(2):345-341, doi:10.5114/aoms.2018.76863
27. Raffaele S, Boccazzi M, Fumagalli M. Oligodendrocyte Dysfunction in Amyotrophic Lateral Sclerosis: Mechanisms and Therapeutic Perspectives. Cells 2021;10(3):565, doi:10.3390/cells10030565
28. Dean DC, Sojkova J, Hurley S, et al. Alterations of Myelin Content in Parkinson’s Disease: A Cross-Sectional Neuroimaging Study. PLOS ONE 2016;11(10):e0163774, doi:10.1371/journal.pone.0163774
29. Bourbon-Teles J, Bells S, Jones DK, et al. Myelin Breakdown in Human Huntington’s Disease: Multi-Modal Evidence from Diffusion MRI and Quantitative Magnetization Transfer. Neuroscience 2019;403(79-92, doi:10.1016/j.neuroscience.2017.05.042
30. Orr ME, Oddo S. Autophagic/lysosomal dysfunction in Alzheimer’s disease. Alzheimer's Research & Therapy 2013;5(5):53, doi:10.1186/alzrt217
31. Ramesh N, Pandey UB. Autophagy Dysregulation in ALS: When Protein Aggregates Get Out of Hand. Frontiers in molecular neuroscience 2017;10(doi:10.3389/fnmol.2017.00263
32. Hou X, Watzlawik JO, Fiesel FC, et al. Autophagy in Parkinson's Disease. Journal of molecular biology 2020;432(8):2651-2672, doi:10.1016/j.jmb.2020.01.037
33. Oh YM, Lee SW, Kim WK, et al. Age-related Huntington’s disease progression modeled in directly reprogrammed patient-derived striatal neurons highlights impaired autophagy. Nature Neuroscience 2022;25(11):1420-1433, doi:10.1038/s41593-022-01185-4
34. Roth KA. Caspases, Apoptosis, and Alzheimer Disease: Causation, Correlation, and Confusion. Journal of neuropathology and experimental neurology 2001;60(9):829-838, doi:10.1093/jnen/60.9.829
35. Sathasivam S, Shaw PJ. Apoptosis in amyotrophic lateral sclerosis—what is the evidence? The Lancet neurology 2005;4(8):500-509, doi:10.1016/S1474-4422(05)70142-3

36. Venderova K, Park DS. Programmed Cell Death in Parkinson's Disease. Cold Spring Harbor Perspectives in Medicine 2012;2(8):a009365-a009365, doi:10.1101/cshperspect.a009365
37. Hickey MA, Chesselet M-F. Apoptosis in Huntington's disease. Progress in neuro-psychopharmacology & biological psychiatry 2003;27(2):255-265, doi:10.1016/s0278-5846(03)00021-6
38. Trayhurn P. Oxygen—A Critical, but Overlooked, Nutrient. Frontiers in nutrition 2019;6(doi:10.3389/fnut.2019.00010
39. Sies H, Jones DP. Reactive oxygen species (ROS) as pleiotropic physiological signalling agents. Nature reviews 2020;21(7):363-383, doi:10.1038/s41580-020-0230-3
40. Ray PD, Huang B-W, Tsuji Y. Reactive oxygen species (ROS) homeostasis and redox regulation in cellular signaling. Cellular Signalling 2012;24(5):981-990, doi:10.1016/j.cellsig.2012.01.008
41. Shahid M, Pourrut B, Dumat C, et al. Heavy-Metal-Induced Reactive Oxygen Species: Phytotoxicity and Physicochemical Changes in Plants. Reviews of Environmental Contamination and Toxicology Volume 232 2014;232(1-44, doi:10.1007/978-3-319-06746-9_1
42. Valavanidis A, Vlachogianni T, Fiotakis K. Tobacco Smoke: Involvement of Reactive Oxygen Species and Stable Free Radicals in Mechanisms of Oxidative Damage, Carcinogenesis and Synergistic Effects with Other Respirable Particles. International Journal of Environmental Research and Public Health 2009;6(2):445-462, doi:10.3390/ijerph6020445
43. Shengchen W, Jing L, Yujie Y, et al. Polystyrene microplastics-induced ROS overproduction disrupts the skeletal muscle regeneration by converting myoblasts into adipocytes. Journal of hazardous materials 2021;417(125962, doi:10.1016/j.jhazmat.2021.125962
44. Libalova H, Milcova A, Cervena T, et al. Kinetics of ROS generation induced by polycyclic aromatic hydrocarbons and organic extracts from ambient air particulate matter in model human lung cell lines. Mutation research 2018;827(50-58, doi:10.1016/j.mrgentox.2018.01.006
45. Azzam EI, Jay-Gerin J-P, Pain D. Ionizing radiation-induced metabolic oxidative stress and prolonged cell injury. Cancer Letters 2012;327(1-2):48-60, doi:10.1016/j.canlet.2011.12.012
46. Turrens JF. Mitochondrial formation of reactive oxygen species. The Journal of physiology 2003;552(2):335-344, doi:10.1113/jphysiol.2003.049478
47. Sandalio LM, Rodríguez-Serrano M, Romero-Puertas MC, et al. Role of Peroxisomes as a Source of Reactive Oxygen Species (ROS) Signaling Molecules. Peroxisomes and their Key Role in Cellular Signaling and Metabolism 2013;69(231-255, doi:10.1007/978-94-007-6889-5_13
48. Ryter SW, Kim HP, Hoetzel A, et al. Mechanisms of Cell Death in Oxidative Stress. Antioxidants & redox signaling 2007;9(1):49-89, doi:10.1089/ars.2007.9.49
49. Tirichen H, Yaigoub H, Xu W, et al. Mitochondrial Reactive Oxygen Species and Their Contribution in Chronic Kidney Disease Progression Through Oxidative Stress. Frontiers in physiology 2021;12(doi:10.3389/fphys.2021.627837
50. Day RM, Suzuki YJ. Cell Proliferation, Reactive Oxygen and Cellular Glutathione. Dose-response : a publication of International Hormesis Society 2005;3(3):dose-response.0, doi:10.2203/dose-response.003.03.010
51. Tsatmali M, Walcott EC, Makarenkova H, et al. Reactive oxygen species modulate the differentiation of neurons in clonal cortical cultures. Molecular and cellular neurosciences 2006;33(4):345-357, doi:10.1016/j.mcn.2006.08.005

52. Wu S-Y, Hou H-S, Sun Y-S, et al. Correlation between cell migration and reactive oxygen species under electric field stimulation. Biomicrofluidics 2015;9(5):054120, doi:10.1063/1.4932662
53. Redza-Dutordoir M, Averill-Bates DA. Activation of apoptosis signalling pathways by reactive oxygen species. Biochimica et biophysica acta 2016;1863(12):2977-2992, doi:10.1016/j.bbamcr.2016.09.012
54. Santos AL, Sinha S, Lindner AB. The Good, the Bad, and the Ugly of ROS: New Insights on Aging and Aging-Related Diseases from Eukaryotic and Prokaryotic Model Organisms. Oxidative Medicine and Cellular Longevity 2018;2018(1-23, doi:10.1155/2018/1941285
55. Birben E, Sahiner UM, Sackesen C, et al. Oxidative Stress and Antioxidant Defense. The World Allergy Organization journal 2012;5(1):9-19, doi:10.1097/wox.0b013e3182439613
56. Hirota K, Murata M, Sachi Y, et al. Distinct Roles of Thioredoxin in the Cytoplasm and in the Nucleus. Journal of Biological Chemistry 1999;274(39):27891-27897, doi:10.1074/jbc.274.39.27891
57. Packer LA. [21] Thioredoxin and thioredoxin reductase. Methods in Enzymology 1995;252(199-208, doi:10.1016/0076-6879(95)52023-6
58. Sarsour EH, Kumar MG, Chaudhuri L, et al. Redox Control of the Cell Cycle in Health and Disease. Antioxidants & redox signaling 2009;11(12):2985-3011, doi:10.1089/ars.2009.2513
59. Baxter PS, Hardingham GE. Adaptive regulation of the brain's antioxidant defences by neurons and astrocytes. Free radical biology & medicine 2016;100(147-152, doi:10.1016/j.freeradbiomed.2016.06.027
60. Barnham KJ, Masters CL, Bush AI. Neurodegenerative diseases and oxidative stress. Nature Reviews Drug Discovery 2004;3(3):205-214, doi:10.1038/nrd1330
61. Huang W-J, Zhang X, Chen W-W. Role of oxidative stress in Alzheimer's disease. Biomedical Reports 2016;4(5):519-522, doi:10.3892/br.2016.630
62. Butterfield DA, Boyd-Kimball D. Oxidative Stress, Amyloid-β Peptide, and Altered Key Molecular Pathways in the Pathogenesis and Progression of Alzheimer's Disease. Journal of Alzheimer's Disease 2018;62(3):1345-1367, doi:10.3233/JAD-170543
63. Perry G, Cash AD, Smith MA. Alzheimer Disease and Oxidative Stress. Journal of Biomedicine and Biotechnology 2002;2(3):120-123, doi:10.1155/s1110724302203010
64. Lovell MA, Gabbita SP, Markesbery WR. Increased DNA Oxidation and Decreased Levels of Repair Products in Alzheimer's Disease Ventricular CSF. Journal of Neurochemistry 1999;72(2):771-776, doi:10.1046/j.1471-4159.1999.0720771.x
65. Nunomura A, Perry G, Aliev G, et al. Oxidative Damage Is the Earliest Event in Alzheimer Disease. Journal of neuropathology and experimental neurology 2001;60(8):759-767, doi:10.1093/jnen/60.8.759
66. Montine KS, Reich E, Neely MD, et al. Distribution of Reducible 4-Hydroxynonenal Adduct Immunoreactivity in Alzheimer Disease is Associated with APOE Genotype. Journal of neuropathology and experimental neurology 1998;57(5):415-425, doi:10.1097/00005072-199805000-00005
67. Münch G, Cunningham AM, Riederer P, et al. Advanced glycation endproducts are associated with Hirano bodies in Alzheimer's disease. Brain research 1998;796(1-2):307-310, doi:10.1016/s0006-8993(98)00328-x
68. Ahmed N, Ahmed U, Thornalley PJ, et al. Protein glycation, oxidation and nitration adduct residues and free adducts of cerebrospinal fluid in Alzheimer's disease and link to cognitive

impairment. Journal of Neurochemistry 2005;92(2):255-263, doi:10.1111/j.1471-4159.2004.02864.x
69. Aksenov MY, Aksenova MV, Butterfield DA, et al. Protein oxidation in the brain in Alzheimer's disease. Neuroscience 2001;103(2):373-383, doi:10.1016/s0306-4522(00)00580-7
70. Butterfield DA, Hensley K, Cole P, et al. Oxidatively Induced Structural Alteration of Glutamine Synthetase Assessed by Analysis of Spin Label Incorporation Kinetics: Relevance to Alzheimer's Disease. Journal of Neurochemistry 2002;68(6):2451-2457, doi:10.1046/j.1471-4159.1997.68062451.x
71. Bürklen TS, Schlattner U, Homayouni R, et al. The Creatine Kinase/Creatine Connection to Alzheimer's Disease: CK Inactivation, APP-CK Complexes and Focal Creatine Deposits. Journal of Biomedicine and Biotechnology 2006;2006(1-11, doi:10.1155/jbb/2006/35936
72. Liu Z, Li T, Li P, et al. The Ambiguous Relationship of Oxidative Stress, Tau Hyperphosphorylation, and Autophagy Dysfunction in Alzheimer's Disease. Oxidative Medicine and Cellular Longevity 2015;2015(e352723, doi:10.1155/2015/352723
73. Yoshida H, Hastie CJ, Mclauchlan H, et al. Phosphorylation of microtubule-associated protein tau by isoforms of c-Jun N-terminal kinase (JNK). Journal of Neurochemistry 2004;90(2):352-358, doi:10.1111/j.1471-4159.2004.02479.x
74. Atwood CS, Scarpa RC, Huang X, et al. Characterization of Copper Interactions with Alzheimer Amyloid β Peptides. Journal of Neurochemistry 2008;75(3):1219-1233, doi:10.1046/j.1471-4159.2000.0751219.x
75. Mandal PK, Goel A, Bush AI, et al. Hippocampal glutathione depletion with enhanced iron level in patients with mild cognitive impairment and Alzheimer's disease compared with healthy elderly participants. Brain communications 2022;4(5), doi:10.1093/braincomms/fcac215
76. Lovell MA, Xie C, Gabbita SP, et al. Decreased thioredoxin and increased thioredoxin reductase levels in Alzheimer's disease brain. Free Radical Biology & Medicine 2000;28(3):418-427, doi:10.1016/s0891-5849(99)00258-0
77. Lubec G, Kim SH, Fountoulakis M, et al. Protein levels of human peroxiredoxin subtypes in brains of patients with Alzheimer's disease and Down Syndrome. Protein Expression in Down Syndrome Brain 2001;223-235, doi:10.1007/978-3-7091-6262-0_18
78. Gsell W, Conrad R, Hickethier M, et al. Decreased Catalase Activity but Unchanged Superoxide Dismutase Activity in Brains of Patients with Dementia of Alzheimer Type. Journal of neurochemistry 1995;64(3):1216-1223, doi:10.1046/j.1471-4159.1995.64031216.x
79. Massaad CA, Pautler RG, Klann E. Mitochondrial superoxide: a key player in Alzheimer's disease. Aging 2009;1(9):758-761, doi:10.18632/aging.100088
80. Tam OH, Rozhkov NV, Shaw R, et al. Postmortem Cortex Samples Identify Distinct Molecular Subtypes of ALS: Retrotransposon Activation, Oxidative Stress, and Activated Glia. Cell Reports 2019;29(5):1164-1177.e5, doi:10.1016/j.celrep.2019.09.066
81. Calingasan NY, Chen J, Kiaei M, et al. β-amyloid 42 accumulation in the lumbar spinal cord motor neurons of amyotrophic lateral sclerosis patients. Neurobiology of disease 2005;19(1-2):340-347, doi:10.1016/j.nbd.2005.01.012
82. Ferrante RJ, Browne SE, Shinobu LA, et al. Evidence of Increased Oxidative Damage in Both Sporadic and Familial Amyotrophic Lateral Sclerosis. Journal of Neurochemistry 2002;69(5):2064-2074, doi:10.1046/j.1471-4159.1997.69052064.x
83. Shaw PJ, Ince PG, Falkous G, et al. Oxidative damage to protein in sporadic motor neuron disease spinal cord. Annals of neurology 1995;38(4):691-695, doi:10.1002/ana.410380424

84. Simpson EP, Henry YK, Henkel JS, et al. Increased lipid peroxidation in sera of ALS patients: A potential biomarker of disease burden. Neurology 2004;62(10):1758-1765, doi:10.1212/wnl.62.10.1758
85. Smith RG, Henry YK, Mattson MP, et al. Presence of 4-hydroxynonenal in cerebrospinal fluid of patients with sporadic amyotrophic lateral sclerosis. Annals of neurology 1998;44(4):696-699, doi:10.1002/ana.410440419
86. Ihara Y, Nobukuni K, Takata H, et al. Oxidative stress and metal content in blood and cerebrospinal fluid of amyotrophic lateral sclerosis patients with and without a Cu, Zn-superoxide dismutase mutation. Neurological research 2005;27(1):105-108, doi:10.1179/016164105x18430
87. Tohgi H, Abe T, Yamazaki K, et al. Remarkable increase in cerebrospinal fluid 3-nitrotyrosine in patients with sporadic amyotrophic lateral sclerosis. Annals of neurology 1999;46(1):129-131, doi:10.1002/1531-8249(199907)46:1<129::aid-ana21>3.0.co;2-y
88. Weishaupt JH, Bartels C, Pölking E, et al. Reduced oxidative damage in ALS by high-dose enteral melatonin treatment. Journal of pineal research 2006;41(4):313-323, doi:10.1111/j.1600-079x.2006.00377.x
89. Mitsumoto H, Santella RM, Liu X, et al. Oxidative stress biomarkers in sporadic ALS. Amyotrophic Lateral Sclerosis 2008;9(3):177-183, doi:10.1080/17482960801933942
90. Agar J, Durham H. Relevance of oxidative injury in the pathogenesis of motor neuron diseases. Amyotrophic lateral sclerosis and other motor neuron disorders : official publication of the World Federation of Neurology, Research Group on Motor Neuron Diseases 2003;4(4):232-242, doi:10.1080/14660820310011278
91. Berdyński M, Miszta P, Safranow K, et al. SOD1 mutations associated with amyotrophic lateral sclerosis analysis of variant severity. Scientific Reports 2022;12(1), doi:10.1038/s41598-021-03891-8
92. Trist BG, Hilton JB, Hare DJ, et al. Superoxide Dismutase 1 in Health and Disease: How a Frontline Antioxidant Becomes Neurotoxic. Angewandte Chemie International Edition 2021;60(17):9215-9246, doi:10.1002/anie.202000451
93. Luquin N, Yu B, Trent RJ, et al. An analysis of the entire SOD1 gene in sporadic ALS. Neuromuscular disorders 2008;18(7):545-552, doi:10.1016/j.nmd.2008.04.013
94. Borchelt DR, Lee MK, Slunt HS, et al. Superoxide dismutase 1 with mutations linked to familial amyotrophic lateral sclerosis possesses significant activity. Proceedings of the National Academy of Sciences 1994;91(17):8292-8296, doi:10.1073/pnas.91.17.8292
95. Reaume AG, Elliott JL, Hoffman EK, et al. Motor neurons in Cu/Zn superoxide dismutase-deficient mice develop normally but exhibit enhanced cell death after axonal injury. Nature genetics 1996;13(1):43-47, doi:10.1038/ng0596-43
96. Ratovitski T, Corson LB, Strain J, et al. Variation in the Biochemical/Biophysical Properties of Mutant Superoxide Dismutase 1 Enzymes and the Rate of Disease Progression in Familial Amyotrophic Lateral Sclerosis Kindreds. Human molecular genetics 1999;8(8):1451-1460, doi:10.1093/hmg/8.8.1451
97. Menzies F. Mitochondrial involvement in amyotrophic lateral sclerosis. Neurochemistry international 2002;40(6):543-551, doi:10.1016/S0197-0186(01)00125-5
98. Ferri A, Cozzolino M, Crosio C, et al. Familial ALS-superoxide dismutases associate with mitochondria and shift their redox potentials. Proceedings of the National Academy of Sciences 2006;103(37):13860-13865, doi:10.1073/pnas.0605814103

99. Stieber A, Gonatas JO, Gonatas NK. Aggregation of ubiquitin and a mutant ALS-linked SOD1 protein correlate with disease progression and fragmentation of the Golgi apparatus. Journal of the neurological sciences 2000;173(1):53-62, doi:10.1016/s0022-510x(99)00300-7
100. Oeda T. Oxidative stress causes abnormal accumulation of familial amyotrophic lateral sclerosis-related mutant SOD1 in transgenic Caenorhabditis elegans. Human molecular genetics 2001;10(19):2013-2023, doi:10.1093/hmg/10.19.2013
101. Jagaraj CJ, Parakh S, Atkin JD. Emerging Evidence Highlighting the Importance of Redox Dysregulation in the Pathogenesis of Amyotrophic Lateral Sclerosis (ALS). Frontiers in cellular neuroscience 2021;14(doi:10.3389/fncel.2020.581950
102. Tiwari A, Hayward LJ. Familial Amyotrophic Lateral Sclerosis Mutants of Copper/Zinc Superoxide Dismutase Are Susceptible to Disulfide Reduction. Journal of Biological Chemistry 2003;278(8):5984-5992, doi:10.1074/jbc.m210419200
103. Przedborski S, Donaldson D, Jakowec M, et al. Brain superoxide dismutase, catalase, and glutathione peroxidase activities in amyotrophic lateral sclerosis. Annals of neurology 1996;39(2):158-165, doi:10.1002/ana.410390204
104. Weiduschat N, Mao X, Hupf J, et al. Motor cortex glutathione deficit in ALS measured in vivo with the J-editing technique. Neuroscience letters 2014;570(102-107, doi:10.1016/j.neulet.2014.04.020
105. Ikawa M, Okazawa H, Tsujikawa T, et al. Increased oxidative stress is related to disease severity in the ALS motor cortex: A PET study. Neurology 2015;84(20):2033-2039, doi:10.1212/wnl.0000000000001588
106. Cova E, Bongioanni P, Cereda C, et al. Time course of oxidant markers and antioxidant defenses in subgroups of amyotrophic lateral sclerosis patients. Neurochemistry international 2010;56(5):687-693, doi:10.1016/j.neuint.2010.02.004
107. Mitchell J, Morris A, de Belleroche J. Thioredoxin reductase 1 haplotypes modify familial amyotrophic lateral sclerosis onset. Free radical biology & medicine 2009;46(2):202-211, doi:10.1016/j.freeradbiomed.2008.09.041
108. Prasad A, Bharathi V, Sivalingam V, et al. Molecular Mechanisms of TDP-43 Misfolding and Pathology in Amyotrophic Lateral Sclerosis. Frontiers in molecular neuroscience 2019;12(doi:10.3389/fnmol.2019.00025
109. Cohen TJ, Hwang AW, Unger T, et al. Redox signalling directly regulates TDP-43 via cysteine oxidation and disulphide cross-linking. The EMBO Journal 2012;31(5):1241-1252, doi:10.1038/emboj.2011.471
110. Shodai A, Morimura T, Ido A, et al. Aberrant Assembly of RNA Recognition Motif 1 Links to Pathogenic Conversion of TAR DNA-binding Protein of 43 kDa (TDP-43). Journal of Biological Chemistry 2013;288(21):14886-14905, doi:10.1074/jbc.m113.451849
111. Ren X, Zou L, Zhang X, et al. Redox Signaling Mediated by Thioredoxin and Glutathione Systems in the Central Nervous System. Antioxidants & Redox Signaling 2017;27(13):989-1010, doi:10.1089/ars.2016.6925
112. Hashimoto S, Matsuba Y, Takahashi M, et al. Neuronal glutathione loss leads to neurodegeneration involving gasdermin activation. Scientific Reports 2023;13(1), doi:10.1038/s41598-023-27653-w
113. Chen JJ, Thiyagarajah M, Song J, et al. Altered central and blood glutathione in Alzheimer's disease and mild cognitive impairment: a meta-analysis. Alzheimer's Research & Therapy 2022;14(1), doi:10.1186/s13195-022-00961-5

114. Chili A, Cucatto A, Terreni AA, et al. Reduced glutathione in amyotrophic lateral sclerosis: an open, crossover, randomized trial. The Italian journal of neurological sciences 1998;19(6):363-366, doi:10.1007/BF02341783
115. Bjørklund G, Peana M, Maes M, et al. The glutathione system in Parkinson's disease and its progression. Neuroscience and biobehavioral reviews 2021;120(470-478, doi:10.1016/j.neubiorev.2020.10.004
116. Arnér ESJ, Holmgren A. Physiological functions of thioredoxin and thioredoxin reductase. European Journal of Biochemistry 2000;267(20):6102-6109, doi:10.1046/j.1432-1327.2000.01701.x
117. Lee S, Kim SM, Lee RT. Thioredoxin and Thioredoxin Target Proteins: From Molecular Mechanisms to Functional Significance. Antioxidants & Redox Signaling 2013;18(10):1165-1207, doi:10.1089/ars.2011.4322
118. Hasan AA, Kalinina E, Tatarskiy V, et al. The Thioredoxin System of Mammalian Cells and Its Modulators. Biomedicines 2022;10(7):1757, doi:10.3390/biomedicines10071757
119. Jiménez A, Zu W, Rawe VY, et al. Spermatocyte/Spermatid-specific Thioredoxin-3, a Novel Golgi Apparatus-associated Thioredoxin, Is a Specific Marker of Aberrant Spermatogenesis. Journal of Biological Chemistry 2004;279(33):34971-34982, doi:10.1074/jbc.m404192200
120. Ouyang Y, Peng Y, Li J, et al. Modulation of thiol-dependent redox system by metal ions via thioredoxin and glutaredoxin systems. Metallomics : integrated biometal science 2018;10(2):218-228, doi:10.1039/c7mt00327g
121. Heppell-Parton A, Cahn A, Bench A, et al. Thioredoxin, a mediator of growth inhibition, maps to 9q31. Genomics 1995;26(2):379-381, doi:10.1016/0888-7543(95)80223-9
122. Oberacker T, Kraft L, Schanz M, et al. The Importance of Thioredoxin-1 in Health and Disease. Antioxidants 2023;12(5):1078, doi:10.3390/antiox12051078
123. Hawkes H-JK, Karlenius TC, Tonissen KF. Regulation of the human thioredoxin gene promoter and its key substrates: A study of functional and putative regulatory elements. Biochimica et biophysica acta 2014;1840(1):303-314, doi:10.1016/j.bbagen.2013.09.013
124. Tonelli C, Chio IIC, Tuveson DA. Transcriptional Regulation by Nrf2. Antioxidants & redox signaling 2018;29(17):1727-1745, doi:10.1089/ars.2017.7342
125. Monteiro HP, Ogata FT, Stern A. Thioredoxin promotes survival signaling events under nitrosative/oxidative stress associated with cancer development. Biomedical journal 2017;40(4):189-199, doi:10.1016/j.bj.2017.06.002
126. D M, CC J, R J, et al. Increased thioredoxin-1 production in human naturally occurring regulatory T cells confers enhanced tolerance to oxidative stress. Blood 2011;117(3), doi:10.1182/blood-2010-09-307041
127. Bertini R, Zack Howard OM, Dong H-F, et al. Thioredoxin, a Redox Enzyme Released in Infection and Inflammation, Is a Unique Chemoattractant for Neutrophils, Monocytes, and T Cells. Journal of Experimental Medicine 1999;189(11):1783-1789, doi:10.1084/jem.189.11.1783
128. Rubartelli A, Bajetto A, Allavena G, et al. Secretion of thioredoxin by normal and neoplastic cells through a leaderless secretory pathway. The Journal of biological chemistry 1992;267(34):24161-24164, doi:10.1016/s0021-9258(18)35742-9
129. TXN - Thioredoxin - Homo sapiens (Human) | UniProtKB | UniProt. 2023. Available from: https://www.uniprot.org/uniprotkb/P10599/entry.

130. Kim H-Y, Kim J-R. Thioredoxin as a reducing agent for mammalian methionine sulfoxide reductases B lacking resolving cysteine. Biochemical and biophysical research communications 2008;371(3):490-494, doi:10.1016/j.bbrc.2008.04.101
131. Haendeler J, Hoffmann J, Tischler V, et al. Redox regulatory and anti-apoptotic functions of thioredoxin depend on S-nitrosylation at cysteine 69. Nature cell biology 2002;4(10):743-749, doi:10.1038/ncb851
132. Tao L, Gao E, Bryan NS, et al. Cardioprotective effects of thioredoxin in myocardial ischemia and the reperfusion role of S-nitrosation. Proceedings of the National Academy of Sciences 2004;101(31):11471-11476, doi:10.1073/pnas.0402941101
133. Weichsel A, Brailey JL, Montfort WR. Buried S- Nitrosocysteine Revealed in Crystal Structures of Human Thioredoxin. Biochemistry 2007;46(5):1219-1227, doi:10.1021/bi061878r
134. Wang Y, Liu T, Wu C, et al. A strategy for direct identification of protein S-nitrosylation sites by quadrupole time-of-flight mass spectrometry. Journal of the American Society for Mass Spectrometry 2008;19(9):1353-1360, doi:10.1016/j.jasms.2008.06.001
135. Wu C, Liu T, Chen W, et al. Redox Regulatory Mechanism of Transnitrosylation by Thioredoxin. Molecular & cellular proteomics 2010;9(10):2262-2275, doi:10.1074/mcp.m110.000034
136. Casagrande S, Bonetto V, Fratelli M, et al. Glutathionylation of human thioredoxin: A possible crosstalk between the glutathione and thioredoxin systems. Proceedings of the National Academy of Sciences 2002;99(15):9745-9749, doi:10.1073/pnas.152168599
137. Go Y-M, Halvey PJ, Hansen JM, et al. Reactive Aldehyde Modification of Thioredoxin-1 Activates Early Steps of Inflammation and Cell Adhesion. The American Journal of Pathology 2007;171(5):1670-1681, doi:10.2353/ajpath.2007.070218
138. TXN2 - Thioredoxin, mitochondrial - Homo sapiens (Human) | UniProtKB | UniProt. 2023. Available from: https://www.uniprot.org/uniprotkb/Q99757/entry.
139. Tanaka T. Thioredoxin-2 (TRX-2) is an essential gene regulating mitochondria-dependent apoptosis. The EMBO Journal 2002;21(7):1695-1703, doi:10.1093/emboj/21.7.1695
140. Nakamura H, Chadwick DJ, Goode J. Extracellular Functions of Thioredoxin. Novartis Foundation Symposia 2008;184-195, doi:10.1002/9780470754030.ch14
141. A M-V, CM S, A J, et al. The mammalian testis-specific thioredoxin system. Antioxidants & redox signaling 2004;6(1), doi:10.1089/152308604771978327
142. Holmgren A, Sengupta R. The use of thiols by ribonucleotide reductase. Free radical biology & medicine 2010;49(11):1617-1628, doi:10.1016/j.freeradbiomed.2010.09.005
143. A H, R S. The use of thiols by ribonucleotide reductase. Free radical biology & medicine 2010;49(11), doi:10.1016/j.freeradbiomed.2010.09.005
144. Nordlund P, Reichard P. Ribonucleotide Reductases. Annual Review of Biochemistry 2006;75(1):681-706, doi:10.1146/annurev.biochem.75.103004.142443
145. Holmgren A. Hydrogen donor system for Escherichia coli ribonucleoside-diphosphate reductase dependent upon glutathione. Proceedings of the National Academy of Sciences 1976;73(7):2275-2279, doi:10.1073/pnas.73.7.2275
146. Yoo M-H, Xu X-M, Carlson BA, et al. Targeting Thioredoxin Reductase 1 Reduction in Cancer Cells Inhibits Self-Sufficient Growth and DNA Replication. PLoS ONE 2007;2(10):e1112, doi:10.1371/journal.pone.0001112
147. Du Y, Zhang H, Lu J, et al. Glutathione and Glutaredoxin Act as a Backup of Human Thioredoxin Reductase 1 to Reduce Thioredoxin 1 Preventing Cell Death by Aurothioglucose. Journal of Biological Chemistry 2012;287(45):38210-38219, doi:10.1074/jbc.m112.392225

148. Rhee SG, Woo HA. Multiple Functions of Peroxiredoxins: Peroxidases, Sensors and Regulators of the Intracellular Messenger H 2 O 2 , and Protein Chaperones. Antioxidants & redox signaling 2011;15(3):781-794, doi:10.1089/ars.2010.3393
149. Kim K, Kim IH, Lee KY, et al. The isolation and purification of a specific "protector" protein which inhibits enzyme inactivation by a thiol/Fe(III)/O2 mixed-function oxidation system. The Journal of biological chemistry 1988;263(10):4704-4711, doi:10.1016/s0021-9258(18)68840-4
150. Neumann CA, Krause DS, Carman CV, et al. Essential role for the peroxiredoxin Prdx1 in erythrocyte antioxidant defence and tumour suppression. Nature 2003;424(6948):561-565, doi:10.1038/nature01819
151. Vogt W. Oxidation of methionyl residues in proteins: Tools, targets, and reversal. Free radical biology & medicine 1995;18(1):93-105, doi:10.1016/0891-5849(94)00158-g
152. Dalle-Donne I, Rossi R, Giustarini D, et al. Methionine oxidation as a major cause of the functional impairment of oxidized actin. Free radical biology & medicine 2002;32(9):927-937, doi:10.1016/s0891-5849(02)00799-2
153. Lee BC, Gladyshev VN. The biological significance of methionine sulfoxide stereochemistry. Free Radical Biology and Medicine 2011;50(2):221-227, doi:10.1016/j.freeradbiomed.2010.11.008
154. Sagher D, Brunell D, Hejtmancik JF, et al. Thionein can serve as a reducing agent for the methionine sulfoxide reductases. Proceedings of the National Academy of Sciences 2006;103(23):8656-8661, doi:10.1073/pnas.0602826103
155. Taggart C. Oxidation of either methionine super351 or methionine super358 in alpha 1-antitrypsin causes loss of anti-neutrophil elastase activity. The Journal of biological chemistry 2000, doi:10.1074/jbc.m004850200
156. Purohit A, Rokita AG, Guan X, et al. Oxidized Ca2+ Calmodulin-Dependent Protein Kinase II Triggers Atrial Fibrillation. Circulation 2013;128(16):1748-1757, doi:10.1161/circulationaha.113.003313
157. Lin Y, Zhou X, Kato M, et al. Redox-mediated regulation of an evolutionarily conserved cross-β structure formed by the TDP43 low complexity domain. Proceedings of the National Academy of Sciences 2020;117(46):28727-28734, doi:10.1073/pnas.2012216117
158. Moskovitz J. Methionine sulfoxide reductases: ubiquitous enzymes involved in antioxidant defense, protein regulation, and prevention of aging-associated diseases. Biochimica et biophysica acta 2005;1703(2):213-219, doi:10.1016/j.bbapap.2004.09.003
159. Renehan AG. What is apoptosis, and why is it important? BMJ 2001;322(7301):1536-1538, doi:10.1136/bmj.322.7301.1536
160. Elmore S. Apoptosis: A Review of Programmed Cell Death. Toxicologic Pathology 2007;35(4):495-516, doi:10.1080/01926230701320337
161. Haanen C, Vermes I. Apoptosis and inflammation. Mediators of Inflammation 1995;4(1):5-15, doi:10.1155/s0962935195000020
162. Nikolaev A, Mclaughlin T, O'Leary DDM, et al. APP binds DR6 to trigger axon pruning and neuron death via distinct caspases. Nature 2009;457(7232):981-989, doi:10.1038/nature07767
163. Crews L, Patrick C, Adame A, et al. Modulation of aberrant CDK5 signaling rescues impaired neurogenesis in models of Alzheimer's disease. Cell Death & Disease 2011;2(2):e120-e120, doi:10.1038/cddis.2011.2

164. Cordeiro MF, Guo L, Coxon KM, et al. Imaging multiple phases of neurodegeneration: a novel approach to assessing cell death in vivo. Cell Death & Disease 2010;1(1):e3-e3, doi:10.1038/cddis.2009.3
165. Alves Da Costa C, Checler F. A novel parkin-mediated transcriptional function links p53 to familial Parkinson's disease. Cell Cycle 2010;9(1):16-17, doi:10.4161/cc.9.1.10420
166. Kim YJ, Yi Y, Sapp E, et al. Caspase 3-cleaved N-terminal fragments of wild-type and mutant huntingtin are present in normal and Huntington's disease brains, associate with membranes, and undergo calpain-dependent proteolysis. Proceedings of the National Academy of Sciences 2001;98(22):12784-12789, doi:10.1073/pnas.221451398
167. Whelan RS, Kaplinskiy V, Kitsis RN. Cell Death in the Pathogenesis of Heart Disease: Mechanisms and Significance. Annual Review of Physiology 2010;72(1):19-44, doi:10.1146/annurev.physiol.010908.163111
168. Fujita T, Ishikawa Y. Apoptosis in Heart Failure - The Role of the .BETA.-Adrenergic Receptor-Mediated Signaling Pathway and p53-Mediated Signaling Pathway in the Apoptosis of Cardiomyocytes -. Circulation Journal 2011;75(8):1811-1818, doi:10.1253/circj.cj-11-0025
169. Cummins NW, Badley AD. Mechanisms of HIV-associated lymphocyte apoptosis: 2010. Cell Death & Disease 2010;1(11):e99-e99, doi:10.1038/cddis.2010.77
170. Nagata S. Autoimmune diseases caused by defects in clearing dead cells and nuclei expelled from erythroid precursors. Immunological reviews 2007;220(1):237-250, doi:10.1111/j.1600-065x.2007.00571.x
171. Eguchi K. Apoptosis in Autoimmune Diseases. Internal Medicine 2001;40(4):275-284, doi:10.2169/internalmedicine.40.275
172. Kawakami A, Matsuoka N, Tsuboi M, et al. CD4+ T Cell-Mediated Cytotoxicity Toward Thyrocytes: The Importance of Fas/Fas Ligand Interaction Inducing Apoptosis of Thyrocytes and the Inhibitory Effect of Thyroid-Stimulating Hormone. Laboratory Investigation 2000;80(4):471-484, doi:10.1038/labinvest.3780053
173. Alberts B, Johnson A, Lewis J, et al. Molecular Biology of the Cell. 2002, doi:https://www.ncbi.nlm.nih.gov/books/NBK21054/
174. Lu J, Holmgren A. Thioredoxin System in Cell Death Progression. Antioxidants & redox signaling 2012;17(12):1738-1747, doi:10.1089/ars.2012.4650
175. Nishinaka Y, Masutani H, Nakamura H, et al. Regulatory roles of thioredoxin in oxidative stress-induced cellular responses. Redox Report 2001;6(5):289-295, doi:10.1179/135100001101536427
176. Islam MI, Nagakannan P, Ogungbola O, et al. Thioredoxin system as a gatekeeper in caspase-6 activation and nuclear lamina integrity: Implications for Alzheimer's disease. Free Radical Biology and Medicine 2019;134(567-580, doi:10.1016/j.freeradbiomed.2019.02.010
177. Mitchell DA, Morton SU, Fernhoff NB, et al. Thioredoxin is required for S-nitrosation of procaspase-3 and the inhibition of apoptosis in Jurkat cells. Proceedings of the National Academy of Sciences 2007;104(28):11609-11614, doi:10.1073/pnas.0704898104
178. Ueda S, Nakamura H, Masutani H, et al. Redox regulation of caspase-3(-like) protease activity: regulatory roles of thioredoxin and cytochrome c. The journal of immunology : official journal of the American Association of Immunologists 1998;161(12):6689-6695
179. Saitoh M. Mammalian thioredoxin is a direct inhibitor of apoptosis signal-regulating kinase (ASK) 1. The EMBO Journal 1998;17(9):2596-2606, doi:10.1093/emboj/17.9.2596
180. Ardestani A, Paroni F, Azizi Z, et al. MST1 is a key regulator of beta cell apoptosis and dysfunction in diabetes. Nature Medicine 2014;20(4):385-397, doi:10.1038/nm.3482

181. Wen W, Zhu F, Zhang J, et al. MST1 Promotes Apoptosis through Phosphorylation of Histone H2AX. Journal of Biological Chemistry 2010;285(50):39108-39116, doi:10.1074/jbc.m110.151753
182. Lee K-K, Yonehara S. Phosphorylation and Dimerization Regulate Nucleocytoplasmic Shuttling of Mammalian STE20-like Kinase (MST). Journal of Biological Chemistry 2002;277(14):12351-12358, doi:10.1074/jbc.m108138200
183. Ura S, Masuyama N, Graves JD, et al. MST1-JNK promotes apoptosis via caspase-dependent and independent pathways. Genes to Cells 2001;6(6):519-530, doi:10.1046/j.1365-2443.2001.00439.x
184. Chae JS, Gil Hwang S, Lim D-S, et al. Thioredoxin-1 functions as a molecular switch regulating the oxidative stress-induced activation of MST1. Free radical biology & medicine 2012;53(12):2335-2343, doi:10.1016/j.freeradbiomed.2012.10.527
185. Boya P, Reggiori F, Codogno P. Emerging regulation and functions of autophagy. Nature Cell Biology 2013;15(7):713-720, doi:10.1038/ncb2788
186. Reggiori F, Klionsky DJ. Autophagy in the Eukaryotic Cell. Eukaryotic cell 2002;1(1):11-21, doi:10.1128/ec.01.1.11-21.2002
187. Wang L, Ye X, Zhao T. The physiological roles of autophagy in the mammalian life cycle. Biological Reviews 2019;94(2):503-516, doi:10.1111/brv.12464
188. Cuervo AM, Bergamini E, Brunk UT, et al. Autophagy and Aging: The Importance of Maintaining "Clean" Cells. Autophagy 2005;1(3):131-140, doi:10.4161/auto.1.3.2017
189. Xie W, Zhou J. Aberrant regulation of autophagy in mammalian diseases. Biology Letters 2018;14(1):20170540, doi:10.1098/rsbl.2017.0540
190. Yang J-S, Lu C-C, Kuo S-C, et al. Autophagy and its link to type II diabetes mellitus. Biomedicine 2017;7(2):8, doi:10.1051/bmdcn/2017070201
191. Fernández-Albarral JA, De Julián-López E, Soler-Domínguez C, et al. The Role of Autophagy in Eye Diseases. Life 2021;11(3):189, doi:10.3390/life11030189
192. Funderburk SF, Marcellino BK, Yue Z. Cell “Self-Eating” (Autophagy) Mechanism in Alzheimer's Disease. Mount Sinai Journal of Medicine: A Journal of Translational and Personalized Medicine 2010;77(1):59-68, doi:10.1002/msj.20161
193. Cataldo AM, Barnett JL, Berman SA, et al. Gene expression and cellular content of cathepsin D in Alzheimer's disease brain: Evidence for early up-regulation of the endosomal-lysosomal system. Neuron 1995;14(3):671-680, doi:10.1016/0896-6273(95)90324-0
194. Yang X, Pan X, Zhao X, et al. Autophagy and Age-Related Eye Diseases. BioMed research international 2019;2019(1-12, doi:10.1155/2019/5763658
195. Yun HR, Jo YH, Kim J, et al. Roles of Autophagy in Oxidative Stress. International Journal of Molecular Sciences 2020;21(9):E3289, doi:10.3390/ijms21093289
196. Lamb CA, Yoshimori T, Tooze SA. The autophagosome: origins unknown, biogenesis complex. Nature Reviews Molecular Cell Biology 2013;14(12):759-774, doi:10.1038/nrm3696
197. Li Y, Chen Y. AMPK and Autophagy. In: Autophagy: Biology and Diseases. Springer Singapore: 2019; pp. 85-108.
198. Klionsky DJ. Look people, “Atg” is an abbreviation for “autophagy-related.” That’s it. Autophagy 2012;8(9):1281-1282, doi:10.4161/auto.21812
199. Suzuki H, Osawa T, Fujioka Y, et al. Structural biology of the core autophagy machinery. Current opinion in structural biology 2017;43(10-17, doi:10.1016/j.sbi.2016.09.010
200. Russell RC, Yuan H-X, Guan K-L. Autophagy regulation by nutrient signaling. Cell Research 2014;24(1):42-57, doi:10.1038/cr.2013.166

201. Scherz-Shouval R, Elazar Z. Regulation of autophagy by ROS: physiology and pathology. Trends in biochemical sciences 2011;36(1):30-38, doi:10.1016/j.tibs.2010.07.007
202. Oka S-I, Hirata T, Suzuki W, et al. Thioredoxin-1 maintains mechanistic target of rapamycin (mTOR) function during oxidative stress in cardiomyocytes. Journal of Biological Chemistry 2017;292(46):18988-19000, doi:10.1074/jbc.m117.807735
203. Oka S-I, Chin A, Park JY, et al. Thioredoxin-1 maintains mitochondrial function via mechanistic target of rapamycin signalling in the heart. Cardiovascular research 2020;116(10):1742-1755, doi:10.1093/cvr/cvz251
204. Nagarajan N, Oka S-I, Nah J, et al. Thioredoxin 1 promotes autophagy through transnitrosylation of Atg7 during myocardial ischemia. Journal of Clinical Investigation 2023;133(3), doi:10.1172/jci162326
205. Hu J, Liu J, Chen S, et al. Thioredoxin-1 regulates the autophagy induced by oxidative stress through
<scp>LC3-II</scp>
in human lens epithelial cells. Clinical and Experimental Pharmacology and Physiology 2023, doi:10.1111/1440-1681.13764
206. Maruyama T, Noda NN. Autophagy-regulating protease Atg4: structure, function, regulation and inhibition. The Journal of Antibiotics 2018;71(1):72-78, doi:10.1038/ja.2017.104
207. Pérez-Pérez ME, Zaffagnini M, Marchand CH, et al. The yeast autophagy protease Atg4 is regulated by thioredoxin. Autophagy 2014;10(11):1953-1964, doi:10.4161/auto.34396
208. Fletcher DA, Mullins RD. Cell mechanics and the cytoskeleton. Nature 2010;463(7280):485-492, doi:10.1038/nature08908
209. Hohmann, Dehghani. The Cytoskeleton—A Complex Interacting Meshwork. Cells 2019;8(4):362, doi:10.3390/cells8040362
210. Kirkpatrick LL, Brady ST. Molecular Components of the Neuronal Cytoskeleton. 1999, doi:https://www.ncbi.nlm.nih.gov/books/NBK28122/
211. Steinmetz MO. Structure and thermodynamics of the tubulin–stathmin interaction. Journal of structural biology 2007;158(2):137-147, doi:10.1016/j.jsb.2006.07.018
212. Gudimchuk NB, Mcintosh JR. Regulation of microtubule dynamics, mechanics and function through the growing tip. Nature Reviews Molecular Cell Biology 2021;22(12):777-795, doi:10.1038/s41580-021-00399-x
213. Cleveland DW, Hwo S-Y, Kirschner MW. Purification of tau, a microtubule-associated protein that induces assembly of microtubules from purified tubulin. Journal of molecular biology 1977;116(2):207-225, doi:10.1016/0022-2836(77)90213-3
214. Dehmelt L, Halpain S. Genome Biology 2004;6(1):204, doi:10.1186/gb-2004-6-1-204
215. Herrmann H, Bär H, Kreplak L, et al. Intermediate filaments: from cell architecture to nanomechanics. Nature Reviews Molecular Cell Biology 2007;8(7):562-573, doi:10.1038/nrm2197
216. Jacque CM, Vinner C, Kujas M, et al. Determination of glial fibrillary acidic protein (GFAP) in human brain tumors. Journal of the neurological sciences 1978;35(1):147-155, doi:10.1016/0022-510X(78)90107-7
217. Windoffer R, Beil M, Magin TM, et al. Cytoskeleton in motion: the dynamics of keratin intermediate filaments in epithelia. Journal of Cell Biology 2011;194(5):669-678, doi:10.1083/jcb.201008095
218. Danielsson F, Peterson M, Caldeira Araújo H, et al. Vimentin Diversity in Health and Disease. Cells 2018;7(10):147, doi:10.3390/cells7100147

219. Dittmer TA, Misteli T. The lamin protein family. Genome Biology 2011;12(5):222, doi:10.1186/gb-2011-12-5-222
220. Li JY, Wu CF. Perspectives on the origin of microfilaments, microtubules, the relevant chaperonin system and cytoskeletal motors— a commentary on the spirochaete origin of flagella. Cell Research 2003;13(4):219-227, doi:10.1038/sj.cr.7290167
221. Vicente-Manzanares M, Ma X, Adelstein RS, et al. Non-muscle myosin II takes centre stage in cell adhesion and migration. Nature Reviews Molecular Cell Biology 2009;10(11):778-790, doi:10.1038/nrm2786
222. Bigarella CL, Liang R, Ghaffari S. Stem cells and the impact of ROS signaling. Development 2014;141(22):4206-4218, doi:10.1242/dev.107086
223. Chalimeswamy A, Thanuja MY, Ranganath SH, et al. Oxidative Stress Induces a Breakdown of the Cytoskeleton and Tight Junctions of the Corneal Endothelial Cells. Journal of Ocular Pharmacology and Therapeutics 2022;38(1):74-84, doi:10.1089/jop.2021.0037
224. Munnamalai V, Suter DM. Reactive oxygen species regulate F-actin dynamics in neuronal growth cones and neurite outgrowth. Journal of Neurochemistry 2009;108(3):644-661, doi:10.1111/j.1471-4159.2008.05787.x
225. Stadtman ER, Berlett BS. Reactive Oxygen-Mediated Protein Oxidation in Aging and Disease. Chemical Research in Toxicology 1997;10(5):485-494, doi:10.1021/tx960133r
226. Landino LM, Iwig JS, Kennett KL, et al. Repair of peroxynitrite damage to tubulin by the thioredoxin reductase system. Free radical biology & medicine 2004;36(4):497-506, doi:10.1016/j.freeradbiomed.2003.11.026
227. Gellert M, Venz S, Mitlöhner J, et al. Identification of a Dithiol-disulfide Switch in Collapsin Response Mediator Protein 2 (CRMP2) That Is Toggled in a Model of Neuronal Differentiation. Journal of Biological Chemistry 2013;288(49):35117-35125, doi:10.1074/jbc.m113.521443
228. Balta E, Kramer J, Samstag Y. Redox Regulation of the Actin Cytoskeleton in Cell Migration and Adhesion: On the Way to a Spatiotemporal View. Frontiers in cell and developmental biology 2021;8(doi:10.3389/fcell.2020.618261
229. Ghezzi P. ReviewRegulation of protein function by glutathionylation. Free Radical Research 2005;39(6):573-580, doi:10.1080/10715760500072172
230. Janssen-Heininger YMW, Mossman BT, Heintz NH, et al. Redox-based regulation of signal transduction: Principles, pitfalls, and promises. Free Radical Biology and Medicine 2008;45(1):1-17, doi:10.1016/j.freeradbiomed.2008.03.011
231. Wang X, Ling S, Zhao D, et al. Redox Regulation of Actin by Thioredoxin-1 Is Mediated by the Interaction of the Proteins via Cysteine 62. Antioxidants & redox signaling 2010;13(5):565-573, doi:10.1089/ars.2009.2833
232. Wiesel P, Foster LC, Pellacani A, et al. Thioredoxin Facilitates the Induction of Heme Oxygenase-1 in Response to Inflammatory Mediators. Journal of Biological Chemistry 2000;275(32):24840-24846, doi:10.1074/jbc.m000835200
233. Takagi Y, Mitsui A, Nishiyama A, et al. Overexpression of thioredoxin in transgenic mice attenuates focal ischemic brain damage. Proceedings of the National Academy of Sciences 1999;96(7):4131-4136, doi:10.1073/pnas.96.7.4131
234. Go Y-M, Ziegler TR, Johnson JM, et al. Selective protection of nuclear thioredoxin-1 and glutathione redox systems against oxidation during glucose and glutamine deficiency in human colonic epithelial cells. Free Radical Biology and Medicine 2007;42(3):363-370, doi:10.1016/j.freeradbiomed.2006.11.005

235. Chittiboyina S, Bai Y, Lelièvre SA. Microenvironment-Cell Nucleus Relationship in the Context of Oxidative Stress. Frontiers in cell and developmental biology 2018;6(doi:10.3389/fcell.2018.00023
236. Schenk H, Klein M, Erdbrügger W, et al. Distinct effects of thioredoxin and antioxidants onthe activation of transcription factors NF-kappa B and AP-1. Proceedings of the National Academy of Sciences 1994;91(5):1672-1676, doi:10.1073/pnas.91.5.1672
237. Freemerman AJ, Gallegos A, Powis G. Nuclear factor kappaB transactivation is increased but is not involved in the proliferative effects of thioredoxin overexpression in MCF-7 breast cancer cells. Cancer research 1999;59(16):4090-4094
238. Kaadige MR, Elgort MG, Ayer DE. Coordination of glucose and glutamine utilization by an expanded Myc network. Transcription 2010;1(1):36-40, doi:10.4161/trns.1.1.12142
239. Makino Y, Yoshikawa N, Okamoto K, et al. Direct Association with Thioredoxin Allows Redox Regulation of Glucocorticoid Receptor Function. Journal of Biological Chemistry 1999;274(5):3182-3188, doi:10.1074/jbc.274.5.3182
240. He F, Ru X, Wen T. NRF2, a Transcription Factor for Stress Response and Beyond. International Journal of Molecular Sciences 2020;21(13):4777, doi:10.3390/ijms21134777
241. Moi P, Chan K, Asunis I, et al. Isolation of NF-E2-related factor 2 (Nrf2), a NF-E2-like basic leucine zipper transcriptional activator that binds to the tandem NF-E2/AP1 repeat of the beta-globin locus control region. Proceedings of the National Academy of Sciences 1994;91(21):9926-9930, doi:10.1073/pnas.91.21.9926
242. Itoh K, Wakabayashi N, Katoh Y, et al. Keap1 represses nuclear activation of antioxidant responsive elements by Nrf2 through binding to the amino-terminal Neh2 domain. Genes & Development 1999;13(1):76-86, doi:10.1101/gad.13.1.76
243. Kobayashi A, Kang M-I, Okawa H, et al. Oxidative Stress Sensor Keap1 Functions as an Adaptor for Cul3-Based E3 Ligase To Regulate Proteasomal Degradation of Nrf2. Molecular and Cellular Biology 2004;24(16):7130-7139, doi:10.1128/mcb.24.16.7130-7139.2004
244. Yamamoto T, Suzuki T, Kobayashi A, et al. Physiological Significance of Reactive Cysteine Residues of Keap1 in Determining Nrf2 Activity. Molecular and Cellular Biology 2008;28(8):2758-2770, doi:10.1128/mcb.01704-07
245. Hansen JM. Compartmentation of Nrf-2 Redox Control: Regulation of Cytoplasmic Activation by Glutathione and DNA Binding by Thioredoxin-1. Toxicological Sciences 2004;82(1):308-317, doi:10.1093/toxsci/kfh231
246. Hirota K, Matsui M, Iwata S, et al. AP-1 transcriptional activity is regulated by a direct association between thioredoxin and Ref-1. Proceedings of the National Academy of Sciences 1997;94(8):3633-3638, doi:10.1073/pnas.94.8.3633
247. Hess J, Angel P, Schorpp-Kistner M. AP-1 subunits: quarrel and harmony among siblings. Journal of Cell Science 2004;117(25):5965-5973, doi:10.1242/jcs.01589
248. Lee W, Haslinger A, Karin M, et al. Activation of transcription by two factors that bind promoter and enhancer sequences of the human metallothionein gene and SV40. Nature 1987;325(6102):368-372, doi:10.1038/325368a0
249. Herdegen T, Waetzig V. AP-1 proteins in the adult brain: facts and fiction about effectors of neuroprotection and neurodegeneration. Oncogene 2001;20(19):2424-2437, doi:10.1038/sj.onc.1204387
250. Benoit B, Baillet A, Poüs C. Cytoskeleton and Associated Proteins: Pleiotropic JNK Substrates and Regulators. International Journal of Molecular Sciences 2021;22(16):8375, doi:10.3390/ijms22168375

251. Ameyar M, Wisniewska M, Weitzman JB. A role for AP-1 in apoptosis: the case for and against. Biochimie 2003;85(8):747-752, doi:10.1016/j.biochi.2003.09.006
252. Angel P, Karin M. The role of Jun, Fos and the AP-1 complex in cell-proliferation and transformation. Biochimica et biophysica acta 1991;1072(2-3):129-157, doi:10.1016/0304-419X(91)90011-9
253. Shen Q, Uray IP, Li Y, et al. The AP-1 transcription factor regulates breast cancer cell growth via cyclins and E2F factors. Oncogene 2008;27(3):366-377, doi:10.1038/sj.onc.1210643
254. Yujiri T, Fanger GR, Garrington TP, et al. MEK Kinase 1 (MEKK1) Transduces c-Jun NH2-terminal Kinase Activation in Response to Changes in the Microtubule Cytoskeleton. Journal of Biological Chemistry 1999;274(18):12605-12610, doi:10.1074/jbc.274.18.12605
255. Wang T-H, Wang H-S, Ichijo H, et al. Microtubule-interfering Agents Activate c-Jun N-terminal Kinase/Stress-activated Protein Kinase through Both Ras and Apoptosis Signal-regulating Kinase Pathways. Journal of Biological Chemistry 1998;273(9):4928-4936, doi:10.1074/jbc.273.9.4928
256. Sadot E, Jaaro H, Seger R, et al. Ras-Signaling Pathways: Positive and Negative Regulation of Tau Expression in PC12 Cells. Journal of Neurochemistry 2002;70(1):428-431, doi:10.1046/j.1471-4159.1998.70010428.x
257. Reynolds CH, Betts JC, Blackstock WP, et al. Phosphorylation Sites on Tau Identified by Nanoelectrospray Mass Spectrometry. Journal of Neurochemistry 2002;74(4):1587-1595, doi:10.1046/j.1471-4159.2000.0741587.x
258. Ploia C, Antoniou X, Sclip A, et al. JNK Plays a Key Role in Tau Hyperphosphorylation in Alzheimer's Disease Models. Journal of Alzheimer's Disease 2011;26(2):315-329, doi:10.3233/jad-2011-110320
259. Duka V, Lee J-H, Credle J, et al. Identification of the Sites of Tau Hyperphosphorylation and Activation of Tau Kinases in Synucleinopathies and Alzheimer's Diseases. PLoS ONE 2013;8(9):e75025, doi:10.1371/journal.pone.0075025
260. Voss K, Koren J, Dickey CA. The Earliest Tau Dysfunction in Alzheimer's Disease? The American Journal of Pathology 2011;179(5):2148-2151, doi:10.1016/j.ajpath.2011.08.020
261. Ruff CA, Staak N, Patodia S, et al. Neuronal c-Jun is required for successful axonal regeneration, but the effects of phosphorylation of its N-terminus are moderate. Journal of Neurochemistry 2012;121(4):607-618, doi:10.1111/j.1471-4159.2012.07706.x
262. Aebi U, Cohn J, Buhle L, et al. The nuclear lamina is a meshwork of intermediate-type filaments. Nature 1986;323(6088):560-564, doi:10.1038/323560a0
263. Burke B, Stewart CL. The nuclear lamins: flexibility in function. Nature reviews 2013;14(1):13-24, doi:10.1038/nrm3488
264. Dobrzynska A, Gonzalo S, Shanahan C, et al. The nuclear lamina in health and disease. Nucleus 2016;7(3):233-248, doi:10.1080/19491034.2016.1183848
265. Zuela N, Bar DZ, Gruenbaum Y. Lamins in development, tissue maintenance and stress. EMBO reports 2012;13(12):1070-1078, doi:10.1038/embor.2012.167
266. Rober RA, Weber K, Osborn M. Differential timing of nuclear lamin A/C expression in the various organs of the mouse embryo and the young animal: a developmental study. Development 1989;105(2):365-378, doi:10.1242/dev.105.2.365
267. Broers JLV, Machiels BM, Kuijpers HJH, et al. A- and B-type lamins are differentially expressed in normal human tissues. Histochemistry and cell biology 1997;107(6):505-517, doi:10.1007/s004180050138

268. Takamori Y, Hirahara Y, Wakabayashi T, et al. Differential expression of nuclear lamin subtypes in the neural cells of the adult rat cerebral cortex. IBRO reports 2018;5(99-109, doi:10.1016/j.ibror.2018.11.001
269. Yang SH, Jung H-J, Coffinier C, et al. Are B-type lamins essential in all mammalian cells? Nucleus 2011;2(6):562-569, doi:10.4161/nucl.2.6.18085
270. Almendáriz-Palacios C, Gillespie ZE, Janzen M, et al. The Nuclear Lamina: Protein Accumulation and Disease. Biomedicines 2020;8(7):188, doi:10.3390/biomedicines8070188
271. Liu Q, Pante N, Misteli T, et al. Functional association of Sun1 with nuclear pore complexes. Journal of Cell Biology 2007;178(5):785-798, doi:10.1083/jcb.200704108
272. Razafsky D, Zang S, Hodzic D. UnLINCing the nuclear envelope: towards an understanding of the physiological significance of nuclear positioning. Biochemical Society Transactions 2011;39(6):1790-1794, doi:10.1042/bst20110660
273. Lei K, Zhang X, Ding X, et al. SUN1 and SUN2 play critical but partially redundant roles in anchoring nuclei in skeletal muscle cells in mice. Proceedings of the National Academy of Sciences 2009;106(25):10207-10212, doi:10.1073/pnas.0812037106
274. Ho CY, Jaalouk DE, Vartiainen MK, et al. Lamin A/C and emerin regulate MKL1–SRF activity by modulating actin dynamics. Nature 2013;497(7450):507-511, doi:10.1038/nature12105
275. Kind J, Pagie L, Ortabozkoyun H, et al. Single-Cell Dynamics of Genome-Nuclear Lamina Interactions. Cell 2013;153(1):178-192, doi:10.1016/j.cell.2013.02.028
276. Guelen L, Pagie L, Brasset E, et al. Domain organization of human chromosomes revealed by mapping of nuclear lamina interactions. Nature 2008;453(7197):948-951, doi:10.1038/nature06947
277. Briand N, Collas P. Lamina-associated domains: peripheral matters and internal affairs. Genome Biology 2020;21(1), doi:10.1186/s13059-020-02003-5
278. Paul JC, Fulka H. Nuclear Lamins: Key Proteins for Embryonic Development. Biology 2022;11(2):198, doi:10.3390/biology11020198
279. Vergnes L, Péterfy M, Bergo MO, et al. Lamin B1 is required for mouse development and nuclear integrity. Proceedings of the National Academy of Sciences 2004;101(28):10428-10433, doi:10.1073/pnas.0401424101
280. Alcorta-Sevillano N, Macías I, Rodríguez CI, et al. Crucial Role of Lamin A/C in the Migration and Differentiation of MSCs in Bone. Cells 2020;9(6):1330, doi:10.3390/cells9061330
281. Kim Y, Zheng X, Zheng Y. Proliferation and differentiation of mouse embryonic stem cells lacking all lamins. Cell Research 2013;23(12):1420-1423, doi:10.1038/cr.2013.118
282. Liu B, Wang J, Chan KM, et al. Genomic instability in laminopathy-based premature aging. Nature Medicine 2005;11(7):780-785, doi:10.1038/nm1266
283. Redwood AB, Perkins SM, Vanderwaal RP, et al. A dual role for A-type lamins in DNA double-strand break repair. Cell Cycle 2011;10(15):2549-2560, doi:10.4161/cc.10.15.16531
284. Bell ES, Shah P, Zuela-Sopilniak N, et al. Low lamin A levels enhance confined cell migration and metastatic capacity in breast cancer. Oncogene 2022;41(36):4211-4230, doi:10.1038/s41388-022-02420-9
285. Fracchia A, Asraf T, Salmon-Divon M, et al. Increased Lamin B1 Levels Promote Cell Migration by Altering Perinuclear Actin Organization. Cells 2020;9(10):2161, doi:10.3390/cells9102161
286. Lindenboim L, Zohar H, Worman HJ, et al. The nuclear envelope: target and mediator of the apoptotic process. Cell Death Discovery 2020;6(1), doi:10.1038/s41420-020-0256-5

287. ÖStlund C, Bonne GL, Schwartz K, et al. Properties of lamin A mutants found in Emery-Dreifuss muscular dystrophy, cardiomyopathy and Dunnigan-type partial lipodystrophy. Journal of Cell Science 2001;114(24):4435-4445, doi:10.1242/jcs.114.24.4435
288. Navarro CL, Cadiñanos J, Sandre-Giovannoli AD, et al. Loss of ZMPSTE24 (FACE-1) causes autosomal recessive restrictive dermopathy and accumulation of Lamin A precursors. Human Molecular Genetics 2005;14(11):1503-1513, doi:10.1093/hmg/ddi159
289. De Sandre-Giovannoli A, Chaouch M, Kozlov S, et al. Homozygous Defects in LMNA, Encoding Lamin A/C Nuclear-Envelope Proteins, Cause Autosomal Recessive Axonal Neuropathy in Human (Charcot-Marie-Tooth Disorder Type 2) and Mouse. The American Journal of Human Genetics 2002;70(3):726-736, doi:10.1086/339274
290. Padiath QS, Fu Y-H. Autosomal Dominant Leukodystrophy Caused by Lamin B1 Duplications: A Clinical and Molecular Case Study of Altered Nuclear Function and Disease. Methods in Cell Biology 2010;98(337-357, doi:10.1016/s0091-679x(10)98014-x
291. Taimen P, Pfleghaar K, Shimi T, et al. A progeria mutation reveals functions for lamin A in nuclear assembly, architecture, and chromosome organization. Proceedings of the National Academy of Sciences 2009;106(49):20788-20793, doi:10.1073/pnas.0911895106
292. Islam MI, Nagakannan P, Shcholok T, et al. Regulatory role of cathepsin L in induction of nuclear laminopathy in Alzheimer's disease. Aging Cell 2022;21(1):e13531, doi:10.1111/acel.13531
293. Frost B. Alzheimer's disease: An acquired neurodegenerative laminopathy. Nucleus 2016;7(3):275-283, doi:10.1080/19491034.2016.1183859
294. Chen X, Xie C, Tian W, et al. Parkinson's disease-related Leucine-rich repeat kinase 2 modulates nuclear morphology and genomic stability in striatal projection neurons during aging. Molecular Neurodegeneration 2020;15(1), doi:10.1186/s13024-020-00360-0
295. Irianto J, Pfeifer CR, Ivanovska IL, et al. Nuclear Lamins in Cancer. Cellular and Molecular Bioengineering 2016;9(2):258-267, doi:10.1007/s12195-016-0437-8
296. Vashisth M, Cho S, Irianto J, et al. Scaling concepts in 'omics: Nuclear lamin-B scales with tumor growth and often predicts poor prognosis, unlike fibrosis. Proceedings of the National Academy of Sciences 2021;118(48):e2112940118, doi:10.1073/pnas.2112940118
297. Roncato F, Regev O, Feigelson SW, et al. Nuclear lamin A/C promotes cancer cell survival and lung metastasis without restricting transendothelial migration. Cold Spring Harbor Laboratory: 2020.
298. Schreiber H, Katherine, Kennedy K, Brian. When Lamins Go Bad: Nuclear Structure and Disease. Cell 2013;152(6):1365-1375, doi:10.1016/j.cell.2013.02.015
299. Cenni V, Capanni C, Mattioli E, et al. Lamin A involvement in ageing processes. Ageing research reviews 2020;62(101073, doi:10.1016/j.arr.2020.101073
300. Tran JR, Chen H, Zheng X, et al. Lamin in inflammation and aging. Current Opinion in Cell Biology 2016;40(124-130, doi:10.1016/j.ceb.2016.03.004
301. Primmer SR, Liao C-Y, Kummert OMP, et al. Lamin A to Z in normal aging. Aging 2022, doi:10.18632/aging.204342
302. Ueno M, Masutani H, Arai RJ, et al. Thioredoxin-dependent Redox Regulation of p53-mediated p21 Activation. Journal of Biological Chemistry 1999;274(50):35809-35815, doi:10.1074/jbc.274.50.35809
303. Liu Y, Min W. Thioredoxin Promotes ASK1 Ubiquitination and Degradation to Inhibit ASK1-Mediated Apoptosis in a Redox Activity-Independent Manner. Circulation Research 2002;90(12):1259-1266, doi:10.1161/01.res.0000022160.64355.62

304. Hwang J, Suh H-W, Jeon YH, et al. The structural basis for the negative regulation of thioredoxin by thioredoxin-interacting protein. Nature Communications 2014;5(1), doi:10.1038/ncomms3958
305. Akterin S, Cowburn RF, Miranda-Vizuete A, et al. Involvement of glutaredoxin-1 and thioredoxin-1 in β-amyloid toxicity and Alzheimer's disease. Cell Death & Differentiation 2006;13(9):1454-1465, doi:10.1038/sj.cdd.4401818
306. Saitoh M, Nishitoh H, Fujii M, et al. Mammalian thioredoxin is a direct inhibitor of apoptosis signal-regulating kinase (ASK) 1. The EMBO Journal 1998;17(9):2596-2606, doi:10.1093/emboj/17.9.2596
307. SI O, A C, JY P, et al. Thioredoxin-1 maintains mitochondrial function via mechanistic target of rapamycin signalling in the heart. Cardiovascular research 2020;116(10), doi:10.1093/cvr/cvz251
308. Morinaka A, Yamada M, Itofusa R, et al. Thioredoxin Mediates Oxidation-Dependent Phosphorylation of CRMP2 and Growth Cone Collapse. Science signaling 2011;4(170):ra26, doi:10.1126/scisignal.2001127
309. Bai J, Nakamura H, Kwon Y-W, et al. Critical Roles of Thioredoxin in Nerve Growth Factor-Mediated Signal Transduction and Neurite Outgrowth in PC12 Cells. The Journal of Neuroscience 2003;23(2):503-509, doi:10.1523/JNEUROSCI.23-02-00503.2003
310. Sartelet H, Rougemont A-L, Fabre M, et al. Activation of the phosphatidylinositol 3′-kinase/AKT pathway in neuroblastoma and its regulation by thioredoxin 1. Human pathology 2011;42(11):1727-1739, doi:10.1016/j.humpath.2011.01.019
311. Chen B, Guan D, Cui ZJ, et al. Thioredoxin 1 downregulates MCP-1 secretion and expression in human endothelial cells by suppressing nuclear translocation of activator protein 1 and redox factor-1. American journal of physiology 2010;298(5):C1170-C1179, doi:10.1152/ajpcell.00223.2009
312. Naranjo-Suarez S, Carlson BA, Tobe R, et al. Regulation of HIF-1α activity by overexpression of thioredoxin is independent of thioredoxin reductase status. Molecules and Cells 2013;36(2):151-157, doi:10.1007/s10059-013-0121-y
313. Guo Y, Einhorn L, Kelley M, et al. Redox Regulation of the Embryonic Stem Cell Transcription Factor Oct-4 by Thioredoxin. STEM CELLS 2004;22(3):259-264, doi:10.1634/stemcells.22-3-259
314. Ago T, Liu T, Zhai P, et al. A Redox-Dependent Pathway for Regulating Class II HDACs and Cardiac Hypertrophy. Cell 2008;133(6):978-993, doi:10.1016/j.cell.2008.04.041
315. Rao AK, Ziegler YS, Mcleod IX, et al. Thioredoxin and thioredoxin reductase influence estrogen receptor α-mediated gene expression in human breast cancer cells. Journal of Molecular Endocrinology 2009;43(6):251-261, doi:10.1677/jme-09-0053
316. King BC, Nowakowska J, Karsten CM, et al. Truncated and Full-Length Thioredoxin-1 Have Opposing Activating and Inhibitory Properties for Human Complement with Relevance to Endothelial Surfaces. The journal of immunology : official journal of the American Association of Immunologists 2012;188(8):4103-4112, doi:10.4049/jimmunol.1101295
317. Nordberg J, Arnér ESJ. Reactive oxygen species, antioxidants, and the mammalian thioredoxin system1 1This review is based on the licentiate thesis “Thioredoxin reductase—interactions with the redox active compounds 1-chloro-2,4-dinitrobenzene and lipoic acid” by Jonas Nordberg, 2001, Karolinska Institute, Stockholm, ISBN 91-631-1064-4. Free radical biology & medicine 2001;31(11):1287-1312, doi:10.1016/s0891-5849(01)00724-9

318. Huang EJ, Reichardt LF. Neurotrophins: Roles in Neuronal Development and Function. Annual Review of Neuroscience 2001;24(1):677-736, doi:10.1146/annurev.neuro.24.1.677
319. Endoh M, Kunishita T, Tabira T. Thioredoxin from Activated Macrophages as a Trophic Factor for Central Cholinergic Neurons in Vitro. Biochemical and biophysical research communications 1993;192(2):760-765, doi:10.1006/bbrc.1993.1479
320. Masutani H, Bai J, Kim Y-C, et al. Thioredoxin as a Neurotrophic Cofactor and an Important Regulator of Neuroprotection. Molecular Neurobiology 2004;29(3):229-242, doi:10.1385/mn:29:3:229
321. Kim M-H, Leem Y-H. Neurogenic effect of exercise via the thioredoxin-1/ extracellular regulated kinase/β-catenin signaling pathway mediated by β2-adrenergic receptors in chronically stressed dentate gyrus. Journal of Exercise Nutrition & Biochemistry 2019;23(3):13-21, doi:10.20463/jenb.2019.0018
322. Tian L, Nie H, Zhang Y, et al. Recombinant human thioredoxin-1 promotes neurogenesis and facilitates cognitive recovery following cerebral ischemia in mice. Neuropharmacology 2014;77(453-464, doi:10.1016/j.neuropharm.2013.10.027
323. Luo Y, Raible D, Raper JA. Collapsin: A protein in brain that induces the collapse and paralysis of neuronal growth cones. Cell 1993;75(2):217-227, doi:10.1016/0092-8674(93)80064-l
324. Tonge D, Chan K, Zhu N, et al. Enhancement of axonal regeneration by in vitro conditioning and its inhibition by cyclopentenone prostaglandins. Journal of Cell Science 2008;121(15):2565-2577, doi:10.1242/jcs.024943
325. Kitaoka Y, Tanito M, Kojima K, et al. Axonal protection by thioredoxin-1 with inhibition of interleukin-1β in TNF-induced optic nerve degeneration. Experimental eye research 2016;152(71-76, doi:10.1016/j.exer.2016.09.007
326. Taoufik E, Kouroupi G, Zygogianni O, et al. Synaptic dysfunction in neurodegenerative and neurodevelopmental diseases: an overview of induced pluripotent stem-cell-based disease models. Open Biology 2018;8(9):180138, doi:10.1098/rsob.180138
327. LoPachin RM, Barber DS. Synaptic Cysteine Sulfhydryl Groups as Targets of Electrophilic Neurotoxicants. Toxicological sciences 2006;94(2):240-255, doi:10.1093/toxsci/kfl066
328. Stemme S, Hansson HA, Holmgren A, et al. Axoplasmic transport of thioredoxin and thioredoxin reductase in rat sciatic nerve. Brain research 1985;359(1-2):140-146, doi:10.1016/0006-8993(85)91421-0
329. Pirazzini M, Azarnia Tehran D, Zanetti G, et al. Thioredoxin and Its Reductase Are Present on Synaptic Vesicles, and Their Inhibition Prevents the Paralysis Induced by Botulinum Neurotoxins. Cell reports 2014;8(6):1870-1878, doi:10.1016/j.celrep.2014.08.017
330. Asahina M, Yamada T, Yoshiyama Y, et al. Expression of Adult T Cell Leukemia-Derived Factor in Human Brain and Peripheral Nerve Tissues. Dementia and geriatric cognitive disorders 1998;9(4):181-185, doi:10.1159/000017044
331. Arodin L, Lamparter H, Karlsson H, et al. Alteration of Thioredoxin and Glutaredoxin in the Progression of Alzheimer's Disease. Journal of Alzheimer's disease 2014;39(4):787-797, doi:10.3233/jad-131814
332. Malaspina A, Kaushik N, de Belleroche J. Differential expression of 14 genes in amyotrophic lateral sclerosis spinal cord detected using gridded cDNA arrays. Journal of neurochemistry 2001;77(1):132-145, doi:10.1046/j.1471-4159.2001.t01-1-00231.x

333. Pennisi G, Cornelius C, Cavallaro MM, et al. Redox regulation of cellular stress response in multiple sclerosis. Biochemical Pharmacology 2011;82(10):1490-1499, doi:10.1016/j.bcp.2011.07.092
334. Sánchez-López F, Tasset I, Agüera E, et al. Oxidative stress and inflammation biomarkers in the blood of patients with Huntington's disease. Neurological research 2012;34(7):721-724, doi:10.1179/1743132812y.0000000073
335. Zhang XY, Chen DC, Xiu MH, et al. Thioredoxin, a novel oxidative stress marker and cognitive performance in chronic and medicated schizophrenia versus healthy controls. Schizophrenia research 2013;143(2-3):301-306, doi:10.1016/j.schres.2012.11.017
336. Owe-Larsson B, Ekdahl K, Edbom T, et al. Increased plasma levels of thioredoxin-1 in patients with first episode psychosis and long-term schizophrenia. Progress in neuro-psychopharmacology & biological psychiatry 2011;35(4):1117-1121, doi:10.1016/j.pnpbp.2011.03.012
337. Zhang QB, Gao SJ, Zhao HX. Thioredoxin: A novel, independent diagnosis marker in children with autism. International Journal of Developmental Neuroscience 2015;40(1):92-96, doi:10.1016/j.ijdevneu.2014.11.007
338. Genc A, Kalelioglu T, Karamustafalioglu N, et al. Level of plasma thioredoxin in male patients with manic episode at initial and post-electroconvulsive or antipsychotic treatment. Psychiatry and Clinical Neurosciences 2015;69(6):344-350, doi:10.1111/pcn.12244
339. Spires-Jones TL, Stoothoff WH, de Calignon A, et al. Tau pathophysiology in neurodegeneration: a tangled issue. Trends in neurosciences 2009;32(3):150-159, doi:10.1016/j.tins.2008.11.007
340. Bjørklund G, Zou L, Peana M, et al. The Role of the Thioredoxin System in Brain Diseases. Antioxidants 2022;11(11):2161, doi:10.3390/antiox11112161
341. Guo Y, Zhang C, Wang C, et al. Thioredoxin-1 Is a Target to Attenuate Alzheimer-Like Pathology in Diabetic Encephalopathy by Alleviating Endoplasmic Reticulum Stress and Oxidative Stress. Frontiers in physiology 2021;12(doi:10.3389/fphys.2021.651105
342. Zhu Y, Romero MI, Ghosh P, et al. Ablation of NF1 function in neurons induces abnormal development of cerebral cortex and reactive gliosis in the brain. Genes & Development 2001;15(7):859-876, doi:10.1101/gad.862101
343. Schoch S, Cibelli G, Thiel G. Neuron-specific Gene Expression of Synapsin I. Journal of Biological Chemistry 1996;271(6):3317-3323, doi:10.1074/jbc.271.6.3317
344. SYN1 protein expression summary - The Human Protein Atlas. 2023. Available from: https://www.proteinatlas.org/ENSG00000008056-SYN1.
345. Melloni RH, Degennaro LJ. Temporal onset of synapsin I gene expression coincides with neuronal differentiation during the development of the nervous system. The Journal of Comparative Neurology 1994;342(3):449-462, doi:10.1002/cne.903420311
346. Rempe D, Vangeison G, Hamilton J, et al. Synapsin I Cre transgene expression in male mice produces germline recombination in progeny. genesis 2006;44(1):44-49, doi:10.1002/gene.20183
347. Sellers SL, Milad N, White Z, et al. Increased nonHDL cholesterol levels cause muscle wasting and ambulatory dysfunction in the mouse model of LGMD2B. Journal of Lipid Research 2018;59(2):261-272, doi:10.1194/jlr.m079459
348. Ihara Y, Tomonoh Y, Deshimaru M, et al. Retigabine, a Kv7.2/Kv7.3-Channel Opener, Attenuates Drug-Induced Seizures in Knock-In Mice Harboring Kcnq2 Mutations. PLOS ONE 2016;11(2):e0150095, doi:10.1371/journal.pone.0150095

349. Dolapchieva S, Eggers R, Kühnel W. Automatic image analysis of the postnatal growth of axons and myelin sheaths in the tibial and peroneal nerves of the rabbit. Annals of anatomy 2000;182(2):133-142, doi:10.1016/S0940-9602(00)80072-2
350. Lam M, Takeo K, Almeida RG, et al. CNS myelination requires VAMP2/3-mediated membrane expansion in oligodendrocytes. Nature Communications 2022;13(1), doi:10.1038/s41467-022-33200-4
351. Shen K, Yuen TJ. Ex Vivo Myelination and Remyelination in Cerebellar Slice Cultures as a Quantitative Model for Developmental and Disease-Relevant Manipulations. Journal of Visualized Experiments 2020;160), doi:10.3791/61044
352. Matsui M, Oshima M, Oshima H, et al. Early Embryonic Lethality Caused by Targeted Disruption of the Mouse Thioredoxin Gene. Developmental biology 1996;178(1):179-185, doi:10.1006/dbio.1996.0208
353. Yamamoto M, Yang G, Hong C, et al. Inhibition of endogenous thioredoxin in the heart increases oxidative stress and cardiac hypertrophy. Journal of Clinical Investigation 2003;112(9):1395-1406, doi:10.1172/jci17700
354. Prigge JR, Coppo L, Martin SS, et al. Hepatocyte Hyperproliferation upon Liver-Specific Co-disruption of Thioredoxin-1, Thioredoxin Reductase-1, and Glutathione Reductase. Cell Reports 2017;19(13):2771-2781, doi:10.1016/j.celrep.2017.06.019
355. Das KC. Thioredoxin-deficient mice, a novel phenotype sensitive to ambient air and hypersensitive to hyperoxia-induced lung injury. American journal of physiology 2015;308(5):L429-L442, doi:10.1152/ajplung.00285.2014
356. Guyenet SJ, Furrer SA, Damian VM, et al. A simple composite phenotype scoring system for evaluating mouse models of cerebellar ataxia. Journal of visualized experiments 2010;39), doi:10.3791/1787
357. Lingor P, Koch JC, Tönges L, et al. Axonal degeneration as a therapeutic target in the CNS. Cell and Tissue Research 2012;349(1):289-311, doi:10.1007/s00441-012-1362-3
358. Seo WM, Yoon J, Lee J-H, et al. Modeling axonal regeneration by changing cytoskeletal dynamics in stem cell-derived motor nerve organoids. Scientific Reports 2022;12(1), doi:10.1038/s41598-022-05645-6
359. Zhang J, Jones MV, Mcmahon MT, et al. In vivo and ex vivo diffusion tensor imaging of cuprizone-induced demyelination in the mouse corpus callosum. Magnetic Resonance in Medicine 2012;67(3):750-759, doi:10.1002/mrm.23032
360. Fluoro-Jade C (FJC) Powder for identifying Degenerating Neurons. 2023;
361. Ohmori I, Ouchida M, Shinohara M, et al. Novel animal model of combined generalized and focal epilepsy. Epilepsia 2022;63(7), doi:10.1111/epi.17295
362. Ohmori I, Ouchida M, Imai H, et al. Thioredoxin deficiency increases oxidative stress and causes bilateral symmetrical degeneration in rat midbrain. Neurobiology of disease 2022;175(105921, doi:10.1016/j.nbd.2022.105921
363. Frost B, Bardai H, Farah, Feany B, Mel. Lamin Dysfunction Mediates Neurodegeneration in Tauopathies. Current Biology 2016;26(1):129-136, doi:10.1016/j.cub.2015.11.039
364. Starr DA, Fridolfsson HN. Interactions Between Nuclei and the Cytoskeleton Are Mediated by SUN-KASH Nuclear-Envelope Bridges. Annual Review of Cell and Developmental Biology 2010;26(1):421-444, doi:10.1146/annurev-cellbio-100109-104037
365. Eftekharzadeh B, Daigle JG, Kapinos LE, et al. Tau Protein Disrupts Nucleocytoplasmic Transport in Alzheimer's Disease. Neuron 2018;99(5):925-940.e7, doi:10.1016/j.neuron.2018.07.039

366. Barbier P, Zejneli O, Martinho M, et al. Role of Tau as a Microtubule-Associated Protein: Structural and Functional Aspects. Frontiers in aging neuroscience 2019;11(doi:10.3389/fnagi.2019.00204
367. Kim S-U, Park Y-H, Kim J-M, et al. Dominant Role of Peroxiredoxin/JNK Axis in Stemness Regulation During Neurogenesis from Embryonic Stem Cells. Stem Cells 2014;32(4):998-1011, doi:10.1002/stem.1593
368. Cole-Edwards KK, Musto AE, Bazan NG. c-Jun N-Terminal Kinase Activation Responses Induced by Hippocampal Kindling Are Mediated by Reactive Astrocytes. The Journal of Neuroscience 2006;26(32):8295-8304, doi:10.1523/jneurosci.1986-05.2006
369. Neddens J, Temmel M, Flunkert S, et al. Phosphorylation of different tau sites during progression of Alzheimer's disease. Acta Neuropathologica Communications 2018;6(1), doi:10.1186/s40478-018-0557-6
370. Sluss HK, Davis RJ. H2AX Is a Target of the JNK Signaling Pathway that Is Required For Apoptotic DNA Fragmentation. Molecular Cell 2006;23(2):152-153, doi:10.1016/j.molcel.2006.07.001
371. Maciejowski J, Hatch EM. Nuclear Membrane Rupture and Its Consequences. Annual Review of Cell and Developmental Biology 2020;36(1):85-114, doi:10.1146/annurev-cellbio-020520-120627
372. Šušnjar U, Škrabar N, Brown A-L, et al. Cell environment shapes TDP-43 function with implications in neuronal and muscle disease. Communications Biology 2022;5(1), doi:10.1038/s42003-022-03253-8
373. Briese M, Saal-Bauernschubert L, Lüningschrör P, et al. Loss of Tdp-43 disrupts the axonal transcriptome of motoneurons accompanied by impaired axonal translation and mitochondria function. Acta Neuropathologica Communications 2020;8(1), doi:10.1186/s40478-020-00987-6
374. Yuan A, Rao MV, Veeranna, et al. Neurofilaments and Neurofilament Proteins in Health and Disease. Cold Spring Harbor Perspectives in Biology 2017;9(4):a018309, doi:10.1101/cshperspect.a018309
375. Aldrich S. MONOCLONAL ANTI-NEUROFILAMENT 200 CLONE NE14. 2023.
376. Hirano A, Nakano I, Kurland LT, et al. Fine Structural Study of Neurofibrillary Changes in a Family with Amyotrophic Lateral Sclerosis. Journal of neuropathology and experimental neurology 1984;43(5):471-480, doi:10.1097/00005072-198409000-00002
377. Activated microglia drive demyelination via CSF1R. GLIA 2021;69(6):1583, doi:10.1002/glia.23980
378. Ryan TA, Li L, Chin LS, et al. Synaptic vesicle recycling in synapsin I knock-out mice. Journal of Cell Biology 1996;134(5):1219-1227, doi:10.1083/jcb.134.5.1219
379. 003966 - Strain Details. 2023;
380. Petr GT, Sun Y, Frederick NM, et al. Conditional Deletion of the Glutamate Transporter GLT-1 Reveals That Astrocytic GLT-1 Protects against Fatal Epilepsy While Neuronal GLT-1 Contributes Significantly to Glutamate Uptake into Synaptosomes. The Journal of Neuroscience 2015;35(13):5187-5201, doi:10.1523/JNEUROSCI.4255-14.2015
381. Denroche HC, Glavas MM, Tudurí E, et al. Disrupted Leptin Signaling in the Lateral Hypothalamus and Ventral Premammillary Nucleus Alters Insulin and Glucagon Secretion and Protects Against Diet-Induced Obesity. Endocrinology 2016;157(7):2671-2685, doi:10.1210/en.2015-1998
382. Zhang Z, Cao M, Chang C-W, et al. Autism-Associated Chromatin Regulator Brg1/SmarcA4 Is Required for Synapse Development and Myocyte Enhancer Factor 2-Mediated

Synapse Remodeling. Molecular and Cellular Biology 2015;36(1):70-83, doi:10.1128/MCB.00534-15
383. He X-P, Kotloski R, Nef S, et al. Conditional Deletion of TrkB but Not BDNF Prevents Epileptogenesis in the Kindling Model. Neuron 2004;43(1):31-42, doi:10.1016/j.neuron.2004.06.019
384. Chauhan P, Philip SE, Chauhan G, et al. The Anatomical Basis of Seizures. In: Epilepsy. Exon Publications: 2022; pp. 15-24.
385. Kandratavicius L, Balista P, Lopes-Aguiar C, et al. Animal models of epilepsy: use and limitations. Neuropsychiatric Disease and Treatment 2014;1693, doi:10.2147/ndt.s50371
386. Dichter MA. Emerging Concepts in the Pathogenesis of Epilepsy and Epileptogenesis. Archives of Neurology 2009;66(4), doi:10.1001/archneurol.2009.10
387. Curtis M, Garbelli R, Uva L. A hypothesis for the role of axon demyelination in seizure generation. Epilepsia 2021;62(3):583-595, doi:10.1111/epi.16824
388. Coulter DA, Steinhauser C. Role of Astrocytes in Epilepsy. Cold Spring Harbor perspectives in medicine 2015;5(3):a022434-a022434, doi:10.1101/cshperspect.a022434
389. Malhas AN, Lee CF, Vaux DJ. Lamin B1 controls oxidative stress responses via Oct-1. The Journal of Cell Biology 2009;184(1):45-55, doi:10.1083/jcb.200804155
390. Matias I, Diniz LP, Damico IV, et al. Loss of lamin-B1 and defective nuclear morphology are hallmarks of astrocyte senescence in vitro and in the aging human hippocampus. Aging Cell 2022;21(1), doi:10.1111/acel.13521
391. Albrecht S, Bourdeau M, Bennett D, et al. Activation of Caspase-6 in Aging and Mild Cognitive Impairment. The American Journal of Pathology 2007;170(4):1200-1209, doi:10.2353/ajpath.2007.060974
392. Angel A, Volkman R, Royal TG, et al. Caspase-6 Knockout in the 5xFAD Model of Alzheimer's Disease Reveals Favorable Outcome on Memory and Neurological Hallmarks. International Journal of Molecular Sciences 2020;21(3):1144, doi:10.3390/ijms21031144
393. Paonessa F, Evans LD, Solanki R, et al. Microtubules Deform the Nuclear Membrane and Disrupt Nucleocytoplasmic Transport in Tau-Mediated Frontotemporal Dementia. Cell Reports 2019;26(3):582-593.e5, doi:10.1016/j.celrep.2018.12.085
394. Milenkovic I, Jarc J, Dassler E, et al. The physiological phosphorylation of tau is critically changed in fetal brains of individuals with Down syndrome. Neuropathology and applied neurobiology 2018;44(3):314-327, doi:10.1111/nan.12406
395. Mondragón-Rodríguez S, Perry G, Zhu X, et al. Phosphorylation of Tau Protein as the Link between Oxidative Stress, Mitochondrial Dysfunction, and Connectivity Failure: Implications for Alzheimer's Disease. Oxidative Medicine and Cellular Longevity 2013;2013(1-6, doi:10.1155/2013/940603
396. Zhu X, Rottkamp CA, Boux H, et al. Activation of p38 Kinase Links Tau Phosphorylation, Oxidative Stress, and Cell Cycle-Related Events in Alzheimer Disease. Journal of neuropathology and experimental neurology 2000;59(10):880-888, doi:10.1093/jnen/59.10.880
397. Olguín-Albuerne M, Morán J. Redox Signaling Mechanisms in Nervous System Development. Antioxidants & redox signaling 2018;28(18):1603-1625, doi:10.1089/ars.2017.7284
398. Przedborski S. Molecular targets for neuroprotection. Amyotrophic lateral sclerosis and other motor neuron disorders : official publication of the World Federation of Neurology, Research Group on Motor Neuron Diseases 2004;5(sup1):14-18, doi:10.1080/1734470410019780

399. Gerace L, Blobel G. Nuclear Lamina and the Structural Organization of the Nuclear Envelope. Cold Spring Harbor Symposia on Quantitative Biology 1982;46(967-978, doi:10.1101/SQB.1982.046.01.090
400. Fu X, Liang C, Li F, et al. The Rules and Functions of Nucleocytoplasmic Shuttling Proteins. International Journal of Molecular Sciences 2018;19(5):1445, doi:10.3390/ijms19051445
401. Suk TR, Rousseaux MWC. The role of TDP-43 mislocalization in amyotrophic lateral sclerosis. Molecular Neurodegeneration 2020;15(1), doi:10.1186/s13024-020-00397-1
402. Coyne AN, Baskerville V, Zaepfel BL, et al. Nuclear accumulation of CHMP7 initiates nuclear pore complex injury and subsequent TDP-43 dysfunction in sporadic and familial ALS. Science translational medicine 2021;13(604):eabe1923, doi:10.1126/scitranslmed.abe1923
403. Chou C-C, Zhang Y, Umoh ME, et al. TDP-43 pathology disrupts nuclear pore complexes and nucleocytoplasmic transport in ALS/FTD. Nature Neuroscience 2018;21(2):228-239, doi:10.1038/s41593-017-0047-3
404. Yang C, Wang H, Qiao T, et al. Partial loss of TDP-43 function causes phenotypes of amyotrophic lateral sclerosis. Proceedings of the National Academy of Sciences 2014;111(12):E1121-E1129, doi:10.1073/pnas.1322641111
405. Alami H, Nael, Smith B, Rebecca, Carrasco A, Monica, et al. Axonal Transport of TDP-43 mRNA Granules Is Impaired by ALS-Causing Mutations. Neuron 2014;81(3):536-543, doi:10.1016/j.neuron.2013.12.018
406. Chien H-M, Lee C-C, Huang JJ-T. The Different Faces of the TDP-43 Low-Complexity Domain: The Formation of Liquid Droplets and Amyloid Fibrils. International Journal of Molecular Sciences 2021;22(15):8213, doi:10.3390/ijms22158213
407. Lefebvre-Omar C, Liu E, Dalle C, et al. Neurofilament accumulations in amyotrophic lateral sclerosis patients' motor neurons impair axonal initial segment integrity. Cellular and Molecular Life Sciences 2023;80(6), doi:10.1007/s00018-023-04797-6
408. Corbo M, Hays AP. Peripherin and Neurofilament Protein Coexist in Spinal Spheroids of Motor Neuron Disease. Journal of neuropathology and experimental neurology 1992;51(5):531-537, doi:10.1097/00005072-199209000-00008